# Characterization of Influenza A:*Streptococcus pneumoniae* Synergistic Disease and Potential for Disease Alleviation via Sphingolipid Therapy

**Amanda Lynn Gasser**

Thesis submitted to the faculty of the Virginia Polytechnic Institute and State University in partial fulfillment of the requirements for the degree of

**Master of Science**

**In**

**Biomedical and Veterinary Sciences**

Paul Christopher Roberts, Chair

Eva M. Schmelz

Lijuan Yuan

July 12, 2013

Blacksburg, VA

Keywords: Influenza A virus, cytokine storm, immunomodulation, sphingosine 1-phosphate, FTY720, sphingosine kinase, Enigmol

# Characterization of Influenza A:*Streptococcus pneumoniae* synergistic disease and Potential for disease alleviation via sphingolipid therapy

Amanda Lynn Gasser

ABSTRACT

Influenza A virus (IAV) is generally associated with the seasonal malady that causes brief respiratory illness during the winter months, known simply as "the flu." Most otherwise healthy individuals will suffer from mild fever, congestion, headaches and myalgia that are resolved within 5-7 days of onset. However, there are nearly 500,000 influenza-related deaths that occur world-wide every year. Many of these casualties and patients hospitalized with influenza also test positive for bacterial pneumonia, the most common agent being *Streptococcus pneumoniae*. Although all individuals are subject to this viral:bacterial synergistic disease, the young, elderly, and immunocompromised are the most susceptible. Previous studies have shown that viral infection creates a prolonged hyper-responsive pro-inflammatory state in the lungs, which increases susceptibility to secondary bacterial infection. Lethality is due to detrimental pulmonary damage from a dysregulated host inflammatory response, known as the "cytokine storm." However, the nature of dual infection has not been well-studied in the elderly demographic. Therefore, we aim to better define this disease synergy in an aged mouse model and explore potential therapeutic alternatives that could be beneficial for the aged and other vulnerable populations.

Sphingolipid modulation has emerged as a potential target to ameliorate the excessive inflammation (cytokine storm) elicited by highly pathogenic influenza. There is particular emphasis on sphingosine 1-phosphate (S1P) signaling, as well as control of intracellular S1P levels

via sphingosine kinases (SK). Sphingolipids are involved in a multitude of cellular processes, and are tightly regulated by their metabolizing enzymes. We hypothesize that manipulation of sphingolipid signaling and alteration of the internal sphingolipid milieu will diminish the inflammatory response elicited by IAV infection. Using fluorescence-activated cell sorting (FACS), real-time PCR and cytometric bead array (CBA) analysis, we evaluated the immunomodulatory effects of systemic sphingosine analog treatment within the lung microenvironment under homeostatic and influenza-infected conditions. FTY720 treatment caused transient, but significant lymphopenia, influx of neutrophils and efflux of macrophages in the lungs, which was enhanced during a mild influenza infectionGene expression in the lungs was generally unaltered, but protein levels showed increases in specific influenza-induced cytokines, suggesting these treatments may have post-transcriptional effects on cytokine expression. To evaluate sphingolipid modulation in specific pulmonary cell types, we next observed the effects of these compounds and sphingosine kinase (SK) inhibitors in epithelial and alveolar macrophage-like cell lines. SK inhibitors and Enigmol demonstrated anti-viral effects in A549 cells, decreasing viral loads by up to 1.5 logs. Real-time PCR and CBA analysis further demonstrated that these effects were associated with alterations in key cytokine expression, including CCL2, CCL5, CXCL10, IL-6, and IL-8. Collectively, these findings indicate that therapeutic sphingolipid modulation has the potential for creating a protective microenvironment in the lungs that could alleviate or even prevent viral:bacterial synergistic disease.

## Acknowledgements

I am fortunate to have so many people in my life who have helped make my graduate career possible. For each of them, I am truly grateful and will never forget the support and encouragement that kept me going through this process.

To my advisor, Dr. Chris Roberts: I deeply appreciate the opportunity you gave me to obtain my master's degree in your lab. Under your guidance, I have become a stronger research scientist, as you have helped develop my ability to think critically and work independently. You motivated me to continuously challenge myself in efforts to expand and evolve my scientific knowledge and reasoning. Thank you for instilling me with these qualities that will be valuable as I move forward in my career.

To my co-mentor, Dr. Schmelz: Thank you for all of your help and direction as you introduced me to the vast world of sphingolipids. Being able to call upon your extensive knowledge in this complex field was tremendously helpful and instrumental to accomplishing this research. To Dr. Yuan: Thank you for all of your contributions as a committee member, and for sharing your expertise and perspectives that helped shape and strengthen my research.

To my fellow lab members: I feel privileged to have worked with you all over the past several years. Thank you to Binu Velayudhan for getting me started in a completely new field of research when I first began my graduate career in the Roberts lab. You taught me many useful techniques that have been essential to the completion of these projects. Thank you to Lynn Heffron, Tila Khan, Courie Cohen, Amanda Shea, and Sungseok Lee for all of your help, support and camaraderie in the lab. I have enjoyed working alongside and learning from you, and value the friendships that have developed from this experience. A special thank you to Lynn Heffron for all of your constant encouragement and invaluable assistance with my experiments. You were

always willing to go above and beyond the call of duty to ensure the lab ran smoothly and that everyone received the help they needed. I also would like to extend my gratitude to the Animal Care Technicians who maintained our mice and the facility necessary to perform these animal studies.

To the many people I have met throughout my time in Blacksburg: I am honored to call you all my friends. I cherish each and every one of you for the friendships and strong sense of home you have given me. There have been so many great times we shared together that I will never forget. From all the laughter to even the tears, every moment with you all has been so very special. You have truly enriched my life by being a part of it.

To my family: There really is no way to adequately convey my gratitude for all that you do. From the beginning, you have been my advocate, and have given me the support and opportunities necessary to succeed. You have seen me at my best and my worst, and throughout it all, you have been right by my side. Your consistent encouragement and unwavering faith in my abilities has given me the confidence to achieve so much more than I could without you. Thank you for being the constant in my life. Your love and support have made my goals attainable, for which I will always be grateful.

## Table of Contents

## Table of Figures

## Table of Tables

# **Chapter One:** Introduction

## Influenza A Virus: A Global Threat

Influenza virus is a highly communicable respiratory pathogen and the causative agent of seasonal and pandemic flu infections. It is an enveloped, negative-sense, single-stranded, segmented RNA virus in the *Orthomyxoviridae* family [1]. This family consists of four genera: influenza A, B, C and thogotovirus. Influenza viruses are classified based on their distinct internal nucleoprotein and matrix proteins, as well as surface proteins, hemagglutinin (HA) and neuraminidase (NA) [2]. While influenza B and C viruses are mostly restricted to human hosts [3], influenza A viruses (IAVs) are zoonotic and infect a wide range of hosts including humans, swine, wild and domestic birds, horses, and dogs [4]. IAV is also highly adaptable due to a variety of mechanisms. An error-prone RNA-dependent RNA polymerase lends to high mutation rates, and reassortment of RNA segments within co-infected cells allows alteration of both genotypic and phenotypic properties [5]. Altogether, these qualities contribute to the virulence of this virus, and thus its ever-present and widespread threat.

Influenza A virus (IAV) is one of the most prevalent causes of upper respiratory tract infections. While IAV infections can strike throughout the year, occurrence is typically seasonal. Regions with temperate climates experience the highest frequency of IAV incidence during the coldest months of the year. In the Northern hemisphere, "flu season" spans from October-April, with infection rates peaking in February [6]. Seasonal flu infection results in an uncomplicated and self-limiting infection that is eliminated by the normal immune response within 7 days of initial insult in otherwise healthy individuals. The host will often experience fever, muscle aches, fatigue, nasal congestion, headaches and a dry cough during infection that may persist into the resolution phase following viral clearance [2]. However, influenza virus has the ability to lead to

more serious disease, especially in the young (under 2 years), elderly (older than 65 years) and immunocompromised. Due to its highly contagious nature, IAV is a particular menace among day care centers, schools, nursing homes and hospitals. In fact, the World Health Organization reports 3-5 million clinical cases and 250-500,000 deaths attributed to influenza A viruses worldwide every year. On average, 36,000 of these deaths occur in the United States, but as many as 52,000 have been recorded since 1976 [7, 8].

Currently, seasonal flu is attributed to variations of influenza A subtypes H1N1 and H3N2, but occasionally novel influenza virus strains are introduced into the population that lead to pandemic outbreaks [7, 9, 10]. The 1918 Spanish Flu was the worst pandemic in recorded history. It affected nearly 30% of the world population and caused a devastating 50 million deaths, which was approximately 2.5% of the world population [11]. Only twenty years ago, RG Webster provided the evidence that wild aquatic avian species maintain the gene pool for these pandemic strains as they are the natural reservoir for all IAV subtypes [4]. Since then, we have seen the emergence of highly pathogenic avian influenza (HPAI) H5N1 and its influence in pandemic outbreaks. HPAI causes extensive disease and economic hardships among poultry farms, as containment practices are limited to widespread culling of flocks. Before 1997, it was not known that avian influenza strains could be transmitted to humans and other mammals. However, studies within the past decade have confirmed not only cross-species transmission, but also the increased mortality rates in humans and mammals. Although efficacy of transmission is potentially reduced compared to seasonal flu strains, HPAI causes fatal disease in 50%-70% of those infected [12].

**Influenza life cycle and pathogenesis**

The influenza A virus genome consists of eight RNA segments that encode 11 viral proteins: PB1, PB2, PA, PB1-F2, HA, NA, NP, M1, M2, NS1 and NS2. PB1, PB2 and PA proteins comprise the viral polymerase complex necessary for genomic viral RNA (vRNA) replication [1]. PB1-F2 is a newly discovered protein linked to enhanced pathogenicity of HPAI and pandemic flu strains [13]. The surface proteins HA and NA serve as the main antigenic factors for subtype classification. HA, of which there are 17 subtypes, is responsible for viral attachment and entry by binding sialic acid receptors on the surface of target cells. NA has 9 subtypes and is key to the release of viral particles from cells via cleavage of sialic acid. Nucleoprotein (NP) binds and packages viral RNA, forming the ribonucleoprotein (RNP) complex [14, 15]. M1 is the structure-providing matrix protein and M2 the integral membrane protein with ion channel activity [16]. Nonstructural proteins 1 and 2 (NS1, NS2) block host cell protein synthesis and innate immune response, and to export viral RNPs from the nucleus, respectively [17].

Influenza virus does not have the means to replicate and produce infectious progeny on its own, so it must first find a living host to undergo this process. IAV surface protein HA attaches to host cells via sialic acid receptors on the cell surface. This binding is preferential, based on the strain of influenza virus. Human IAV strains favor sialic acid on glycoproteins with α2,6 linkages, which are primarily expressed on mammalian respiratory mucosal cells. Avian strains instead favor α2,3 linkages, which are most commonly found on cells in the avian gut, but also selectively on human airway cells [18]. Limited expression of α2,3 linkages among human airway cells is one factor that restricts the efficiency of human-human transmission of avian influenza viruses. HA is then cleaved by respiratory-specific extracellular proteases to expose the fusion peptide necessary for infectivity of virus as it allows the fusion of viral and endosomal membranes [19].

Binding then triggers endocytosis and the virus becomes enclosed in clathrin-dependent endosomal vesicles. Acidification within the endosomes and shuttling of protons through the M2 ion channel causes the release of viral RNP from M1 [19]. Fusion of viral envelope and endosomal membrane is mediated by viral HA protein. Viral RNPs are released into the cytoplasm and then translocated to the nucleus. Viral RNA-dependent RNA polymerase, comprised of PB1, PB2 and PBA proteins, initiates viral mRNA synthesis for subsequent viral protein translation and genomic vRNA synthesis for progeny [20]. Newly synthesized HA, NA and M2 are transported from the ER, through the ER and preferentially gather near lipid raft regions at the apical surface of infected epithelial cells [21, 22]. NP and M1 translocate into the nucleus, where they bind vRNA to form the M1-RNP complexes. These complexes facilitate nuclear export and subsequent association with structural proteins assembled at the apical surfaces. M1 association with the cytoplasmic tails

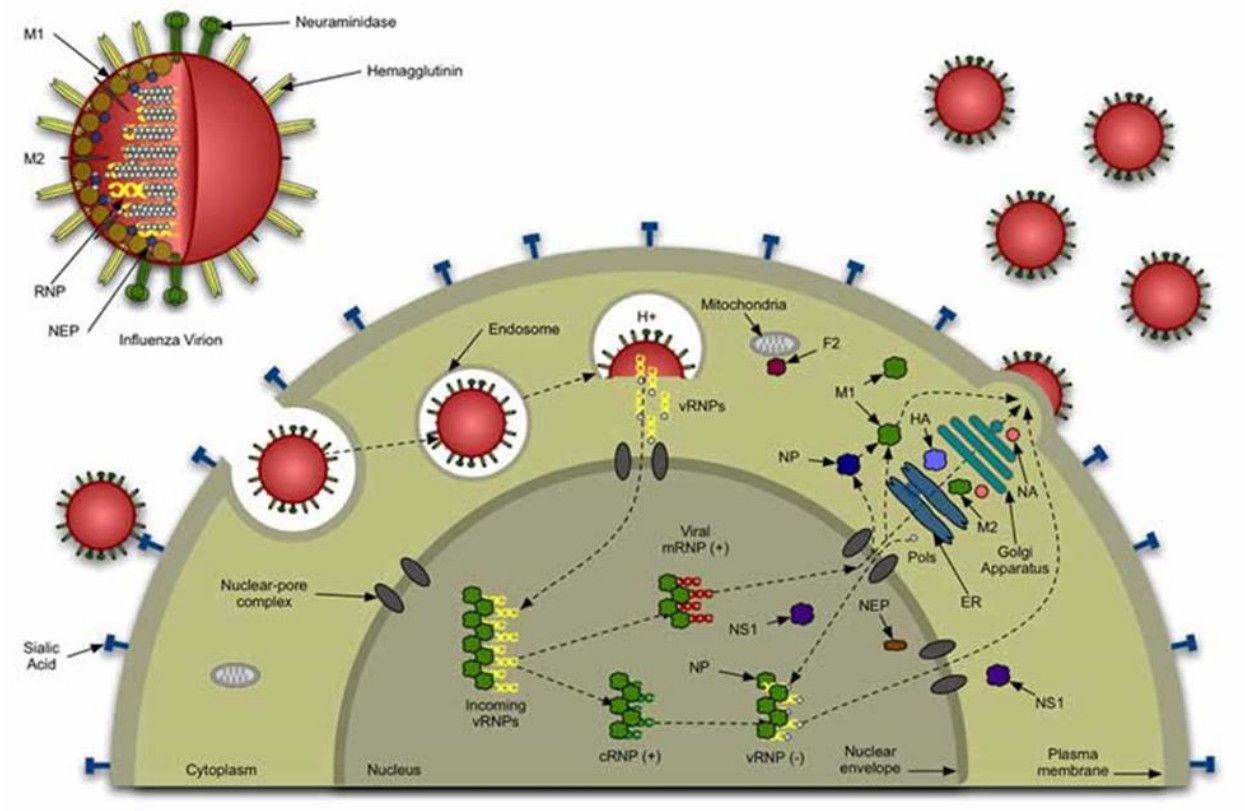


**Figure 1-1. Overview of influenza viral life cycle.**
http://gallus.reactome.org/cgi-bin/eventbrowser?DB=test_gallus_reactome_release_2_myisam&ID=168255. May 5, 2013. Used under fair use, 2013.

of HA and NA which initiates viral budding. As the virus buds, it acquires part of the cell membrane, which becomes the HA/NA-expressing viral envelope. Budding virions are then released into the extracellular spaces by NA cleavage of sialic acid [23-26].

**Innate immune response to influenza infection**

There are several pattern recognition receptors (PRRs) by which the innate immune system identifies and responds to influenza viruses. These include toll-like receptors (TLRs), retinoic acid inducible gene-I (RIG-I) and the NOD-like receptor family pryin domain containing 3 (NLRP-3) protein [27]. Intranuclear TLRs 7/8 recognize genomic ssRNA and recruit MyD88 containing TIR domain. Further downstream, MyD88 signaling leads to the production of anti-viral type I interferons and pro-inflammatory cytokines through activation of IRF and NFκB transcription factors [28, 29]. RLRs are a redundant innate viral recognition mechanism that also initiate signaling via NFκB and IRF [30]. However, these receptors function in the cytoplasm of influenza-infected cells by recognizing genomic triphosphate ssRNA [31]. Finally, NLRP3 is triggered by the M2 ion channel activity of influenza, and subsequently leads to the activation of IL-1β, a cytokine key to antigen-specific CD4+ T cell expansion [32].

Respiratory epithelial cells (ECs), resident alveolar macrophages (AMs) and respiratory dendritic cells (rDCs) are among the first cell types to encounter the influenza virus. Epithelial cells differ based upon their location in the respiratory tract, but all provide the primary site and machinery for influenza viral replication. Alveolar epithelial cells (AECs) are particularly important to evaluate because severe influenza viral and/or polymicrobial infections involve the cells of the lower respiratory tract [33]. There are two types of AECs: alveolar type I (ATI) and alveolar type II (ATII). ATIs specialize in gas exchange, and fluid and ion transport [34], whereas ATIIs play a role in innate defense through secretion of cytokines and surfactant proteins, ion and

fluid transport, and alveolar repair [35]. These cells also generate many of the pro-inflammatory cytokines that recruit leukocytes, namely neutrophils and monoctyes, from the periphery to clear infection. These cytokines include TNFα, IL-1, CCL2, CCL5, CXCL8, CXCL10, IFNγ and many others [36, 37]. Epithelial cells are essentially responsible for the coordination, maintenance and balance of phagocyte-mediated anti-viral host response [38].

As the primary phagocyte of the respiratory tract, resident AMs are critical in limiting viral spread. In addition to phagocytosis of influenza-infected cells, they also produce cytotoxic NOS2 and TNFα [39]. Though AMs can directly be infected by influenza A virus, it typically results in an abortive infection with very few infectious viral particles produced. Like respiratory ECs, AMs also secrete a host of immune cell-recruiting chemokines. Upregulation of type I interferons (α/β) and CXCL11 genes are notable in the early response to IAV (4hpi), and IFN-inducible genes CXCL9, -10,-11 dominate the late response (24hpi) [40]. In direct contrast to their pro-inflammatory response, alveolar macrophages also regulate the resolution of inflammation to bring the airways back to their homeostatic state. This quality is essential as the respiratory tract is constantly exposed to airborne allergens and inflammation-inducing antigens [41]. AMs perform this anti-inflammatory duty through phagocytosis of apoptotic neutrophils, reduction of pro-inflammatory cytokine expression and upregulation of inflammation-suppressing TGFβ and prostaglandin $E_2$ [42].

Respiratory dendritic cells (rDCs) represent another critical immune cell involved in the innate response to influenza viral infection. They serve a unique role as the gateway between the innate and adaptive immune response [43]. There are many subsets of CD11c+ dendritic cells each with specialized functions, but generally speaking rDCs originate from bone marrow derived precursors that migrate through the bloodstream to the airways. After entering the lungs, these

precursors undergo maturation and acquire their essential antigen uptake and presentation functions [44]. Mature rDCs are positioned between the airway epithelium and basal membrane, and survey the airway with their outstretched dendrites that extend into the lumen [45]. Upon recognition of IAV via microbial PRRs like TLR7, signaling cascades within the cell are initiated, resulting in anti-viral and inflammatory cytokine production. In addition, DCs acquire viral antigen by either direct infection with IAV or the phagocytosis of nearby apoptotic virus-infected cells [46, 47]. Antigen-expressing DCs then migrate to the mediastinal lymph node (MLN), the regional LN for the lungs, to initiate clonal expansion of T helper cells (CD4+) and cytotoxic T lymphocytes (CD8+) by antigen presentation via major histocompatibility complexes. These lymphocytes travel to the lungs to aid in viral clearance by secreting anti-viral IFNγ or direct cell killing, respectively [44].

**Cytokine storm**

Cytokine storm is the term used for the robust and dysregulated inflammatory immune response elicited by the host following innate pathogen recognition, often resulting in increased morbidity and mortality. It is characterized by an excessive production of cytokines, including interferons, interleukins, chemokines, colony-stimulating factors (CSFs) and tumor necrosis factors (TNFs) [48]. Chemokines, the largest of the cytokine families, function to recruit immune cells, such as neutrophils, monocytes and lymphocytes, to the site of infection [49]. In macaques infected with lethal H1N1 influenza (1918 pandemic strain), cytokine storm is marked by enhanced gross pathologic pulmonary lesions (60-90% of lung affected) and prolonged alveolar damage [50]. Microarray and protein analysis reveal substantial increased expression of IL-6, IL-8, CCL2, and CCL5 among other cytokines. While a mild seasonal influenza infection does not

typically prompt such an exuberant response alone, it does generate a pre-disposed state in the lungs. This leaves the host vulnerable to secondary bacterial infection and the resultant cytokine storm induced by polymicrobial infection.

**Secondary bacterial infection**

Seasonal influenza virus infection is rarely fatal, but it does leave the host highly susceptible to lethal bacterial superinfection, especially during pandemic years. In fact, over half of the patients hospitalized with influenza test positive for bacterial pneumonia [51]. *Streptococcus pneumoniae* (*S. pneumoniae*) is the most common agent, but other isolates include *Staphylococcus aureus* and *Haemophilus influenzae* [52]. *S. pneumoniae* is a commensal microorganism that colonizes the nasopharynx of 20-50% of healthy children and 8-30% of healthy adults [53]. McCullers (2006) outlines the virus-induced changes in the respiratory tract that allow this opportunistic pathogen to invade the lower respiratory tract and cause severe disease. Such factors include epithelial damage, altered airway function and innate immune responses, and upregulation of receptors [54]. Previous studies in the Roberts' lab have shown that viral:bacterial synergistic disease results in mortality due to septicemia, enhanced inflammatory infiltrates and dysregulated cytokine production [55]. However, the same disease state is not achieved when the order of infection is reversed [56]. These findings indicate that it is in fact the primary influenza infection that alters the lung environment, causing a susceptibility to polymicrobial infection and resulting cytokine storm.

**Current influenza vaccination and treatment methods**

Annual immunization against seasonal strains of influenza virus is a commonly implemented preventative treatment used worldwide. There are two main varieties of vaccines used in the United States: inactivated trivalent vaccine (TIV) and live attenuated vaccine (LAIV) [57]. TIVs are comprised of two IAV strains and one IBV strain, and induce high neutralizing antibody titers against HA and NA, which are modified each year based on current circulating strains. The humoral response mounted by TIVs is driven by $T_h2$-mediated immunity and influenza-specific serum IgG [78-82]. Although the vaccine is effective in eliciting a response to neutralize virus infection, it does not offer much cell-mediated protection, which is key for cytotoxic T cell viral clearance [83-84]. Therefore, vaccine efficacy is generally limited to healthy individuals between the ages of 3 and 65, and successful prediction of HA/NA viral proteins [74]. On the other hand, LAIV utilizes live, temperature-sensitive (attenuated) strains of IAV and IBV [87]. This vaccine is given as a nasal mist and mimics an actual IAV infection, ideally without the severity [88]. It stimulates influenza-specific IgA, IgM and IgG, as well as anti-viral IFNγ secretion and cytotoxic T cell responses [81]. LAIV is nearly 85-93% effective depending on antigenic match, but only approved for healthy individuals between 2-50 years of age because of asthma-causing potential in children and weakened immunity in the elderly [89]. Overall, these vaccination strategies are efficacious, but for only a specific population. This leaves the very young, elderly, and immune-challenged without an effective means of protection.

Though many individuals do not seek anti-viral treatment when suffering from a seasonal flu infection, there are treatments available. Still, these treatments are not without their downfalls. There are two classes of anti-viral drugs currently approved: M2 ion channel-blockers (amantadine and rimantadine) and neuraminidase inhibitors (oseltamivir/Tamiflu and zanamivir/Relenza) [58].

In 2006, the CDC advised against M2-blockers due to adverse effects, limitation to only influenza A viruses, and the rapid emergence of drug-resistant influenza viral strains [59]. Since 2010, neuraminidase inhibitors (NAIs) are the only anti-viral treatment recommended by the WHO. At this time, IAV strains have demonstrated extremely low rates of NAI resistance. However, as NAIs have become the prevalent treatment of influenza, selective pressure and the ability of influenza viruses to rapidly mutate has resulted in increasing rates of resistance to these drugs as well [59].

**Sphingolipids**

Sphingolipids are a major constituent of the eukaryotic plasma membrane and are comprised of a sphingoid long-chain base (sphingosine) and amide-linked fatty acid chain. There are numerous sphingolipid metabolites within the pathway; those important for this thesis are sphingomyelin, ceramide, ceramide 1-phosphate, sphingosine, and sphingosine 1-phosphate (Fig. 1-2) [60]. Sphingosines and ceramides exist in many permutations, which vary in fatty acid chain length and substituents, such as double bonds and hydroxyl groups [61]. As bioactive mediators,

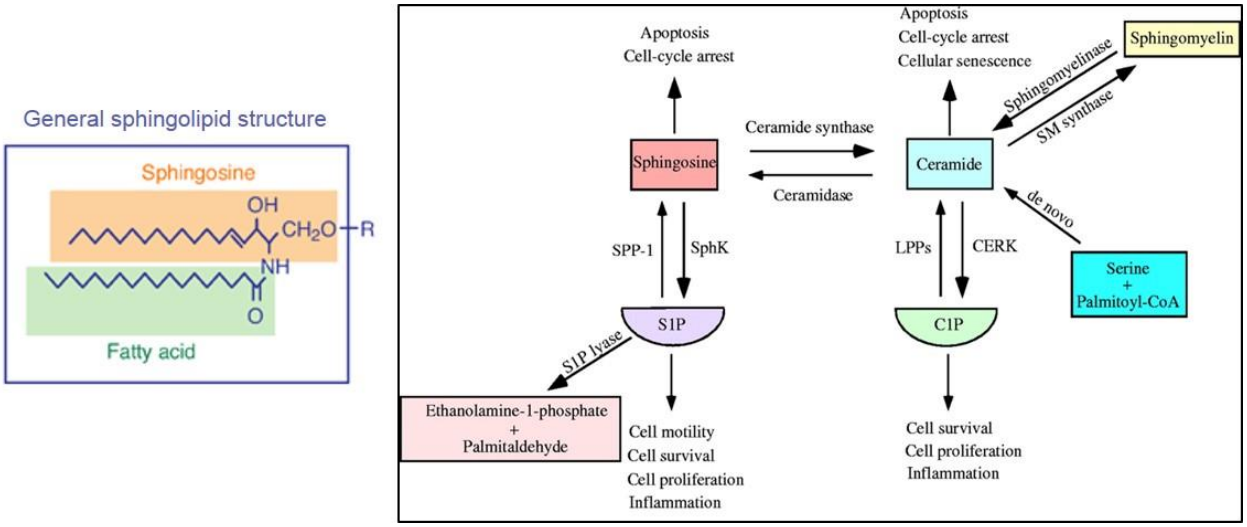


**Figure 1-2. Sphingolipid structure and metabolic pathway overview.**
http://journals.cambridge.org/fulltext_content/ERM/ERM4_28/S146239940200546Xsup004.htm (structure)
http://jcs.biologists.org/content/118/20/4605/F1.large.jpg (pathways). June 1, 2013. Used under fair use, 2013.

they are involved in a variety of cellular activities and essential functions. Ceramide and sphingosine typically induce cell growth arrest and cell death, whereas their phosphorylated forms promote cellular proliferation and survival, intracellular trafficking [62], and many other functions. The levels of these sphingolipids are tightly controlled by their metabolizing enzymes, especially those responsible for sphingosine 1-phosphate (S1P) metabolism. Sphingosine kinases (SKs) catalyze the phosphorylation of sphingosine to S1P, and exists in two forms: SK1 and SK2. SK2 has been even further into the original short SK2(S) and newly-discovered species-specific long SK2(L) isoforms [63]. Although both SKs catalyze the same biochemical reaction, they have different substrate specificities and intracellular localizations. The subcellular location of these kinases dictates their activity and the cellular response. SK1 is highly expressed in many tissues and does not seem to have a membrane-docking sequence, so it is thought to be a soluble enzyme primarily found in the cytosol [64-67]. It is activated by a variety of factors, including TNFα, IL-1β, PDGF, VEGF and S1P itself [68-71]. Upon activation, SK1 is translocated to the plasma membrane where it catalyzes SO phosphorylation [72]. SK2 is expressed at lower levels than SK1, and is mostly found in the nucleus and cytoplasm. Exact location has been found to be cell type and condition dependent [67]. Sphingosine 1-phosphate phosphatase (SPP) catalyzes the reversal of this reaction to cleave the phosphate group from S1P, returning it to sphingosine. Finally, sphingosine 1-phosphate lyase (SPL) catalyzes the degradation of S1P into its metabolites, ethanolamine phosphate and hexadecenal [73].

**Sphingosine 1-phosphate signaling**

Over the past twenty years, interest in sphingosine 1-phosphate signaling has grown exponentially because of its complexity and therapeutic potential in inflammatory disease. S1P

acts in two distinct manners: as an agonist for five extracellular S1P receptors ($S1P_{1-5}$), and as an intracellular second messenger. Therefore, after sphingosine is phosphorylated by SKs within the cell, the resulting S1P is either shuttled out to act in an autocrine or paracrine fashion on S1P receptors, or remains intracellular to signal from within [74].

$S1P_{1-5}$ are high-affinity G-protein-coupled receptors that are expressed on numerous cell types, of both hematopoietic and non-hematopoietic origins. Through the use of the promiscuous S1P receptor pro-drugs FTY720 and AAL-R, extracellular S1P signaling has been described *in vivo*. The S1P-S1P receptor axis controls the migration and trafficking of immune cells such as T and B lymphocytes, natural killer T cells, macrophages, neutrophils and dendritic cells using a S1P gradient [43, 75, 76]. Platelets secrete large amounts of S1P, and thus the blood contains a high concentration of S1P (1-3μM) compared to lymph and tissues (100nM). While in circulation, $S1P_1$ on migrating T lymphocytes is internalized due to these high levels, but re-expressed upon entering secondary lymphoid tissue under steady state conditions. It is at this point when S1P-based

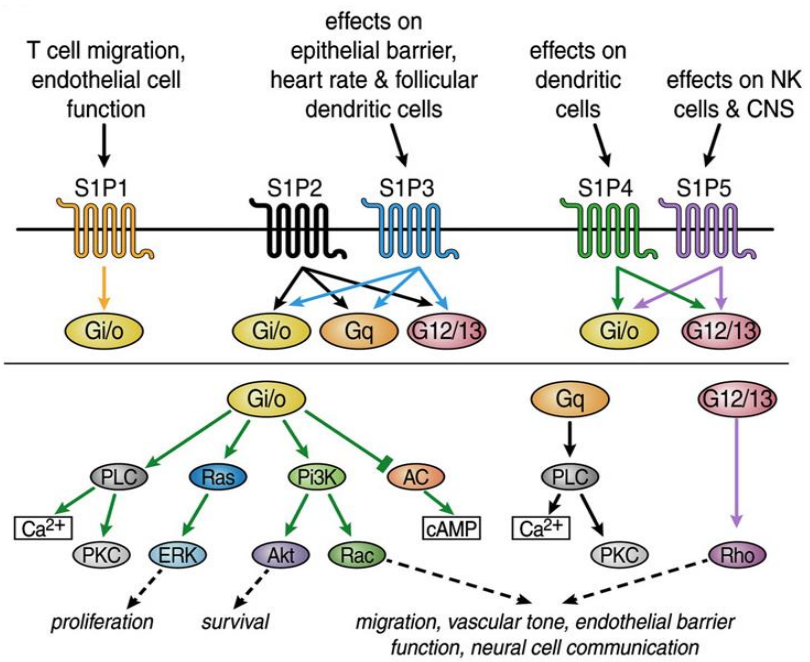


**Figure 1-3. S1P receptor signaling cascade.** (Oldstone et al., 2013 [77]) Used under fair use, 2013.

therapies can be utilized to bind and internalize $S1P_1$ to prevent T cell exit and migration to sites of inflammation [75]. In addition, $S1P_{3,4}$ have also been implicated in DC migration, indirectly through activation of Rac [78], and $S1P_5$ with egress of NKT cells from lymph nodes and bone marrow (Fig 1-3) [77, 79].

Intracellular S1P signaling has also been linked to the modulation of cytokines levels associated with inflammatory diseases. TNF signaling is known to activate SK1 and cause its translocation to the plasma membrane [80, 81]. The resulting S1P generated by SK1 is exported out of the cell to act in an autocrine manner. It is thought that this signaling pathway may enhance certain TNF functions, such as nitric oxide synthase (NOS) expression and enhancement of endothelial microvascular tone. Furthermore, S1P receptor-independent intracellular S1P signaling can even activate the key transcription factor activate NF-κB, causing an upregulation in the expression of select set of genes [82].

In order to achieve the immunomodulating effects of sphingosine 1-phosphate, many utilize synthetic sphingosine analogs. These particular sphingosine analogs are abundant and varied in structure, but they all share the property of $S1P_1$ agonism without the potential to be degraded to S1P metabolites or N-acylated to ceramide. Here, we discuss two unique sphingosine analogs: AAL-R and FTY720. Many studies with AAL-R, and a few with FTY720, have shown great therapeutic potential in the treatment and alleviation of cytokine storm associated with lethal influenza viral infection.

**Sphingosine analogs as immunosuppressive therapeutics**

*AAL-R*: (R)-2-amino-4-(4-heptyloxyphenyl)-2-methylbutanol; AAL-R was synthesized as a FTY720 analog that is more readily phosphorylated *in vivo* by SK2 due to the removal of the C2

hydroxyl group [83]. Phosphorylation converts AAL-R to (*R*)-2-amino-4-(4-(heptyloxy) phenyl)-2-methylbutyl dihydrogen phosphate (AFD-R). AFD-R either remains in the cell and induces apoptosis after significant accumulation, or is secreted from the cell to act on $S1P_{1,3-5}$. AAL-S, a chiral enantiomer of AAL-R, cannot be phosphorylated, thus it is used as a control for discerning phosphorylation-dependent activity [84, 85].

In 2008, Oldstone et al. first published their findings that demonstrated the protective effects of locally-administered AAL-R therapy against lethal influenza A viral infection. They observed a marked reduction in influenza-specific CD8+ T cells, as well as some of the major pro-inflammatory cytokines (IL-6, CCL2, IL-1β and TNFα) in the lungs at 6 days post viral infection. Furthermore, the DC population in the lungs was not reduced, but DC accumulation in the mediastinal lymph node was inhibited. Importantly, these immunosuppressive effects were only achieved with local (intratracheal), but not systemic (intraperitoneal) administration of AAL-R, and not AAL-S [85]. Subsequent studies revealed that the dampening of influenza-specific T cell accumulation did not prevent the production of anti-influenza neutralizing antibodies that are crucial to a protective memory response. Interestingly, AAL-R impaired the antigen-presenting capacity of pulmonary DCs by downregulating their surface expression of MHC-I, MHC-II and B7-2, which is likely a significant cause of reduced T cell clonal expansion following viral infection [86]. As a culmination of these effects, survival rates were remarkably increased after challenge with pathogenic A/WSN/33 (H1N1), and attributed to decreased pulmonary inflammation/injury, cytokine production and cellular infiltrates [87]. Due to the fact that AAL-R is an analog of FTY720, and that FTY720 is a commercially-available, FDA-approved drug use in multiple sclerosis treatment [88], we decided to repurpose FTY720 in our animal and cell culture studies.

*FTY720 (Fingolimod):* (2-amino-2-(2-[4-octylphenyl]ethyl)-1,3- propanediol) was first synthesized in 1992 from myriocin (ISP-1), a metabolite of the fungus *Isaria sinclairii* with potent immunosuppressive properties, in efforts to minimize toxicity of the metabolite for use in allograft rejection treatment [89]. FTY720 is a pro-drug that is preferentially and rapidly phosphorylated by SK2 within the cell, converting it to its bioactive form FTY720 phosphate (FTY720-P). FTY720-P can then bind and activate downstream signaling events through $S1P_{1,3-5}$ with even higher affinity than S1P [89]. At therapeutically relevant levels, FTY720-P induces lymphopenia *in vivo* by sequestering mature T and B lymphocytes the thymus and secondary lymphoid organs. Lymphocytes are prevented from migrating out of the lymph nodes because of $S1P_1$ internalization caused by FTY720-P binding. Notably, this property does not impair antigen-driven T- and B-cell activation and proliferation necessary for both innate and adaptive immunity [90, 91]. In October of 2010, Novartis released FTY720 commercially as Gilenya® (Fingolimod) for use as treatment for multiple sclerosis (MS) in humans due to its effectiveness against autoimmune diseases and ability to cross the blood-brain barrier. It is the first oral MS treatment, and has the potential to promote both neuroprotection and neurorepair via direct interaction with receptors on neurons and glia [92-94].

The targets and mechanisms of FTY720 immunomodulation are varied, complex and are not yet fully understood. This analog has many molecular targets, some of which are independent of its phosphorylated biologically active form, FTY720-P (Fig 1-4). For this reason, FTY720 is an appealing candidate for therapeutic treatment of other inflammatory diseases such as diabetes, arthritis, atherosclerosis, asthma, and cardiac/cerebral ischemia injuries. Pitman et al. (2012) described these novel cellular "off-targets" in their thorough review of FTY720 studies in the literature [95]. Like AAL-R, when FTY720 is given at high concentration, it induces apoptotic

cell death via caspase activation and Bcl-2 overexpression [96], which makes it a potential cancer treatment. However, this dosage is 5-10 time greater than that in MS treatment and is associated with adverse side effects. Phosphorylation-independent activity of FTY720 is even more diverse and is elusive as far as the full impact of these actions. Briefly, non-phosphorylated FTY720 has been implicated in the activation of protein phosphatase 2A (PP2A), a tumor-suppressor that is downregulated in numerous cancers [97]. Additionally, FTY720, but not FTY720-P, has inhibitory effects on the sphingolipid-metabolizing enzymes ceramide synthase (CerS), sphingosine kinase 1 (SK1) and sphingosine 1-phosphate lyase (SPL). CerS dampening is thought to be attributed to acyl-CoA chain length and allosteric inhibition [98], SK1 diminished activity due to competitive inhibition with sphingosine [99], but the SPL inhibitory mechanism still remains unclear [100]. There are several other interesting targets outlined by Pitman et al. (Fig 1-4) in addition to those mentioned here [95].

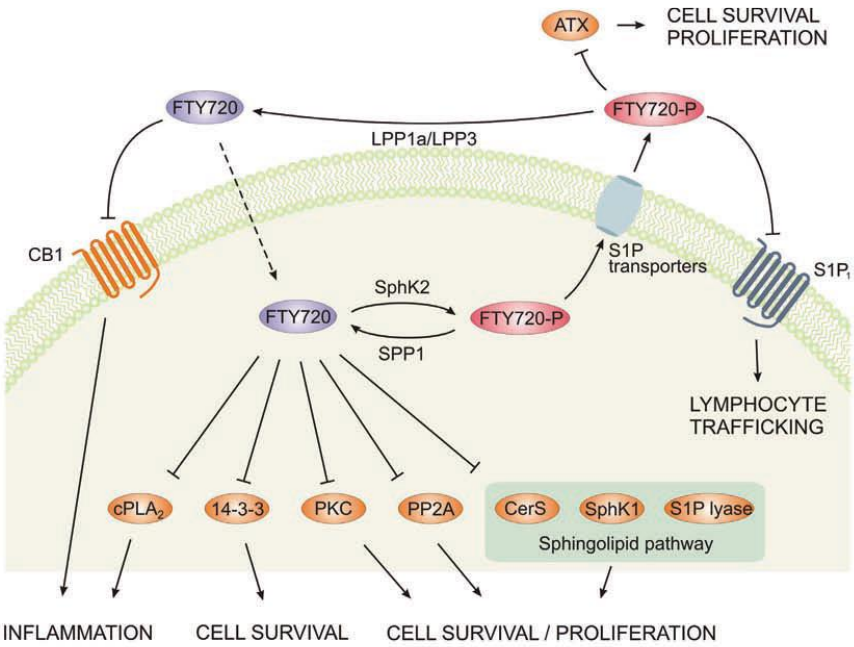


**Figure 1-4. Cellular targets of FTY720 and FTY720-P.** (Pitman et al, 2012 [95])

There have been limited studies reporting the efficacy of FTY720 in immunosuppression and protection during influenza A viral infections, all of which focus exclusively on the cytokine storm elicited by highly pathogenic IAV. However, because of the evident success of FTY720-analog AAL-R therapy and the comparable hallmarks of cytokine storm in our polymicrobial infection model, we believe that this immune-modulating drug will also be effective in synergistic disease alleviation.

**Enigmol**

Enigmol ((2S,3S,5S)-2-amino-3,5-dihydroxyoctadecane) is a novel sphingosine analog that was synthesized for use in cancer treatment [101]. Unlike AAL-R and FTY720, Enigmol cannot be phosphorylated to act in a S1P-like manner. Furthermore, its conversion to ceramide is negligible due to inefficient N-acylation by ceramide synthase. Together, these qualities result in a highly stable, and thus potent, sphingosine analog. Sphingosine and ceramide are favorable targets for cancer control because of their inhibition of cell growth and promotion of apoptosis [102]. These effects are achieved only when the compounds accumulate to high intracellular concentrations. When administered in large doses, Enigmol is indeed an effective anti-cancer drug. Given systemically to mice, Enigmol was able to suppress prostate cancer tumor growth without signs of host toxicity. Enigmol has also been implicated in immunomodulation and may share a number of off-targets with FTY720 at lower doses, but these properties have yet to be elucidated [101].

**Specific Aims**

**Specific Aim 1: Characterize influenza A:*Streptococcus pneumoniae* synergistic disease in aged mice.** *Working hypothesis*: Aged Balb/c mice (18 months) will be more susceptible to single influenza or *Streptococcus pneumoniae* infections than young mice. Aged mice will also be vulnerable to secondary bacterial infection for an extended period of time following primary viral infection.

**Specific Aim 2: Evaluate the impact of systemic sphingosine analog therapy on the lung microenvironment.** *Working hypothesis*: Treating mice with sphingosine analogs immediately following an influenza A viral infection will alleviate disease complications associated with secondary bacterial infection by diminishing the pro-inflammatory response.

**Specific Aim 3: Define the cell type-specific effects of sphingolipid treatment during influenza A viral infection.** *Working hypothesis*: Treatment with S1P and FTY720 will suppress the expression of pro-inflammatory mediators in A549 and MH-S cells following high dose influenza A challenge. Treatment with sphingosine kinase inhibitors SK1i, SK2i and DMS will dampen pro-inflammatory mediator expression in MH-S and A549 cells, as well as decrease viral loads in A549 and MDCK cells.

## Chapter Two

Characterization of influenza A:*Streptococcus pneumoniae* synergistic disease in aged mice

**Abstract**

Seasonal influenza A viral infection typically results in a self-limiting upper respiratory tract infection with mild symptoms of sore throat, fever, head and muscle aches, and lethargy. Complications arise when the host encounters a secondary bacterial challenge, typically *S. pneumoniae* or *S. aureus*. Studies show that the host is susceptible to secondary infection even after recovery from the initial flu infection. The lethality of this synergistic disease still remains to be fully elucidated. Our lab has been able to model and characterize this disease pathology in young (6-8 weeks) Balb/c mice, as previously reported [55]. The elderly (> 65 years) are a population at greater risk for morbidity and mortality due to viral:bacterial dual infection. Due to inefficient vaccination strategies for the aged, immunosenescence and longer recovery time following influenza infection, they may be vulnerable to secondary bacterial infection for an extended period of time [103]. We hypothesized that aged Balb/c mice (18 months) would be more susceptible to single influenza or *Streptococcus pneumoniae* infections than young mice. In addition, vulnerability to secondary bacterial infection would be extended in aged mice following primary viral infection. We found that aged mice had greater weight loss following low-dose influenza A viral infection and a pro-longed recovery period. At 21 days post-viral infection, 100% of 18m Balb/c mice succumbed to secondary pneumococcal infection. Lethality was accompanied by rapid and extreme weight loss, sepsis, enhanced pathology and bacterial loads in the lungs. Real-time PCR and Bioplex cytokine array analysis revealed synergistic upregulation of both gene and protein expression of cytokines and chemokines associated with detrimental cytokine storm. Therefore, we concluded that aged mice develop more severe disease from single mild influenza and pneumococcal infection and that susceptibility to bacterial superinfection is sustained for a longer period of time.

## Methods and Materials

### Cell culture and virus propagation

Madin-Darbin canine kidney (MDCK) cells were grown and maintained in Dulbecco's modified Eagle's medium (DMEM; Mediatech) supplemented with 10% fetal bovine serum (Atlanta Biologicals) and penicillin/streptomycin (100U/100ug per ml). Stocks of influenza A/Udorn/72 (H3N2) virus, a filamentous laboratory-adapted human clinical isolate, were prepared in MDCK cells. Briefly, cells were infected with influenza A/Udorn/72 (H3N2) at a low multiplicity of infection (0.001) for 1 h. Following virus adsorption, DMEM supplemented with 2ug/ml TPCK-treated trypsin (Sigma) was added to the cells, and virus was allowed to replicate for 48h at 37°C, 5% $CO_2$. Supernatants were collected and pre-cleared by centrifugation at 3000rpm for 10 min. Virus titer was determined using a tissue culture infectious dose (TCID) assay, which determines the dose required to cause cytopathic effect in 50% of the cells [104].

### Bacterium propagation and bacterial load assays

*Streptococcus pneumoniae,* serotype 3 (ATCC 6303) was grown in brain heart infusion broth to mid-logarithmic phase as determined by $OD_{600}$ measurement. The culture was diluted to $1x10^4$ CFU/50µl in sterile PBS-/- for mouse inoculation. The titer was confirmed by plating in triplicate on blood agar plates (trypticase soy agar plates supplemented with 5% defibrinated sheep's blood; BBL Inc). Aliquots of tissue homogenate were serially diluted, and 100µl of selected dilutions were plated in duplicate onto blood agar plates. Plates were incubated for 18-24 hours at 37˚C in 5% $CO_2$. Colonies were counted on plates within the 30-300 CFU range, and multiplied by 10 to obtain CFU/ml. To calculate CFU/g lung tissue, this value was then divided by the wet lung weight (in grams).

**Dual infection study in aged mice and tissue collection**

Animal experiments were performed in accordance with NIH guidelines and with approval by the Institutional Animal Care and Use Committee of Virginia Polytechnic Institute and State University. Mice were obtained from NCI, Charles River Laboratories and housed within a BSL2-approved animal facility in sterile microisolators. Aged (18 month old) female Balb/c mice were lightly anesthetized via isoflurane inhalation and intranasally infected with 50µl PBS (mock) or $1x10^4$ $TCID_{50}$ IA/Udorn/72. Lungs were collected from 3 influenza-infected mice at 3, 7, 14 and 21dpi to determine infection status. At 21 days after primary infection, mice were again anesthetized and intranasally infected with 50µl PBS (mock) or $1x10^4$ CFU *Streptococcus pneumoniae*, serotype 3 (ATCC 6303). At 2d and 4d post-secondary bacterial infection, mice were euthanized via intraperitoneal injection of a lethal dose of sodium pentobarbital (Fatal Plus). All mice were monitored and weighed daily throughout the entire study. After secondary bacterial infection, mice were monitored every 6-8 hours until end point. Mice were humanely euthanized upon reaching the pre-determined end point. Viral and bacterial doses were chosen based on preliminary studies that have shown that $1x10^4$ $TCID_{50}$ IA/Udorn/72 or $1x10^4$ CFU *Streptococcus pneumoniae* individually cause a mild and self-limiting infection with transient viremia or bacteremia.

At the time of necropsy, blood and lungs were collected from each mouse post-mortem. All tissues were kept on ice until analysis or were flash frozen. Blood was collected by retro-orbital bleeding into tubes with 100µM EDTA to prevent coagulation. Lung collection occurred in two phases. First, the chest cavity was opened and the lungs were perfused with 3-4ml PBS. The right lobes were clamped at the trachea, which was then exposed up to the neck. A small nick was made in the trachea distal to the lungs for insertion of a 26G gavage needle. The trachea was

tied off around the gavage needle, and 2ml of 10% formalin was used to inflate the left lobes. The left lobes were then removed and placed in a vial with 10% formalin, to be used for histopathologic analysis. The right lobes were removed and minced. Portions of the right lobes were weighed and placed in RNA*later* TissueProtect (Qiagen), or 2 separate microfuge tubes containing DMEM.

**Lung homogenization**

Two separate pre-weighed lung portions were homogenized in DMEM using a TissueTearor® homogenizer. For protein analysis, tissue debris was removed by centrifugation (10,000 rpm x 10 min, 4˚C). Supernatants were transferred to new microfuge tubes, flash-frozen in liquid nitrogen and stored at -80˚C until use. To determine bacterial loads in the lungs and blood, homogenates were brought up to a 1 ml volume, and the spread plate method was used (see 2.2).

**Histopathological analysis of lung sections**

Formalin-inflated lungs were embedded in paraffin, sectioned, mounted on slides and stained with hematoxylin and eosin by VMRCVM Clinical Laboratory Services. The slides were blinded to remove potential bias and evaluated by Dr. Tanya LeRoith. Lung sections were scored based on degree of peribronchiolitis, perivasculitis, interstitial inflammatory cells, and bronchiolitis/alveolitis. Each category was based on a scale of 0-4, with a score of 4 indicating maximum tissue pathology. Overall scores ranged from 0 to 16.

**RNA extraction and cDNA synthesis**

A small piece of lung (~30mg) was removed from RNA*later* TissueProtect and blotted dry on a Kim Wipe. RNA was extracted following the RNeasy Mini Kit protocol. Briefly, lung tissue was homogenized in 600µl RLT lysis buffer. Tissue debris was pelleted and supernatants were transferred to a new microfuge tube. An equal volume of 70% ethanol was added to the supernatants and mixed, then transferred to a mini spin-column with collection tube to bind RNA. After DNA clean-up with RNase-free DNase I (Qiagen) and washing with RW and RPE wash buffers, RNA was eluted in 30-50µl nuclease free $dH_2O$. RNA was quantified using a NanoDrop spectrophotometer.

Complementary DNA (cDNA) was synthesized using the iScript cDNA synthesis kit from Bio-Rad. Briefly, 4ul 5x reaction mix and 1ul reverse transcriptase was added to 500ng of RNA template in 0.2ml PCR tubes. The volume was brought up to 20µl with nuclease free $dH_2O$, and samples were incubated at 42˚C in a water bath for 30 minutes. The reverse transcriptase was deactivated by incubation at 85˚C for 5 minutes in a heat block or thermocycler. Tubes were spun down to remove condensation from lid and sides, then samples were diluted 1:10 with nuclease free $dH_2O$.

**Real-time PCR analysis**

Quantitative real-time PCR was performed according to the SensiMix™ SYBR & Fluorescein kit (Bioline) instructions. All primers used (Supplemental Table S1) were designed with a $T_m$ of 58-60˚C and 80-120 bp amplicon. Each reaction consisted of 7.5ng cDNA template, 0.5uM forward primer, 0.5uM reverse primer and 1x SensiMix™ in a total volume of 15ul. Real-time PCR analysis was conducted with the Bio-Rad iQ5 Thermal Cycler with the following

reaction conditions: 95˚C x 10 min for polymerase activation, then 45 cycles of denaturation (95˚C x 15s), annealing (60˚C x 15s), elongation (72˚C x 30s) and fluorescence acquisition. A melt curve analysis was performed at the end of cycle 45 to ensure product specificity. Relative quantification of transcripts were determined with the $2^{-\Delta\Delta Ct}$ method as previously described [105].

**Bio-Plex cytokine array**

Using a custom twelve-plex murine Bioplex array (IL-10, IL-12p40, G-CSF, CXCL1, CCL2, CCL3, TNFa, IL-12p70, IL-1b, GM-CSF, IFNg and IL-2) according to the manufacturer's protocol (Bio-Rad), cytokines and chemokines were measured in lung homogenates diluted 1:2 in DMEM.

**Statistical analysis**

Statistical analysis was conducted with Prism software (GraphPad). Difference in weight loss, gene and protein expression were analyzed with Two-way ANOVA using Dunnett's multiple comparisons test. Bacterial titers and histopathology scores were analyzed with One-way ANOVA using Dunnett's or Sidak's multiple comparisons test, as specified.

## Results

### Single IA/Udorn/72 and *Streptococcus pneumoniae* infections result in enhanced, but non-lethal disease in aged mice

As we aimed to simulate a mild seasonal flu-like disease that is typically seen in the clinical setting, we chose the filamentous influenza A/Udorn/72 viral strain at a dose of $1x10^4$ $TCID_{50}$ per mouse. In young and adult Balb/c mice, this dose of IA/Udorn allows for detectable levels of viral replication in the respiratory tract between days 2-7 post-infection, and complete viral clearance by 8dpi. Weight loss is minimal, usually reaching a maximum of -2 to -3% body weight at day 3 following influenza infection. Mice return to starting weight by day 6 with subsequent steady weight gain or maintenance on par with mock-infected mice. Some mice are asymptomatic, while others show brief signs of influenza-related illness such as ruffled fur, slight respiratory distress and lethargy between days 3-4 post-influenza. These symptoms are also resolved within 6 days of infection. Low dose of *Streptococcus pneumoniae* serotype 3 ($1x10^4$ CFU per mouse) results in a similar disease state in young and adult mice. Mild pneumococcal disease is marked by minor weight loss and a transient bacteremia in about 30% of infected mice that is cleared by day 7 [55].

Intranasal infection with $1x10^4$ $TCID_{50}$ IA/Udorn/72 resulted in comparable, but heightened disease in 18 month aged Balb/c mice. Aged mice experienced greater weight loss that was both delayed and sustained compared to young mice (Fig. 2-2A). Weight loss and influenza-associated symptoms began around day 3 following primary viral infection and peaked at day 5, with an average and significant 6% body weight reduction. Weight gain and resolution of disease signatures, specifically ruffled fur and lethargy, were much more gradual than in young mice. In fact, influenza-infected aged mice did not regain all weight lost, but remained at -2% starting body

weight until secondary infection at day 21. This suggests that aged mice undergo a prolonged recovery period that may extend to 14 days post-influenza infection or longer (indicated by dashed line in Figure 2-2A).

Single low-dose bacterial infection with *Streptococcus pneumoniae*, serotype 3 mimicked clinical parameters previously seen in young and adult mice. Of the three mice intranasally challenged with *S. pneumoniae*, only one (33%) had measurable bacteremia at 2dpi (Fig. 2-2B). Respiratory distress symptoms and weight loss were negligible and even improving at 4dpi, which suggest a complete recovery from single respiratory pneumococcal infection. However, histopathological analysis of the lungs at 2d post-bacterial challenge revealed that single *S. pneumoniae* infection did cause notable tissue damage (Fig. 2-2C, 2-3C). This enhanced tissue damage occurred regardless of prior viral infection, which differs from the insignificant pathology observed in young mice following single bacterial challenge.

**Susceptibility to viral:bacterial synergistic disease is prolonged in aged mice**

To determine susceptibility to polymicrobial infection, aged mice previously infected with influenza were superinfected with low dose *Streptococcus pneumoniae* at 21dp influenza. At this point, virus had been fully cleared and was no longer detectable within the lungs (data not shown). In 6-8 week old Balb/c mice, vulnerability to secondary bacterial infection persists until day 14 following influenza infection. The survival rate of these mice is 10%, with lethality occurring by day 4 post-secondary infection. By day 21 post-influenza, young mice are largely no longer subject to fatal synergistic disease (data not shown). However, in our aged mouse model, we still observed 100% mortality from dual infection when secondary bacterial challenge occurred at 21 days post-influenza viral infection. Signs of morbidity and mortality developed rapidly, and mice

met end-point parameters within 96 hours of secondary bacterial challenge. End point parameters were pre-determined to be 20% body weight loss, severe respiratory distress and inactivity. At 48hpi, all mice infected with *S. pneumoniae* demonstrated some degree of clinical symptoms including hunched posture, lethargy, decreased appetite, slight weight loss and ruffled fur. While mice infected with *S. pneumoniae* alone began to recover over the next 48 hours, the health of dual infection mice continued to decline to end point conditions.

**Fatal viral:bacterial disease is marked by septicemia and increased lung pathology**

In addition to substantial weight loss and clinical symptoms, dual infection was associated with significant increases in bacterial loads in the target tissues at 2 days post-*S. pneumoniae* (Fig. 2-2B). There was a 1.5 log increase in recovered *S. pneumoniae* from the lungs of previously influenza-infected mice compared to singly infected mice (6.2 $\log_{10}$ CFU/g versus 4.7 $\log_{10}$ CFU/g). An even greater difference was found in bacteria circulating in the blood (4.0 $\log_{10}$ CFU/ml versis 1.9 $\log_{10}$ CFU/ml). Whereas only one of three mice infected with *S. pneumoniae* alone had a measurable, but likely transient, bacterial load in the blood, all five superinfected mice demonstrated fatal septicemia. Gross pathology observed at the time of necropsy further supported augmented bacterial loads. Consolidation in the lungs of dually-infected mice was noticeably greater than that of single bacterial-infected mice.

Histopathology of lungs were somewhat enhanced, but not significantly when compared to single bacterial infection due to biological variability (Fig. 2-2C and 2-3). Minor local lung tissue damage was observed in both 21d post-influenza and even mock-infected mice. This is not surprising though, as other non-viral related factors including age can impact tissue integrity over time. Microscopic examination of lungs from mice 2d post-*S. pneumoniae* showed varying

degrees of peribronchiolitis and immune cell infiltration, chiefly neutrophil influx into the intra-alveolar spaces. Mice infected 21 days prior with influenza had more severe pathology and greater neutrophil invasion of the lung than those not pre-disposed by viral infection. Furthermore, several dual infection mice also exhibited pulmonary edema and hemorrhage in the lungs.

**Mild influenza A viral infection induces a sustained increase in pro-inflammatory mediator expression**

Quantitative real-time PCR analysis of influenza-infected aged mice was used to give an insight into the lung microenvironment over the course of infection (Fig. 2-4). At 3, 7, 14 and 21 days post-infection, lungs were collected and RNA was extracted from homogenized lung samples. A panel of 18 genes was evaluated for expression levels during the acute phase of infection (3dpi), upon viral clearance (7dpi) and throughout the recovery phase (14 and 21dpi). Normalized Ct values (ΔCt; Figure 2-4B) are presented in a heat map (Fig. 2-4A) to show the change in expression levels of these key mediators. In contrast to fold values ($2^{-\Delta\Delta Ct}$), the lower the ΔCt, the higher the expression of that mRNA transcript. Gene expression in the lungs at 21dp PBS (mock) was used to establish the basal levels of these cytokines in aged mice, and is represented in the top row of the heat map. Although introduction of fluid into the lungs itself causes a slight inflammatory reaction, it is typically resolved well before 21dpi. Here, we can see that the majority of these inflammatory genes are induced by influenza A virus and peak between days 3 and 7 post-infection. Several chemokines, such as CCL4, CCL5, CXCL1, CXCL2 and CXCL10 are constitutively expressed at fairly high levels in the homeostatic aged lung, but are still inducible to even higher levels after viral infection. Although virus is cleared from the lungs between days 7-10 in aged mice (determined by other studies), mRNA transcripts of many pro-inflammatory

mediators are still elevated at 14dpi. These chemokines are expressed by a wide array of activated cells to perpetuate recruitment and activation of other immune cells. Specifically, CCL3 and CCL4 chemokines are crucial during acute inflammation for bringing neutrophils to the site of inflammation [106]. While recruitment of neutrophils is important for limiting spread and clearance of the virus during early stages (2-3dpi), it becomes detrimental during the recovery phase when the lung must undergo repair and remodeling of damaged tissues. This prolonged inflammatory state may play a key role in the extended recovery phase following influenza viral infection.

**Cytokine gene expression is synergistically upregulated in superinfected mice**

Single influenza and *S. pneumoniae* respiratory infections both elicit a robust, but regulated pro-inflammatory response that is necessary for pathogen containment and elimination via direct action or recruitment of innate immune cells. Soon after initial viral infection of naïve mice, respiratory epithelial cells, resident macrophages and dendritic cells begin synthesizing and secreting these chemotactic proteins. Revisiting Figure 2-4, we see the hallmark early innate response to IA/Udorn at 3dpi. Influenza infection upregulates several CC and CXC chemokines responsible for recruiting monocytes, polymorphonuclear leukocytes (PMNs) and T lymphocytes. Expression of these mRNA transcripts continues to increase until at least day 7, but then begins to wane, essentially returning to basal levels by 21dpi. Similarly, *S. pneumoniae* infection of naïve mice induces moderate upregulation of many of the same cytokine transcripts at 2dpi, especially CXCL10, CXCL11, CCL2, CCL3 and G-CSF (Fig. 2-4A).

However, in contrast to single pathogen-infected mice, superinfected mice demonstrated a synergistic upregulation, or exacerbation, of several cytokines. We have defined synergistic

upregulation as a response that is greater than the additive effect of the individual stimuli. Although only CXCL11 (~1500-fold) reaches significant levels with ANOVA, CXCL2 (120-fold), CXCL10 (100-fold), CCL2 (150-fold) and G-CSF (300-fold) are also subject to this exacerbative effect. These genes did not meet criteria for significance using Dunnett's multiple comparisons test due to the variability inherent to biological replicates. Although other tissues were not evaluated in this study, systemic spread of bacteria due to superinfection suggests that elevated levels of these chemokines would also be found at other sites, including the spleen and brain as previously published [55].

**Select cytokine protein upregulation correlates with gene upregulation**

In order to determine whether the exacerbative effect observed at the gene expression level of key inflammatory cytokines translated to elevated protein levels, we used a 12-plex Bioplex cytokine array quantify proteins in lung homogenates (Fig. 2-4B). Negligible amounts of CXCL1, CCL2, IL-12p40, TNFα and G-CSF were measured in mock-infected mice (21d PBS + 2d PBS). As CXCL1, CCL2 and TNFα are constitutively expressed at intermediate levels ($\Delta$Ct value < 8; Supplemental Table S2), control of these proteins is likely post-transcriptional. Although CCL2 gene expression has returned to basal levels by 21dp IA/Udorn, Bioplex analysis reveals that protein expression was still elevated compared to mock. This finding further supports the probability of post-transcriptional control, considering previously influenza-infected lungs express CCL2 transcripts at the same level as mock lungs, yet more CCL2 protein was detected in the former.

Corresponding with real-time PCR analysis, CCL2, CCL3 and G-CSF protein levels were elevated in the lungs at 2 days after single *S. pneumoniae* infection. CXCL1 protein was also

elevated, but only marginally at the gene expression level. Superinfection of predisposed mice caused more dramatic augmentation of protein expression, synergistically affecting CXCL1, CCL2, IL-12p40, TNFα and G-CSF proteins. Most of these proteins also displayed exacerbated mRNA transcripts. Dysregulation of these specific proteins is linked to the increased neutrophil influx as determined by histopathologic analysis of dual-infected lung tissue. CXCL1 and CCL2 chemokines are known PMN chemoattractants. Additionally, G-CSF supports proliferation and activation of recruited neutrophils that can then produce and secrete IL-12p40. TNFα is greatly versatile, as it acts as both a neutrophil chemoattractant and activator. High levels of TNFα are related septic shock, which corresponds with the fatal septicemia resulting from dual infection.

**Not all cytokines are subject to viral:bacterial exacerbation**

Although synergistic disease is derived from an aberrant inflammatory response known as cytokine storm, it is important to note that not all cytokines are involved in this exacerbated response. Figure 2-5C illustrates numerous chemokines and cytokines that are induced equally by *S. pneumoniae* infection, regardless of pre-disposition from previous influenza A viral infection. Lymphocyte-recruiting chemokines CXCL3, 9 and 13 are upregulated considerably by bacterial infection alone, but are not dysregulated with pre-disposing influenza infection. Interestingly, TNFα was found to be exacerbated at the protein, but not gene expression, level. Also, CCL3 gene and protein expression were elevated by *S. pneumoniae* infection, but mRNA transcript levels were decreased with a prior influenza infection. Protein levels, however, remained unaffected.

## Discussion

Our findings demonstrated that aged Balb/c mice, like young mice, are subject to the lethal synergistic influenza:*Streptococcus pneumoniae* dual infection. This synergistic disease was marked by the dysregulated innate host immune response associated with the "cytokine storm." As hypothesized, aged mice developed more severe disease than young mice after single low-dose IA/Udorn/72 or *S. pneumoniae* respiratory infections. Enhanced influenza-induced disease was indicated by the significant and sustained weight loss after challenge, as mice lost up to 6% body weight, compared to 2-3% in young mice [55]. Aged mice did not fully regain the weight that was lost, but plateaued at a maintenance weight by 14 days post-influenza infection. However, single bacterial infection did not cause a more notable weight loss in aged, but instead elicited increased lung histopathology at 2 days post challenge. Young mice did not demonstrate this level of local tissue damage at 2dpi, unless subjected to influenza infection up to 14 days prior. In sum, aged mice were not able to recover from mild single infections at the rate in which young mice can. This extended recovery period, particularly post-influenza infection, was likely a substantial factor in the prolonged susceptibility of aged mice to secondary bacterial infection. Again, we have found that young mice no longer succumb to *S. pneumoniae* superinfection at 21d post-influenza, yet this dual infection remained fully lethal among aged mice. As all aged mice met endpoint parameters within 4 days of secondary infection, we expect that this vulnerability continues even further than 21d post-influenza infection.

These results suggest age-related changes that alter host response to single infections (immunosenescence), that causes older mice to be more vulnerable these respiratory pathogens individually. Although the causes of immunosenescence are not yet fully understood, many advances in our understanding of this phenomenon have been made over the past 5 years [107].

Until recently, the common misconception was that the immune response diminished to an overall hypo-responsive state over time. Yet, now research has shown that some responses, such as CD8+ T cell function [108], are not altered or are actually enhanced (macrophage cytokine production) with age [109]. The robust pro-inflammatory response that we observed over the course of low-dose influenza infection, and at 2d post-bacterial infection both indicate that the greater disease state resulting from these challenges are not a consequence of a dulling of the immune response in the aged.

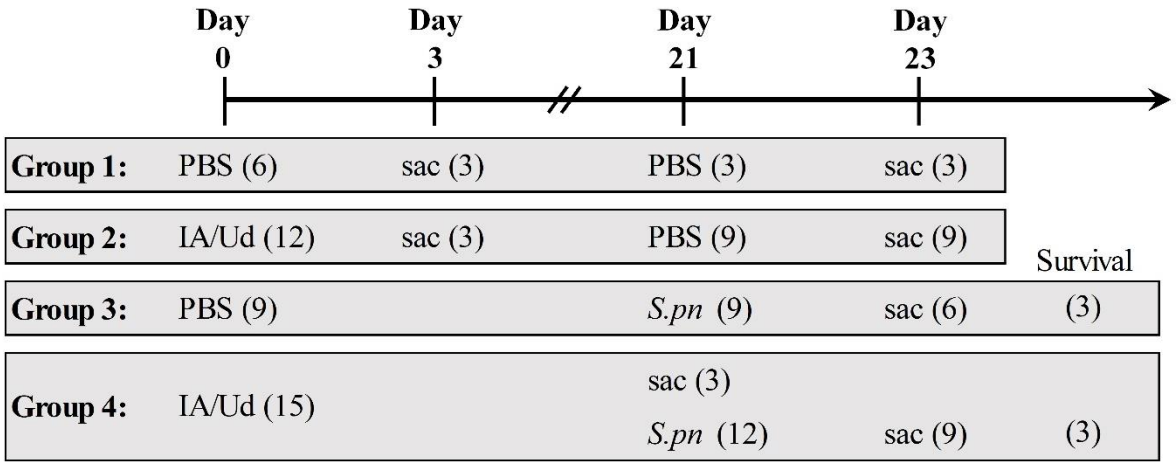


**Figure 2-1. Experimental schematic for inducing and evaluating viral:bacterial synergistic disease in aged mice.** Aged (18m) female Balb/c mice were infected with influenza (IA/Ud) or *S. pneumoniae* (*S.pn*) on days 0 and 21 as shown in the schematic. Mice were anesthetized via isoflurane inhalation and intranasally inoculated with PBS (mock) or specified agent in 50uL PBS. Doses were $1x10^4$ $TCID_{50}$ IA/Udorn/72 and $1x10^4$ CFU *S. pneumoniae* per mouse. Mice were weighed and monitored daily for the duration of the experiment. On days that mice were sacrificed (sac) and necropsied, whole blood and lungs were collected for analysis. Three mice in Groups 3 and 4 were monitored for survival after secondary infection on day 21 and euthanized at a pre-determined endpoint. Numbers in parentheses indicate the number of mice.

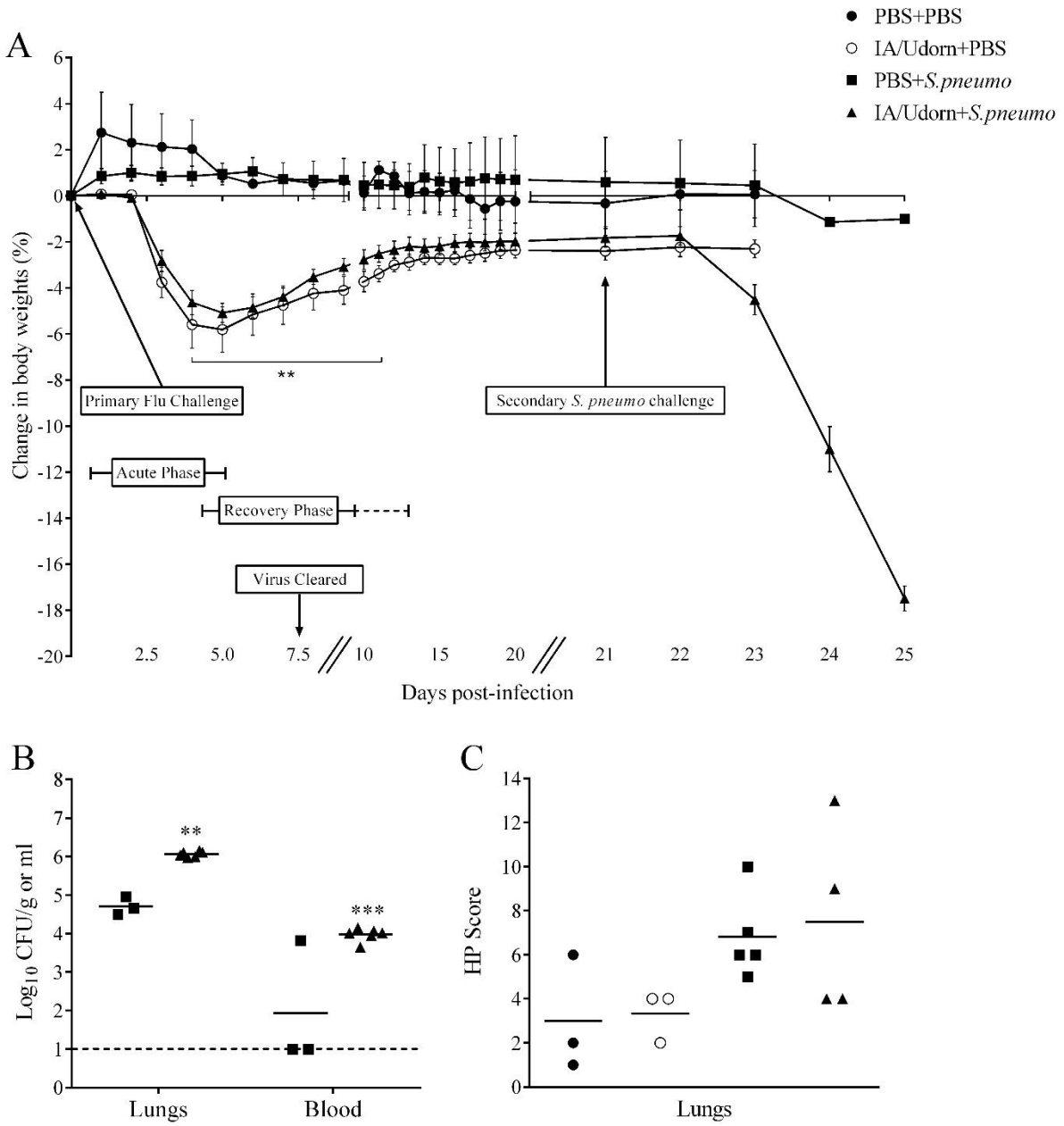


**Figure 2-2. Clinical symptoms of viral:bacterial synergistic disease in aged mice.** Weights from each mouse were recorded on a daily basis following primary infection (day 0) through the end of the study (day 25). Change in percentage of starting weight was calculated for each mouse and plotted (A). Bacterial loads were measured in the lungs and blood of mice 2 days after *S.pneumoniae* secondary challenge and reported as $\log_{10}$ colony-forming unit (CFU) per gram of lung tissue or milliliter of blood (B). Local pulmonary tissue damage was evaluated by histopathology scores of lung sections from mice superinfected at day 21 post-virus infection (C). ANOVA, Dunnett's (A) or Sidak's (B,C) multiple comparisons test (** $p < 0.01$, *** $p < 0.005$). Dashed line (- - -) indicates the bacterial load assay detection limit.

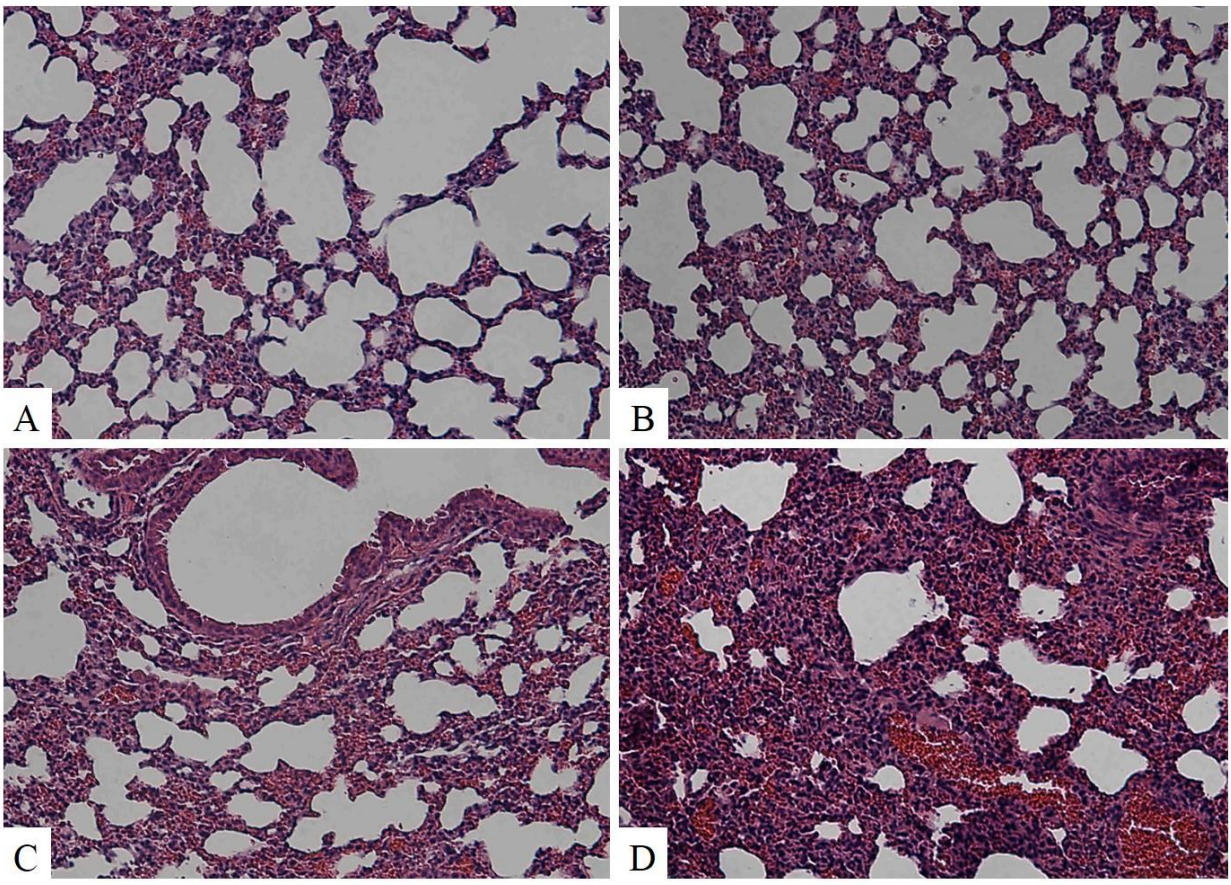


**Figure 2-3. Histopathology of lungs recovered from mock and infected mice.** H&E-stained sections of the left lung lobes from mice 21dp mock (A), 21dp IA/Udorn (B), 2dp *S. pneumoniae* (C), and 21dp IA/Udorn + 2d *S. pneumoniae* dual infection (D) are shown here. The lungs of mock and influenza-infected mice demonstrated normal, unremarkable pathology. Histopathology of lungs 2dp single bacterial infection ranged from mild to moderate, while that of dually-infected lungs ranged from moderate to acute. Both sets of lungs exhibited degrees of peribronchiolitis and immune cell infiltration with greater severity in dual infection lungs. Lungs of dual infection mice also exhibited pulmonary edema and hemorrhage. Magnification, x200.

A

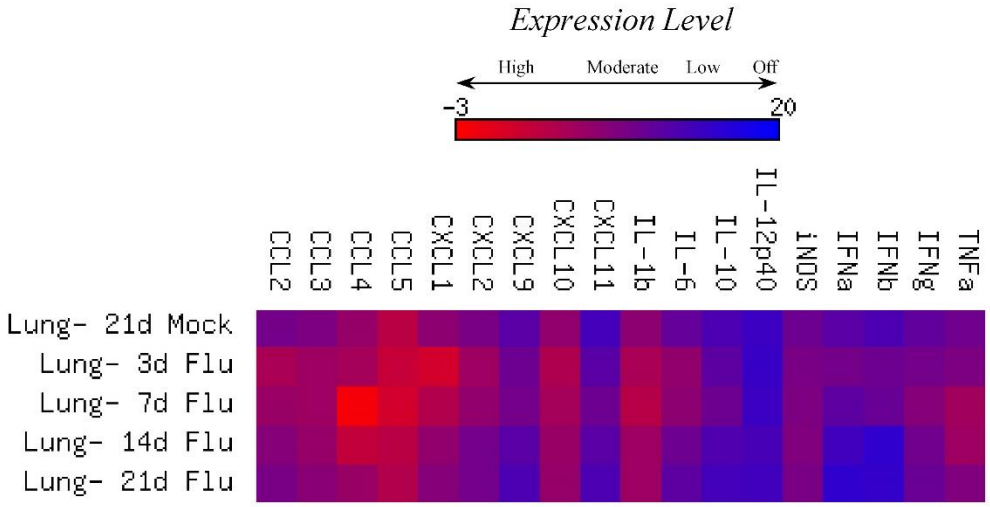


B

| | CCL2 | CCL3 | CCL4 | CCL5 | CXCL1 | CXCL2 |
|---|---|---|---|---|---|---|
| Lung- 21d Mock | 9.52 (0.66) | 8.69 (0.38) | 6.5 (0.15) | 3.31 (0.22) | 7.13 (0.99) | 8.89 (0.94) |
| Lung- 3d Flu | 4.55 (0.36) | 5.65 (0.21) | 5.18 (1.84) | 2.33 (0.30) | 1.17 (1.17) | 5.98 (0.32) |
| Lung- 7d Flu | 6.02 (0.27) | 5.96 (1.02) | -2.16 (0.95) | 1.28 (0.56) | 4.00 (0.57) | 7.05 (0.49) |
| Lung- 14d Flu | 7.96 (0.67) | 6.55 (0.81) | 2.55 (1.11) | 3.18 (0.88) | 6.80 (0.70) | 9.33 (0.35) |
| Lung- 21d Flu | 9.12 (0.27) | 7.60 (0.15) | 6.01 (0.33) | 4.02 (1.08) | 7.87 (0.56) | 9.29 (0.57) |

| | CXCL9 | CXCL10 | CXCL11 | IL-1β | IL-6 | IL-10 |
|---|---|---|---|---|---|---|
| Lung- 21d Mock | 12.05 (2.12) | 6.72 (1.15) | 13.87 (1.64) | 7.35 (0.39) | 10.88 (0.69) | 13.01 (0.60) |
| Lung- 3d Flu | 10.23 (0.42) | 4.22 (0.54) | 11.80 (0.83) | 4.88 (0.48) | 6.86 (0.26) | 11.46 (0.4) |
| Lung- 7d Flu | 9.33 (0.98) | 5.10 (0.66) | 9.99 (0.55) | 3.57 (0.48) | 7.26 (0.13) | 10.08 (0.34) |
| Lung- 14d Flu | 12.01 (0.62) | 6.06 (0.30) | 11.90 (0.68) | 5.94 (0.15) | 10.02 (0.33) | 12.49 (0.58) |
| Lung- 21d Flu | 13.1 (1.93) | 6.68 (0.10) | 12.89 (0.80) | 5.66 (0.24) | 11.71 (0.28) | 13.89 (0.31) |

| | IL-12p40 | iNOS | IFNα | IFNβ | IFNγ | TNFα |
|---|---|---|---|---|---|---|
| Lung- 21d Mock | 14.6 (0.53) | 10.24 (0.57) | 11.81 (2.35) | 12.85 (0.54) | 11.34 (0.21) | 9.78 (0.63) |
| Lung- 3d Flu | 14.86 (0.80) | 8.93 (0.53) | 9.55 (1.14) | 10.20 (0.85) | 9.48 (0.55) | 8.55 (0.37) |
| Lung- 7d Flu | 14.36 (0.74) | 8.62 (0.28) | 11.62 (1.54) | 10.30 (1.01) | 8.04 (0.36) | 5.41 (0.95) |
| Lung- 14d Flu | 13.25 (0.31) | 8.21 (0.48) | 14.09 (1.02) | 15.65 (0.77) | 9.83 (0.36) | 5.82 (1.00) |
| Lung- 21d Flu | 13.92 (0.89) | 9.09 (0.45) | 15.46 (1.28) | 15.12 (0.69) | 10.53 (0.12) | 8.20 (1.14) |

**Table 2-1. Gene expression over the course of a mild influenza A viral infection in aged mice.** Aged (18m) female Balb/c mice were intranasally inoculated with $1x10^4$ $TCID_{50}$ IA/Udorn/72 or PBS (mock). At 3, 7, 14 and 21 dpi, mice were sacrificed and lungs were collected. RNA was isolated from the lung tissue, and mRNA levels were quantified using real-time PCR. All Ct values were normalized to L19, a murine house-keeping gene, to obtain a ΔCt value. A heat map (A) was generated from these ΔCt values (B), shown here as ΔCt (±SEM).

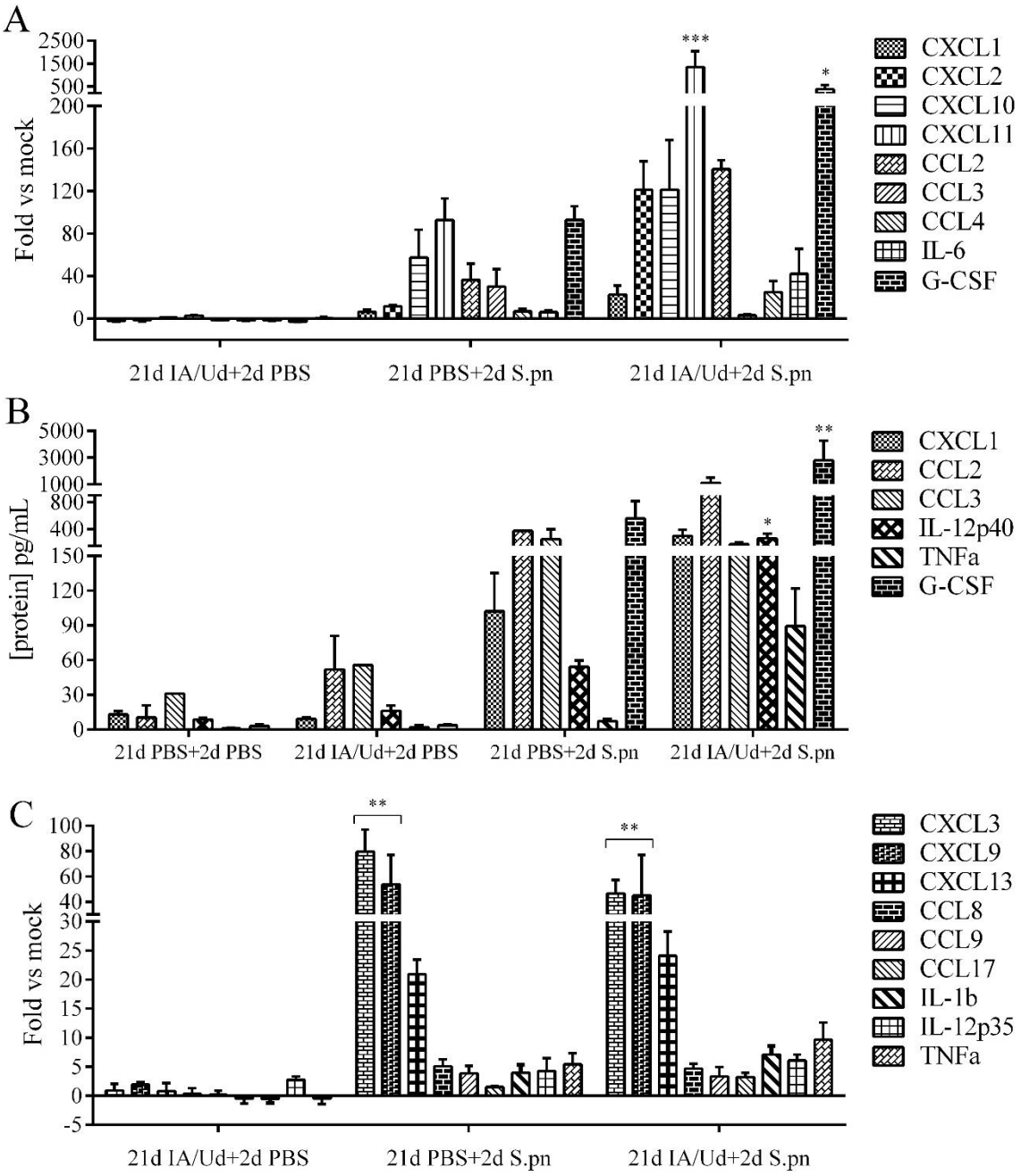


**Figure 2-4. Gene and protein expression following viral:bacterial dual infection at 21dp IA/Udorn infection.** Cytokine mRNA expression levels (A,C) and protein expression (B) were evaluated in the lungs of mice superinfected with *S. pneumoniae* at 21 days post virus infection. RNA was isolated from the lung tissue 2 days after secondary infection, and mRNA levels of were measured using real-time PCR. Values are expressed as fold change over mock infection (21d PBS+2d PBS) after normalization to L19 mRNA. Protein expression was quantified from lung homogenates using the Bio-Plex suspension array system. Statistical analysis was used to compare viral:bacterial dual infection to single bacterial infection (A-C) and single bacterial infection to mock (C). ANOVA, Dunnett's multiple comparisons test (* $p < 0.05$, ** $p < 0.01$, *** $p < 0.005$).

## Chapter Three

Evaluate the impact of systemic sphingosine analog therapy on the lung microenvironment

**Abstract**

The host immune response to influenza A viral infection is a complex interplay between the airway epithelial cells, resident alveolar macrophages, neutrophils, NK cells, dendritic cells and T- and B-lymphocytes. Sphingosine 1-phosphate (S1P) signaling is known to influence a variety cellular functions, including inflammation and immune cell trafficking. For this reason, we wanted to evaluate the impact of the phosphorable sphingosine analog FTY720 on the lung microenvironment. FTY720 is a commercially-available, FDA-approved immunomodulator that targets extracellular S1P receptors, a multitude of diverse intracellular molecules, and induces a transient lymphopenia of the blood and spleen. FTY720 therapy during influenza infection has not been well studied, but the protective effect of its chiral analog AAL-R against HP influenza has been reported. In contrast, the novel sphingosine analog Enigmol is non-phosphorable and therefore cannot be converted to S1P. Enigmol is a highly stable compound that has demonstrated potential for anti-cancer therapy. We hypothesized that treating mice with these sphingosine analogs would alter the host lung microenvironment and inflammatory profile under homeostatic conditions or low-dose influenza A viral infection. Our results showed that systemic treatment with FTY720 and, to a lesser extent, Enigmol, altered select cytokine expression profile in the lungs at 2 days post-challenge. There was a trend towards upregulation of pro-inflammatory cytokines such as CCL2, IL-6, CXCL10 and TNFα. FTY720 treatment induced a clear lymphopenic state in the blood and lungs at 2d post-treatment that was resolved by day 7. Interestingly, FTY720 treatment alone mimicked a mild influenza infection regarding and efflux of macrophages and influx of PMNs at 2dpi, but suppressed the influenza-induced sustained PMN presence at 7dpi. Enigmol had little effect on pulmonary immune cell composition, with the exception of an increase in PMNs and slight decrease in macrophages on day 5 of treatment. Our

findings indicate that systemic FTY720 treatment alone and during influenza infection does modulate the immune response and cell recruitment. These immunomodulatory properties are function of its phosphorylation and specific intracellular targets, but not necessarily sphingosine signaling. However, its ability to confer protection against the cytokine storm elicited by secondary bacterial infection requires further investigation.

## Methods and Materials

### Cell culture and virus propagation

Madin-Darby canine kidney (MDCK) cells were grown and maintained in Dulbecco's modified Eagle's medium (DMEM; Mediatech) supplemented with 10% fetal bovine serum (Atlanta Biologicals) and penicillin/streptomycin (100U/100μg per ml). Stocks of influenza A/Udorn/72 (H3N2) virus, a laboratory-adapted human clinical isolate, were prepared in MDCK cells. Briefly, cells were infected with influenza A/Udorn/72 (H3N2) at a low multiplicity of infection (0.001) for 1 h. Following virus adsorption, DMEM supplemented with 2ug/ml TPCK-treated trypsin (Sigma) was added to the cells, and virus was allowed to replicate for 48h at 37°C, 5% $CO_2$. Supernatants were collected and pre-cleared by centrifugation at 3000rpm for 10 min.

### Virus titration and viral loads

Virus titer was determined using the previously described Reed-Muench 50% tissue culture infectious dose ($TCID_{50}$) assay in a 96-well TC plate format. In short, serial 10-fold dilutions of virus stock or pre-cleared lung homogenates were incubated with MDCK cells for 1 hour (37˚C, 5% $CO_2$) to allow for virus adsorption. Inoculum was aspirated from cells, which were then incubated with 2μg/ml TPCK-treated trypsin in DMEM for 72 hours (37˚C, 5% $CO_2$). Cytopathic effect was recorded and used to calculate titers, expressed in $TCID_{50}$/ml.

### Sphingosine and sphingosine analogs: preparation and doses

FTY720·HCl (2-amino-2-[2-(4-octylphenyl)ethyl]-1,3-propanediol, hydrochloride; Cayman Chemical), D-erythro-sphingosine ((2S,3R,4E)-2-amino-4-octadecene-1,3-diol; Avanti Polar Lipids, Inc.) and Enigmol ((2S,3S,5S)-2-aminooctadecane-3,5-diol; generously donated by

A.H. Merrill at Emory University) were used as systemic treatments in the reported mouse studies. FTY720 was prepared at a stock concentration of 100mg/ml in dimethylsulfoxide (DMSO). Sphingosine and Enigmol had previously been prepared in a 1:1 molar complex with fatty-acid free bovine serum albumin (FAF-BSA; Calbiochem). All stocks were diluted to working concentration in 200µl sterile water for intraperitoneal injection. Based on efficacy and toxicity studies, the systemic doses used were 100µg/kg FTY720, 0.5mg/kg sphingosine or 0.5mg/kg Enigmol. Vehicle used for FTY720 studies was 0.03% DMSO in sterile water, which is well below toxicity. The vehicle used for sphingosine and Enigmol study was 0.25% FAF-BSA in sterile water.

**FTY720 treatment of influenza-infected mice**

Animal experiments were performed in accordance with NIH guidelines and with approval by the Institutional Animal Care and Use Committee of the Virginia Polytechnic Institute and State University. Mice were obtained from NCI, Charles River Laboratories and housed within a BSL2 facility in sterile microisolators. In two separate studies, 12 adult female mice (3 month Balb/c; Harlan Laboratories) were divided into four groups of three mice. Mice were lightly anesthetized via isoflurane inhalation and intranasally inoculated with PBS (mock; Groups 1 and 3) or low-dose influenza A ($1x10^4$ $TCID_{50}$ IA/Udorn; Groups 2 and 4) in a 50µl inoculum volume. Four hours later mice were given a single 200µl intraperitoneal injection of vehicle (Groups 1 and 2) or 100µg/kg FTY720 (Groups 3 and 4). For the first study, we evaluated the tissues of mice at 2 days post-infection and treatment during peak influenza infection and FTY720 lymphopenic effect. In the second study, we evaluated the same tissues at 7 days post-infection and treatment.

| | | | Treatments | |
|---|---|---|---|---|
| | Graph label | n | IA/Udorn | FTY720 |
| Group 1 | PBS+Vehicle | 3 | - | - |
| Group 2 | IA/Udorn+Vehicle | 3 | + | - |
| Group 3 | PBS+FTY720 | 3 | - | + |
| Group 4 | IA/Udorn+FTY720 | 3 | + | + |

Mice were monitored and weighed daily for the duration of the experiment. On days 2 and 7 of the respective studies, mice were euthanized via lethal sodium pentobarbital i.p. injection. Whole blood was collected by cardiac puncture into EDTA-coated blood collection tubes to prevent coagulation. The chest cavity was then opened and lungs were perfused with 3-4ml PBS. All lung lobes were carefully removed, rinsed in PBS, then coarsely minced. Approximately one-third of the minced lung was placed in digestion buffer on ice (for FACS analysis). A few small pieces were placed in RNA*later* Tissue Protect (Qiagen), and the remainder was weighed then transferred to microfuge a tube with DMEM for homogenization.

**Sphingosine and Enigmol treatment**

As a follow-up to the FTY720 treatment studies, we wanted to evaluate the effects of systemic sphingosine and Enigmol, another sphingosine analog. For this study, 15 adult female mice (3 month Balb/c, Harlan Laboratories) were divided into three groups of five mice. Mice received 4 daily intraperitoneal injections of vehicle (Group 1), 0.5mg/kg sphingosine (Group 2) or 0.5mg/kg Enigmol (Group 3) in a 200µl volume. On the fifth day, mice were euthanized and lungs were collected as above.

**Lung homogenization**

Pre-weighed lung portions were homogenized in DMEM immediately after collection using a TissueTearor® homogenizer. Tissue debris was removed by centrifugation (10,000 rpm

x 10 min, 4˚C). Supernatants were transferred to new microfuge tubes, and the volume was brought up to 1ml with DMEM. Half (500µl) of the diluted supernatant was transferred to another microfuge tube. One tube was designated for viral load titration, and the other for protein analysis. All tubes were flash-frozen in liquid nitrogen and stored at -80˚C until use.

**Enzymatic lung digestion**

To obtain a single cell suspension from harvested lung tissue, lungs were digested using the method previously described [110]. In short, lungs were finely minced in enzymatic digestion buffer: 1.8mg/ml Collagenase type 4 (Worthington Biochemical), 0.1mg/ml DNaseI (Invitrogen), 10% FBS in GKN buffer (137mM NaCl, 5mM KCl, 25 mM $Na_2HPO_4$, 5.5 mM $NaH_2PO_4 \cdot 2H_2O$, 11 mM D-(+)-glucose, pH 7.4). Lung suspension was transferred to sterile 14ml culture tubes with caps and incubated at 37˚C for 30 minutes in a shaking incubator. Samples were passed through a 20G needle several times, and filtered first through a 40 micron and then 20 micron cell strainer. Red blood cells were removed by incubation with RBC lysis buffer (155 mM $NH_4Cl$, 12 mM $NaHCO_3$, 0.1 mM EDTA in sterile $dH_2O$) for 5 minutes on ice. Cells were pelleted (1300rpm x 5 min, 4˚C) and resuspended in cold flow buffer (2% BSA in PBS deficient).

**FACS analysis**

Cells were incubated for 10 minutes at 4°C with rat anti-mouse CD16/32 (BD Pharmingen) diluted to 1 µg per million cells in flow buffer (FB). The following antibodies were used at pre-determined dilutions in FB in various experiments in differing combinations, depending on cell type analyzed: CD45-FITC, CD45-APC-af780, CD3-V500, CD4-PE-Cy7, CD8a-ACP-H7, CD19-ef450, CD19-APC, B220-APC-af780, CD11b-V500, CD11b-APC, CD11c-PE-Cy7,

SiglecF-PE, Ly6C-PerCp-Cy5.5 and Ly6G-V450. Cells were incubated with antibodies for 20 minutes at 4°C on a rotating rack. Following incubation, cells were washed and resuspended in PBS deficient for analysis. FACS analysis was performed with BD FACSAria Cell Sorter in the VT Flow Core. Data analysis was completed using FlowJo software.

**RNA extraction and cDNA synthesis**

A small piece of lung (~30mg) was removed from RNA*later* TissueProtect and blotted dry on a Kim Wipe. RNA was extracted following the RNeasy Mini Kit protocol. Briefly, lung tissue was homogenized in 600µl RLT lysis buffer. Tissue debris was pelleted and supernatants were transferred to a new microfuge tube. An equal volume of 70% ethanol was added to the supernatants and mixed, then transferred to a mini spin-column with collection tube to bind RNA. After DNA clean-up with RNase-free DNase I (Qiagen) and washing with RW and RPE wash buffers, RNA was eluted in 30-50µl nuclease free $dH_2O$. RNA was quantified using a NanoDrop spectrophotometer.

Complementary DNA (cDNA) was synthesized using the iScript cDNA synthesis kit from Bio-Rad. Briefly, 4µl 5x reaction mix and 1µl reverse transcriptase was added to 500ng of RNA template in 0.2ml PCR tubes. The volume was brought up to 20µl with nuclease free $dH_2O$, and samples were incubated at 42˚C in a water bath for 30 minutes. The reverse transcriptase was deactivated by incubation at 85˚C for 5 minutes in a heat block or thermocycler. Tubes were spun down to remove condensation from lid and sides, then samples were diluted 1:10 with nuclease free $dH_2O$.

**Real-time PCR analysis**

Quantitative real-time PCR was performed according to the SensiMix™ SYBR & Fluorescein kit (Bioline) instructions. All primers used (Supplemental Table S1) were designed with a $T_m$ of 58-60˚C and 80-120 bp amplicon. Each reaction consisted of 7.5ng cDNA template, 0.5µM forward primer, 0.5µM reverse primer and 1x SensiMix™ in a total volume of 15µl. Real-time PCR analysis was conducted with the Bio-Rad iQ5 Thermal Cycler with the following reaction conditions: 95˚C x 10 min for polymerase activation, then 45 cycles of denaturation (95˚C x 15s), annealing (60˚C x 15s), elongation (72˚C x 30s) and fluorescence acquisition. A melt curve analysis was performed at the end of cycle 45 to ensure product specificity. Relative quantification of transcripts were determined with the $2^{-\Delta\Delta Ct}$ method as previously described [105].

**Cytometric Bead Array (CBA) Assay**

Key cytokine protein levels were measured in lung homogenates using a Mouse Inflammation CBA kit (BD) as per manufacturer's protocol. This 6-plex kit quantitated levels of IL-12p70, TNF, IFNγ, CCL-2, IL-10 and IL-6. CBA samples were acquired with BD FACSAria Cell Sorter in the VT Flow Core. Data analysis was completed using FCAP Array software.

**Statistical analysis**

Statistical analysis was conducted with Prism software (GraphPad). Difference in viral loads, gene and protein expression were analyzed with two-way ANOVA using Dunnett's multiple comparisons test or Kruskal-Wallis test for non-parametric data. FACS results were analyzed with two-way ANOVA using Tukey's multiple comparisons test.

## Results

### FTY720 treatment does not reduce viral loads or viral gene transcript levels

Following a mild influenza A viral infection, young adult Balb/c mice were mostly asymptomatic, except for slight weight loss (Fig. 3-3A). Between days 2-3 post-infection, mice lost 1-2% body weight, which was subsequently regained. Mice treated systemically with 100ug/kg FTY720 after infection lost an additional 1% body weight and regained less than non-treated mice, but this difference was insignificant.

Viral loads recovered from the lungs at 2dpi were around $1x10^6$ $TCID_{50}$ per gram of lung tissue, regardless of treatment. Virus was still detectable at 7dpi but was reduced by 3 logs, again not affected by FTY720 treatment (Fig. 3-3B). Correspondingly, real-time PCR evaluation of IA/Udorn HA mRNA transcript levels revealed ΔCt values around 2 at 2dpi that increased to 5 at 7dpi, translating to a substantial decrease in gene expression (Fig. 3-3C). There was slight consolidation of the lungs collected at 2dpi, particularly in influenza-infected mice, but no difference between FTY720-treated and non-treated.

### Systemic FTY720 marginally alters the inflammatory gene profile

As we have seen in our other studies, pro-inflammatory gene expression peaked around day 2-3 post-influenza infection in young mice. This response diminished over the next few days, but was still elevated at least until day 7 post-infection. Chemokines essential to recruiting the necessary immune cells for viral clearance were especially high at day 2, including CXCL10 and CXCL11 at significant levels; also CCL2, CCL4 and IL-6, but to a lesser extent (Fig. 3-4A). By day 7 post-infection, expression of these cytokines was reduced, but still above mock levels. CXCL10 and CXCL11 were still expressed at significantly high levels, though decreased to about

half the amount at day 2. Importantly, IL-10 was elevated at day 7 after infection. Expression of this interleukin is crucial to the recovery phase following viral clearance as it inhibits pro-inflammatory cytokine synthesis to support regeneration and repair of the respiratory tract.

FTY720 treatment alone had a marginal overall pro-inflammatory effect on gene expression in the lungs of non-infected mice (Fig. 3-4B). At 2 days post-treatment, IL-6 was expressed at a 15-fold greater level than vehicle treatment. CXCL10 and TNFα were also increased, but to a lesser extent (3-5 fold). In contrast, CCL3 was actually decreased by 4-fold in comparison to vehicle. By day 7 post-FTY720 treatment, expression levels of these transcripts had all returned to basal levels. Systemic FTY720 treatment had an even less effect on gene expression in the lungs of influenza-infected mice (Fig. 3-4C). Of the genes measured, we only found a minor increase (2-fold) in CCL2 and IL-6 at 2 days post-infection compared to non-treated infected mice. At day 7 post-infection, CCL2 was expressed 4-fold higher than non-treated, but IL-6 remained at around a 2 to 3-fold increase. Interferon levels also seemed to be affected by FTY270 treatment alone and during influenza infection, but the amount of biological variation between mice was too great to claim significance. This indicates that FTY720 treatment given at the time of infection was not able to overcome the rapid effects of influenza A virus. All real-time PCR results for the transcripts measured in these mice can be found in Supplemental Table S3, expressed as ΔCt (±SEM).

**Systemic FTY720 increases protein expression of select cytokines**

To determine if protein expression reflected the observed changes in gene expression, we ran a 6-plex cytometric bead array mouse inflammation kit to measure levels of CCL2, IL-6, TNF, IFNγ, IL-10 and IL-12p70. Although IL-10 and IL-12p70 were not measurable in any of these

samples, we did find interesting changes in the other analytes (Fig. 3-4D). CCL2, TNF, IL-6 and IFNγ were all elevated at 2 days following mild influenza infection. Influenza challenge increased CCL2 levels significantly, almost 10-fold from 300 to 2,000pg per gram of lung tissue. CCL2 remained elevated at 7dpi as well, but only 3-fold higher than mock. TNF, IL-6 and IFNγ protein levels were increased about 2-fold at day 2 after influenza. By day 7, TNF expression had essentially returned to basal levels and IL-6 was undetectable. IFNγ expression was increased further at 7 days after infection compared to mock, which did not contain measurable IFNγ protein. These findings supported the results of real-time PCR analysis shown in Figure 3-4(A-C) and Table S3.

Interestingly, FTY720 treatment had a greater effect on protein expression than what was revealed by gene expression analysis. While treatment alone marginally increased CCL2 expression only, treatment during influenza infection demonstrated a greater effect. On day 2 post-infection, influenza-induced expression of CCL2 and IL-6 was amplified 3-fold by FTY720 treatment. FTY720 also enhanced TNF and IFNγ expression during early stages of infection, but to a much lesser extent. However, these effects were generally no longer observed at day 7 post-infection as the pro-inflammatory response had diminished.

**Systemic FTY720 causes transient lymphopenia in the blood and lungs**

To ensure that systemic treatment with 100μg/kg FTY720 was in fact reaching target cells and functioning *in vivo*, we utilized the property of phosphorylated form of FTY720 (FTY720-P) to induce lymphophenia. To evaluate the lymphopenic response, blood and lung tissue collected on days 2 and 7 of these studies were analyzed by FACS (Fig. 3-5 and 3-6). Based on CD45, CD3, CD4, CD8, CD19 and B220 cell surface expression, we determined the change in T- and B-

lymphocyte populations in these tissues. At day 2 post-FTY720 treatment, there was a substantial decrease in both the T- and B-lymphocyte populations in the blood (Fig. 3-5A). Only T-, not B-, cells were decreased in the lungs at this time (Fig. 3-6A). In both tissues, total T cell population was decreased by nearly 70%. CD4+ and CD8+ T cells were reduced equally, keeping a constant 3:1 ratio. By day 7 following FTY720 administration, these changes in the T-lymphocyte populations were no longer evident as there was no difference from mock levels (Fig. 3-5B and 3-6C). However, the circulating B cell population remained diminished at 7 days post-treatment compared to vehicle control. These findings confirm that the FTY720 treatment was functional and effective in these mice. FTY720 was successfully phosphorylated intracellularly to FTY720-P, released from cells and acted upon $S1P_1$ to induce lymphopenia in the blood and lungs.

**FTY720-induced lymphopenic state is enhanced during influenza viral infection**

In the early stages of influenza viral infection, T-lymphocytes, both CD4+ and CD8+, were decreased in the blood and lungs. Influenza reduced the total T-cell population by 25-30% in each of these tissues at 2 days post-infection. This decrease was reflected proportionately in CD4+ and CD8+ T cells, maintaining the 3:1 ratio of these subsets. In contrast, B cells were increased by about 20% in the blood and lungs at day 2. FTY720 treatment given systemically 4 hours after infection either compounded or negated these effects from influenza infection alone. The T cell population was reduced to the same level as FTY720 alone in the blood (Fig. 3-5A), but was reduced even more than that of FTY720 alone in the lungs (Fig. 3-6A). Again, CD4+ and CD8+ T cell subsets were evenly depleted. Similarly, B cell numbers were decreased by FTY720 given subsequent to influenza infection to the same level as FTY720 alone, or even further reduced. However, it is important to note that this reduction was even more substantial because of the

influenza-induced increase in the B lymphocyte population. This means that FTY720 treatment was able to overcome the effects of influenza infection, even when given after intranasal challenge, indicating the rapidity of therapeutic action.

At 7dpi, influenza had caused a slight increase in T-cell numbers in both the blood (Fig. 3-5B) and lungs (3-6B), with a slight preference toward CD4+ T cells, compared to mock. FTY720 dampened this increase slightly so that the T lymphocyte populations were equal to mock. This pattern was also found in the B cell population in the lungs at 7dpi, but not the blood. Circulating B cells were significantly reduced by day 7 following influenza infection compared to mock, which was also seen in mice treated with FTY720 alone. Treatment with FTY720 after viral infection did not augment this effect.

**Influenza and FTY720 treatment independently cause efflux of macrophages and influx of PMNs in the lungs**

To determine how the cell trafficking control of FTY720-P affected other immune cells, we performed FACS analysis of infected and treated lungs to evaluate these specific populations (Fig. 3-6B,D). At 2 days post-influenza infection or FTY720 treatment, the CD11b-/CD11c+ macrophage population was decreased compared to the non-treated mock lung (Fig. 3-6B). Macrophages were decreased from 25% of the total CD45+ population to 19% with influenza infection. FTY720 had a greater effect, reducing the macrophage population to a mere 8%. By 7 days post-infection, macrophages had repopulated the lungs to around the same level as non-treated mock (Fig. 3-6D). Though not statistically significant, there were slightly more macrophages (3%) in the lungs of FTY720-treated mice than those infected with influenza at this time point. In contrast, the CD11b+/CD11c-/Ly6C+/Ly6G$^{hi}$ PMN population in the lungs was

doubled by influenza infection or FTY720 treatment independently at day 2. Interestingly, at 7dpi, the PMN population in influenza-infected mice was reduced from heightened levels at 2dpi, but remained elevated compared to FTY720-treated mice.

**FTY720 promotes resolution of PMN infiltration without altering acute-phase recruitment during influenza infection**

As noted above, FTY720 treatment alone elevated PMN levels in the lungs almost to the same extent as influenza viral infection at day 2 post-treatment or infection. When mice were treated with FTY720 4 hours following influenza infection, PMN recruitment was slightly greater, resulting in a total of 25% of all CD45+ cells. Although FTY720 treatment enhanced PMN recruitment to a degree in infected mice at 2dpi, treated mice exhibited a notable reduction in this population at 7dpi compared to non-treated mice (Fig. 3-6B,D). Though the reduction did not meet significance, FTY720 treatment caused a decrease of 10% between the PMN population at 2dpi (25%) and at 7dpi (15%). Non-treated mice only saw a 6% reduction from 24% at 2dpi to 18% at 7dpi.

**FTY720 treatment decreases the dendritic cell population in the lungs**

Dendritic cells (DCs) are another essential player in the immune response after influenza infection. Their activity as antigen-presenting cells are vital for both innate cell-mediated and adaptive immunity [111]. CFSE staining has revealed that there is a regular, albeit minor, emigration of rDCs to regional lymph nodes under homeostatic conditions that can be hastened by respiratory insults. Influenza viral infection briefly accelerates this emigration from the lungs within hours of challenge, the effect typically lasting only 24 hours. To balance efflux, the

respiratory DC population is continuously being re-established by recruitment of DC precursors from the bone marrow [112, 113].

On day 2 of these studies, the total lung CD45+ cell population from influenza-infected mice consisted of 16% DCs, whereas the lungs of FTY720 treated mice consisted only of 8% (Fig. 3-6B). Control mice revealed a norm of 12% DCs in the lungs. Assuming the normal migration of virus-activated DCs to the regional lymph nodes occurred, mild influenza infection enhanced the early-stage repopulation and recruitment of DCs by 30% compared to mock. Since influenza viral replication usually peaks around 48hpi, the greater numbers of DCs seen in the lungs are mostly enlisted for the purpose of antigen presentation and recruitment of lymphocytes. This increase was no longer found at 7dpi, and there was no difference in DC numbers between influenza-infected and mock mice. In contrast, FTY720 actually decreased the pulmonary dendritic cell population by 30% compared to vehicle control mice. The reduction was also temporary, as there was no substantial difference between DC populations by 7 days post-treatment.

**Systemic treatment with sphingosine or Enigmol has negligible effect on the normal lung microenvironment**

In order to better understand the specific effects of FTY270 treatment, we evaluated the ability of treatment with sphingosine and Enigmol, a non-phosphorable sphingosine analog, to alter the lung microenvironment under mock conditions. Daily systemic treatment with these compounds over the course of 4 days caused only slight measurable change in the cellular composition of the lungs (Fig 3-7). Both treatments marginally decreased the B-cell lymphocyte population (6-12%), but this was insignificant due to the variability among the vehicle control

mice (Fig 3-7A). However, the T lymphocyte population in the lungs was generally unaffected. This suggests that introducing exogenous sphingosine does not necessarily increase the levels of S1P just by introducing more substrate for sphingosine kinases. If the exogenous sphingosine was phosphorylated within cells, the resultant S1P did not act upon $S1P_1$ to generate a lymphopenic effect, as seen with FTY720 and S1P administration.

The remaining CD45+ immune cell population did demonstrate some minor, but notable, changes with these treatments (Fig 3-7B). With the addition of SiglecF staining, we were able to clearly discern alveolar (SiglecF+) from non-alveolar (SiglecF-) macrophages ($CD11b^-/CD11c^+$), as well as eosinophils (SiglecF+) from the general SiglecF- PMN population ($CD11b^+/CD11c^-$). FACS analysis revealed an increase in the alveolar macrophage population with treatment, especially sphingosine (~25% increase). Otherwise, sphingosine did not alter the other leukocyte populations evaluated. The effects of Enigmol treatment were slightly more notable, particularly among PMN, eosinophil and non-alveolar macrophage populations. Enigmol actually increased the PMN population by a significant 35%, and eosinophils to a lesser extent. In contrast, the non-alveolar macrophage population was decreased by 20% with Enigmol.

Cytokine gene and protein expression was generally unaffected by treatment, with the exception of the monocyte chemotactic protein CCL2 (Supplemental Table S4; Fig 3-7D). Neither sphingosine nor Enigmol induced an increase in CCL2 expression, but quantification of protein in lung homogenates exhibited a marked increase in protein expression. CCL2 protein level was elevated 2.5- to 3-fold, from 5μg/g to 12-15μg/g lung tissue.

## Discussion

The ability to repurpose FTY720 as a therapeutic treatment against seasonal influenza infection would be an auspicious step toward a greater understanding of the influenza-induced pre-disposed state, and protection against lethal bacterial superinfection. Some of our findings were surprising in that treatment with a single systemic dose of FTY720 actually elicited a slight transient pro-inflammatory gene response in the lungs during homeostatic conditions. This effect was actually heightened during an active low-dose influenza infection, and translated to protein expression as well. These results are in direct contrast to the cytokine dampening observed with AAL-R treatment during highly pathogenic (HP) influenza infection [87]. Walsh et al. (2011) reported the reduction of the influenza-induced elevated levels of IL-6, CCL2, TNFα and CXCL10 in the BAL fluid with AAL-R local treatment. This difference is likely due in most part to the innate pro-inflammatory response produced by HP versus mild influenza infection. HP influenza infection itself elicits the cytokine storm leading to mortality, whereas low-dose IA/Udorn/72 mimics a milder seasonal influenza infection. This suggests a necessity to reach a threshold level of cytokine gene expression in order to achieve the anti-inflammatory effects of FTY720. For this reason, FTY720 may be better suited as a treatment during a secondary bacterial infection rather than during the primary viral infection.

There is a delicate balance regarding the recruitment of immune cells during respiratory viral infection. Systemic administration of FTY720 clearly has a significant, and transient, effect on these populations in the lungs. Notably, FTY720 treatment under mock conditions resulted in a shift in immune cell populations that mimicked mild influenza infection at 2dpi. There was a considerable decrease in T-lymphocytes and macrophages, but increase in PMNs. Furthermore, when mice were treated with FTY720 during viral infection, these acute-phase effects were

compounded to varying extents. There are many reports that have demonstrated the lymphopenic effect of FTY720, which our study confirmed in both the blood and lungs [88, 95, 114]. It is important to note that FTY720 treatment significantly reduces, but does not completely eliminate, the T-lymphocyte population in the lungs at day 2. This allows the host to still mount complete and effective innate and adaptive immune responses. AAL-R treatment of mice following HP influenza infection diminishes the accumulation of influenza-specific CD8+ T cell recruitment to the lungs, but does not interfere with the host ability to produce anti-influenza neutralizing antibodies [86, 87]. We confirmed that FTY720 shares this quality with AAL-R in subsequent studies involving treatment following low-dose IA/Udorn infection. Mice treated with FTY720 during mild influenza challenge were still protected against lethal influenza challenge at 3 months post primary viral infection.

Macrophages and PMNs are important for clearing the virus by killing and removing virus-infected cells. However, their cytotoxic effects are also detrimental to the healthy cells surrounding the sites of inflammation. It is just as important that these immune cells are eliminated after acute infection for recovery and repair to take place as it is for their initial recruitment. FTY720 seems to have a dual ability to both enhance early PMN recruitment, and to encourage a more rapid elimination of these cytotoxic cells is a promising feature for its use as a therapeutic for influenza infection. It is not surprising that we did not see a reduction in viral loads at days 2 or 7 post-infection even with increased PMN infiltration. As the dose and strain of virus used in these studies elicits a mild, self-limiting infection with relatively low viral loads, there may not have been a strong enough response for FTY720 to demonstrate a difference in viral loads. However, increased PMN levels would be greatly beneficial for combating highly pathogenic influenza or secondary bacterial infections. Conversely, efflux of PMNs from the lungs after viral

clearance is essential to recovery and repair within the respiratory tract. PMNs cause severe tissue damage, so it is important that they are no longer recruited or linger in the alveolar spaces after active infection.

Unlike the other immune cell populations, FTY720 and influenza had opposing effects on the DC population in the lungs at 2dpi. Whereas DCs are recruited to the lungs and 2 days post-influenza, FTY720 instead resulted in a decrease of this population at 2d post-treatment. Together, these effects seemed to negate each other, and the DC population was no different from mock. This effect of FTY720 treatment could be on account of various factors, individually or in conjunction. It is possible that FTY720, like influenza, causes increased migration of DCs to the lymph nodes, but on a slightly delayed and/or extended time line. FTY720 could also prevent DC precursors either from exiting the bone marrow, much like it prevents lymphocyte egress from lymphoid tissues, or from entering the lungs to become mature rDCs. Lan et al. observed a rapid depletion of DCs in the spleen and lymph nodes, but an increase in circulating DCs 24 hours after a systemic dose of 3.5mg/kg FTY720 was given [115]. Furthermore, this dose of FTY720, which was 35 times more than the dose we administered, also decreased cell surface expression of adhesion molecules PECAM-1 (CD31) and ICAM-1 (CD54), as well as the transendothelial migratory chemokine receptor CCR7, when given *in vivo*, but not *in vitro*. These findings suggest that decreased DC numbers in the lungs following FTY720 treatment could be a combination of the short-term downregulation of select dendritic cell surface markers and possible slight increase in efflux from the lungs. However, when FTY720 was given just after influenza infection, the individual effects were modulated, resulting in the same number of rDCs in the lungs as mock/vehicle mice. This apparent attenuation of influenza-induced dendritic cell recruitment into the lungs is an interesting prospective for FTY720 therapeutic potential. Decreasing DCs could

result in mitigating the damaging effects of cytotoxic T cell recruitment, without compromising the host's ability to eliminate the virus or mount an adequate adaptive immune response.

Our preliminary findings with Enigmol treatment establish that a 4-day course of systemic administration of 1μM Enigmol is non-toxic and relatively inert under homeostatic conditions *in vivo*. Enigmol did cause a few alterations to the lung microenvironment, including a reduction in macrophages, significant influx of PMNs, and increase in CCL2 protein expression in the lungs. The increase in CCL2, a monocyte chemotactic protein, would suggest an increase in macrophages, yet we observed a decrease in non-alveolar (SiglecF-) macrophages. This may indicate that Enigmol somehow influences macrophage/monocyte migration via sphingosine-like signaling. Interestingly, the influx of PMNs was not accompanied by an increase in key chemotactic proteins, such as CXCL1 and CXCL2, nor the proteins typically generated by PMNs. However, recent studies have demonstrated that CCL2 can indirectly recruit neutrophils through the induction of platelet activating factor [116]. PMN recruitment to the lungs could be advantageous in protection against secondary bacterial infection in our dual infection model. The initial immune cell responsible for bacterial pathogen clearance is the neutrophil [117]. Perhaps by populating the lungs with PMNs just prior to bacterial infection would allow for expedited clearance of bacteria, and thus greatly mitigate the course and severity of infection. Future studies include applying this method of Enigmol treatment to our mouse model in order to determine the potential protective effects of the compound against single and dual infections.

A

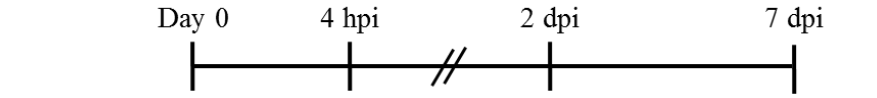


| | | | | |
|---|---|---|---|---|
| **Group 1:** | PBS (6) | Vehicle i.p. | sac (3) | sac (3) |
| **Group 2:** | IA/Ud (6) | Vehicle i.p. | sac (3) | sac (3) |
| **Group 3:** | PBS (6) | FTY720 i.p. | sac (3) | sac (3) |
| **Group 4:** | IA/Ud (6) | FTY720 i.p. | sac (3) | sac (3) |

B

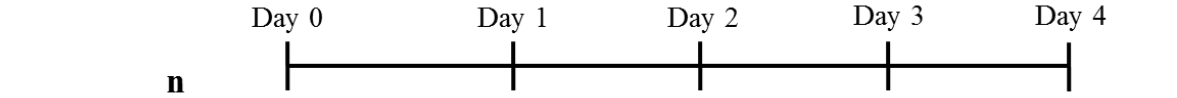


| | **n** | | | | | |
|---|---|---|---|---|---|---|
| **Group 1:** | **(5)** | Vehicle i.p. | V | V | V | sac (5) |
| **Group 2:** | **(5)** | Sphingosine i.p. | SO | SO | SO | sac (5) |
| **Group 3:** | **(5)** | Enigmol i.p. | E | E | E | sac (5) |

**Figure 3-1. Schematics of sphingosine analog mouse studies.** Study schematics for FTY720 treatment during influenza infection (A), or 4 day systemic treatment with sphingosine and Enigmol (B). In two separate studies, 3m Balb/c mice were intranasally infected with 50ul PBS or $1x10^4$ $TCID_{50}$ IA/Udorn. At 4hpi, mice were given an i.p. injection of vehicle or 100ug/kg FTY720, then euthanized at 2dpi or 7dpi for tissue analysis (A). In another mouse study, daily i.p. injections of vehicle "V", 0.5mg/kg sphingosine "SO" or 0.5mg/kg Enigmol "E" were given to 3m Balb/c mice for 4 days. Mice were euthanized and tissues collected for analysis the day after the fourth treatment (B).

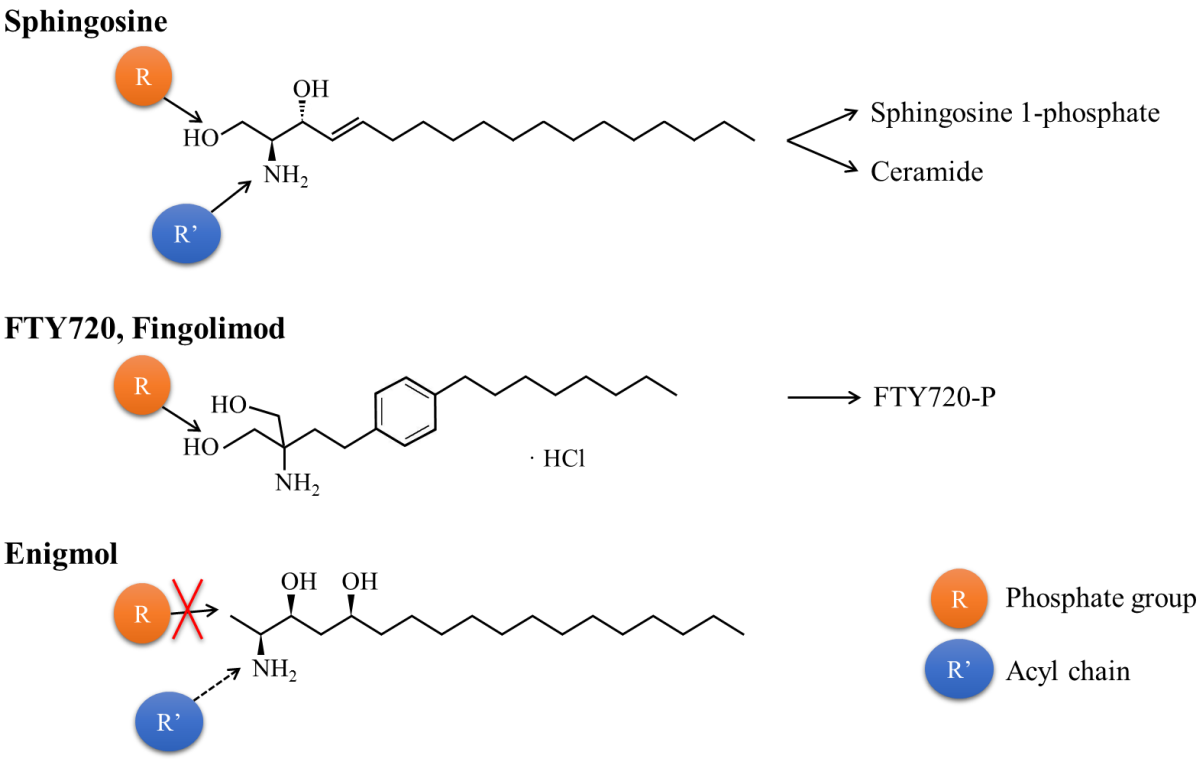


**Figure 3-2. Sphingosine and sphingosine analogs.** Sphingosine and the sphingosine analogs FTY720 and Enigmol were used to treat adult Balb/c mice. Depicted here are the chemical structures and key phosphorylation (orange) or acylation (blue) sites. Phosphorylation is catalyzed by sphingosine kinase (SK), whereas acylation is catalyzed by ceramide synthase (CS). Sphingosine, a naturally-occurring molecule, can be phosphorylated at C1 and converted to sphingosine-1-phosphate, or N-acylated to ceramide. FTY720, a myriocin derivative, can be phosphorylated to FTY720-P, but not acylated. Enigmol is a highly stable sphingoid base analog that cannot be phosphorylated and is very poorly acylated.

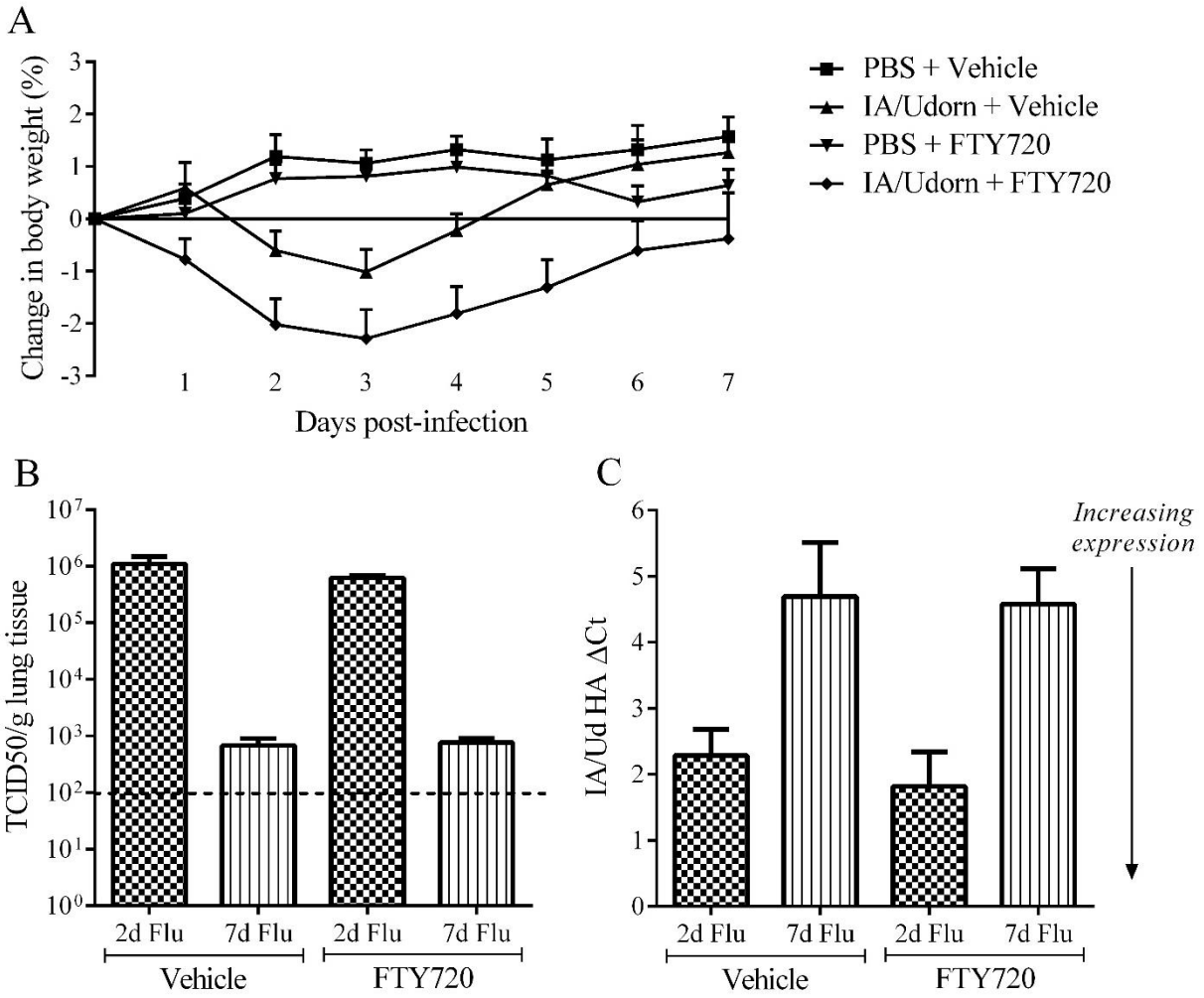


**Figure 3-3. Systemic FTY720 treatment effect on clinical parameters during influenza infection.** Balb/c mice were intranasally infected with PBS (mock) or $1x10^4$ $TCID_{50}$ IA/Udorn/72, then given an intraperitoneal injection of vehicle or 100ug/kg FTY720 4 hours later. Mice were weighed daily (A) and observed for clinical symptoms. At days 2 and 7 post-infection, mice were euthanized and lungs were collected for viral loads (B) and IA/Udorn HA mRNA expression analysis (C). ANOVA, Dunnett's multiple comparisons test was used to compare difference between influenza infection with FTY720 treatment and without treatment. Dashed line (- - -) indicates detection limit of viral load assay.

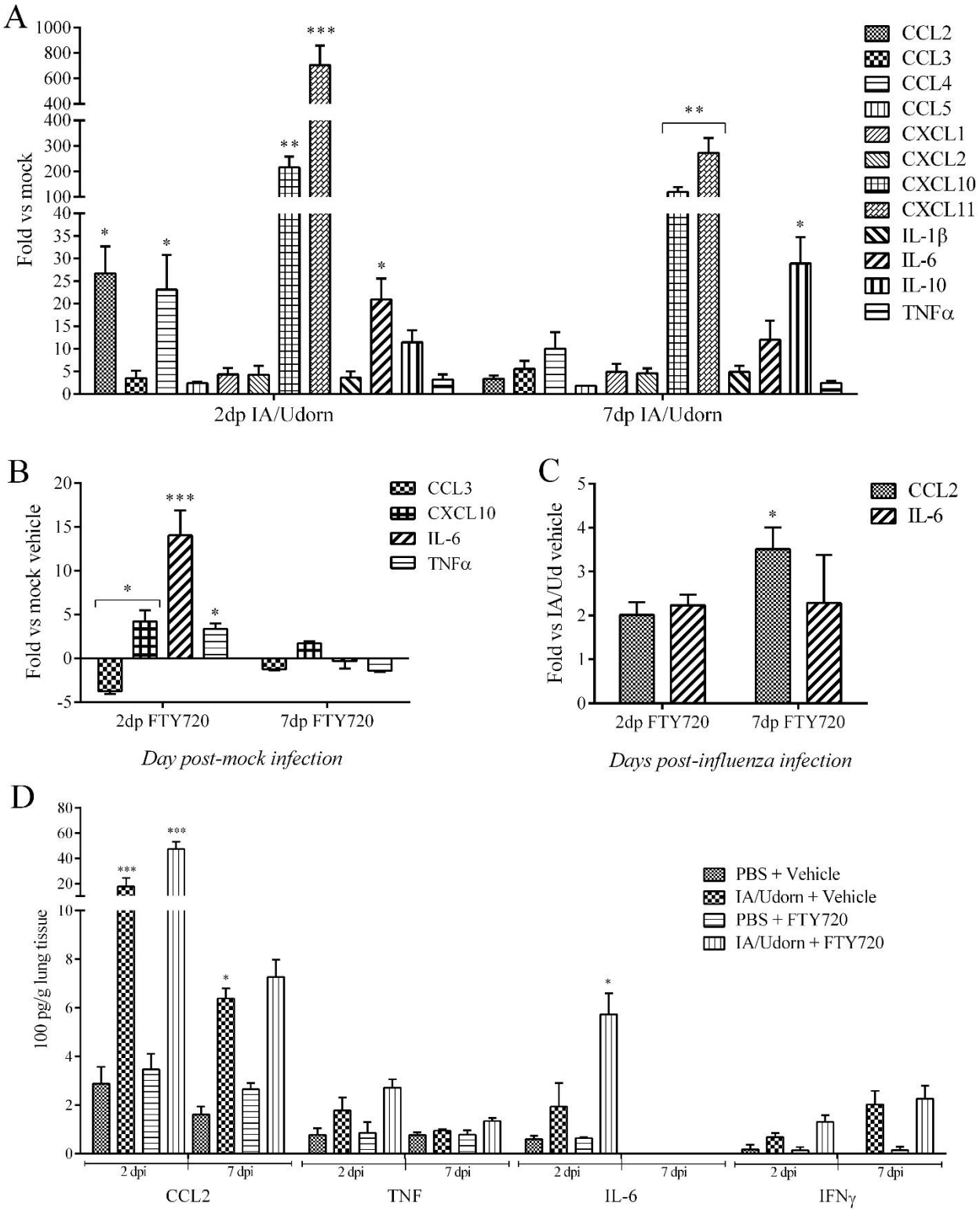
A
Fold vs mock
2dp IA/Udorn
7dp IA/Udorn
CCL2
CCL3
CCL4
CCL5
CXCL1
CXCL2
CXCL10
CXCL11
IL-1β
IL-6
IL-10
TNFα
B
Fold vs mock vehicle
CCL3
CXCL10
IL-6
TNFα
2dp FTY720
7dp FTY720
Day post-mock infection
C
Fold vs IA/Ud vehicle
CCL2
IL-6
2dp FTY720
7dp FTY720
Days post-influenza infection
D
100 pg/g lung tissue
PBS + Vehicle
IA/Udorn + Vehicle
PBS + FTY720
IA/Udorn + FTY720
2 dpi
7 dpi
CCL2
TNF
IL-6
IFNγ

**Figure 3-4. Systemic FTY720 treatment effect on gene and protein expression in the lung.** Balb/c mice were intranasally infected with sham (PBS) or $1x10^4$ $TCID_{50}$ IA/Udorn/72, then given an intraperitoneal injection of vehicle or 100ug/kg FTY720 4 hours later. At days 2 and 7 post-infection, mice were euthanized and lungs were collected for mRNA expression analysis (A-C) and cytokine protein analysis (D). Cytokine mRNA expression levels at 2 and 7dp influenza without treatment (A), with FTY720 treatment (C) and non-infected with FTY720 treatment (B) were evaluated using real-time PCR. Values are expressed as fold change over mock (PBS) or vehicle after normalization to L19 mRNA. ANOVA, Dunnett's multiple comparisons test. Cytokines were quantified from whole lung homogenates and are plotted as 100pg/g of lung tissue (D). ANOVA, Dunnett's multiple comparisons test was used to determine significance of IA/Udorn or FTY720 treatment alone to mock, non-treated mice and significance of treatment versus non-treated infected mice (* $p < 0.05$, ** $p < 0.01$, *** $p < 0.005$).

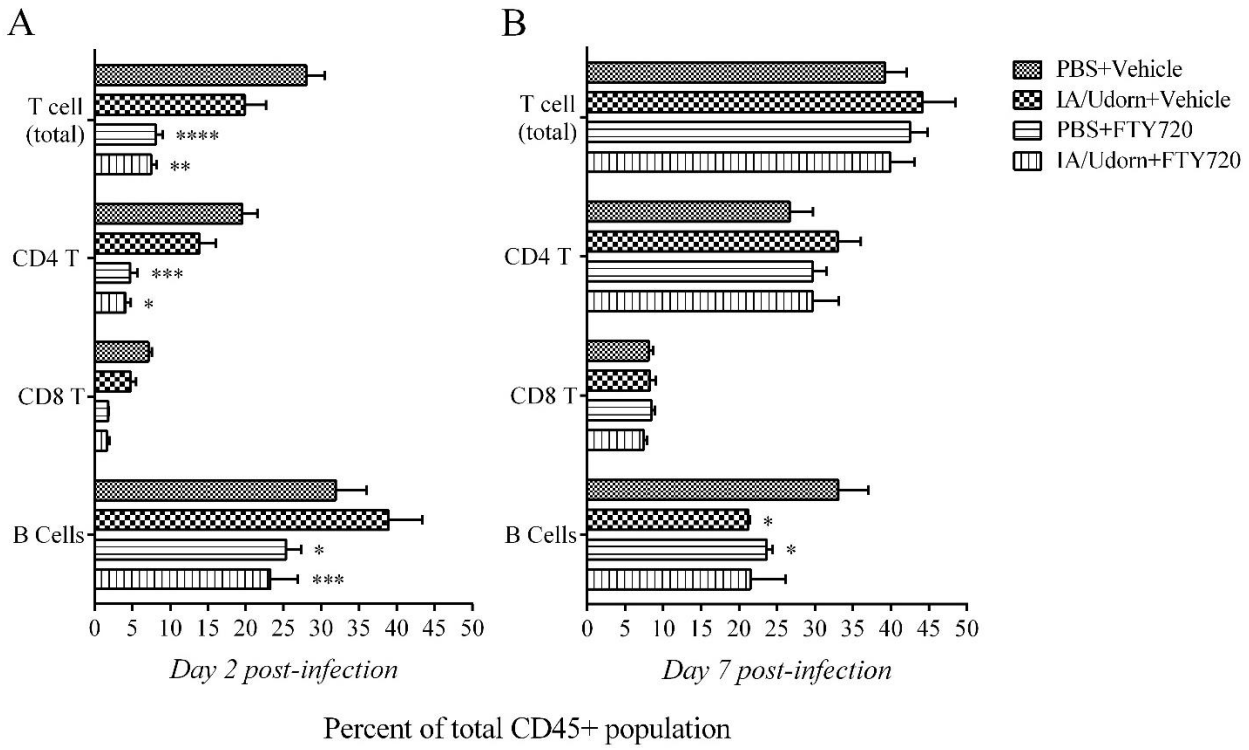


**Figure 3-5. Transient lymphopenia in the blood following influenza infection and systemic FTY720 treatment.** Balb/c mice were intranasally infected with mock (PBS) or $1x10^4$ $TCID_{50}$ IA/Udorn/72, then given an intraperitoneal injection of vehicle or 100ug/kg FTY720 4 hours later. At day 2 (A) and day 7 (B) post-infection, mice were euthanized and blood was collected for FACS analysis. Lymphocyte sub-populations are reported as percentage of the total CD45+ myeloid-lineage population. ANOVA, Tukey's multiple comparisons test was used to determine significance of IA/Udorn or FTY720 treatment alone to mock, non-treated mice and significance of treatment versus non-treated infected mice (* $p < 0.05$, ** $p < 0.01$, *** $p < 0.005$, **** $p < 0.001$).

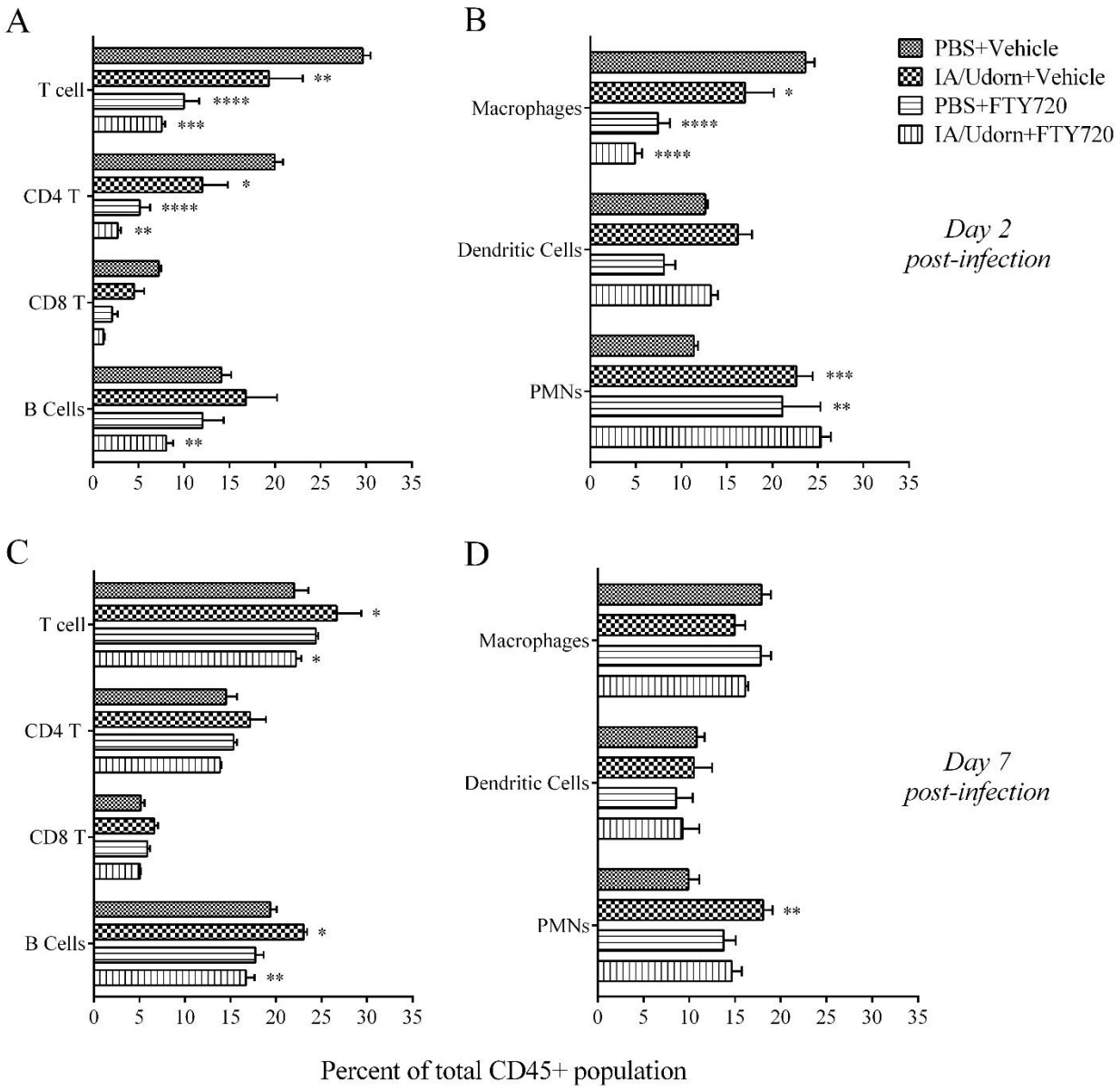


**Figure 3-6. Systemic FTY720 treatment effect on cellular composition in the lungs during influenza infection.** 3m female Balb/c mice were intranasally infected with mock (PBS) or $1x10^4$ $TCID_{50}$ IA/Udorn/72, then given an i.p. injection of vehicle or 100ug/kg FTY720 4 hours later. At day 2 (A,B) and day 7 (C,D) post-infection, mice were euthanized and lungs were collected for FACS analysis. Lymphocyte (A,C) and other leukocyte (B,D) sub-populations are reported as percentage of the total CD45+ myeloid-lineage population. ANOVA, Tukey's multiple comparisons test was used to compare individual IA/Udorn infection and FTY720 treatment to PBS+vehicle, and flu-infected mice treated with FTY720 to non-treated flu-infected mice (* $p < 0.05$, ** $p < 0.01$, *** $p < 0.005$, **** $p < 0.001$).

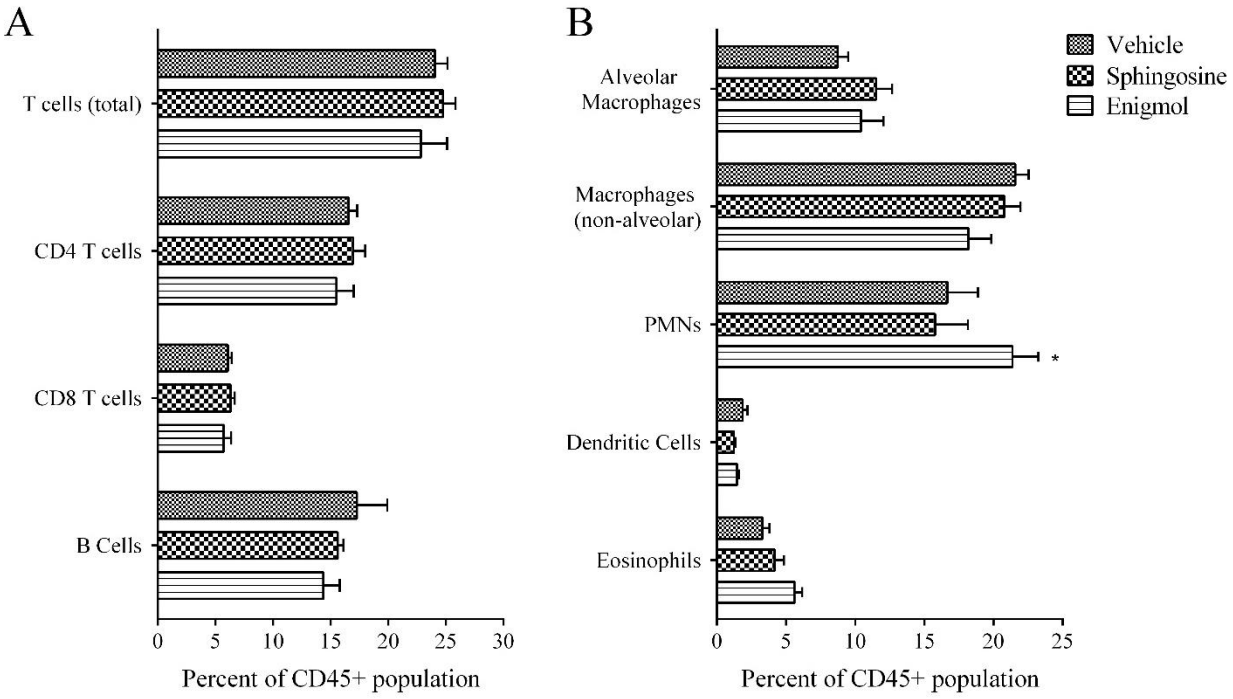


C

| Sub-population | Phenotype |
|---|---|
| T cells (total) | CD3+/CD19-/B220- |
| CD4+ T cells | CD3+/CD4+/CD8- |
| CD8+ T cells | CD3+/CD4-/CD8+ |
| B cells | CD3-/CD19+/B220+ |
| Alveolar Macrophages | $CD11b^{lo}/CD11c^{hi}$/SiglecF+ |
| Macrophages (non-alveolar) | CD11b-/CD11c+/SiglecF- |
| PMNs | CD11b+/CD11c-/Ly6C+/$Ly6G^{hi}$ |
| Dendritic Cells | CD11b+/CD11c+/SiglecF- |
| Eosinophils | CD11b+/CD11c-/SiglecF+ |

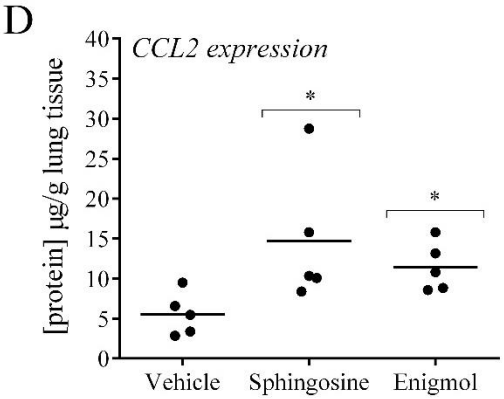


**Figure 3-7. Systemic sphingosine and Enigmol effect on the lung microenvironment.** Balb/c mice were treated daily for 4 days with intraperitoneal injections of vehicle, 0.5mg/kg sphingosine or 0.5mg/kg Enigmol. On the fifth day, mice were euthanized and lungs were collected for FACS, qRT-PCR (Supplemental Table S4) and protein analysis. For FACS analysis, lymphocyte (A) and other leukocyte (B) sub-populations are reported as percentage of the total CD45+ myeloid-lineage population based on phenotype (C). ANOVA, Tukey's multiple comparisons test (* $p < 0.05$). CCL2 protein was also measured in whole lung homogenates and plotted as µg/g lung tissue (D). ANOVA, Kruskal-Wallis test (* $p < 0.05$).

## Chapter Four

Define the cell type-specific effects of sphingolipid treatment during influenza A viral infection

**Abstract**

Influenza infection induces a robust pro-inflammatory response in many cell types, which contributes to the cytokine storm associated with disease lethality. Animal models encompass innumerable interactions between cells and cellular products, making it impossible to illuminate mechanisms and direct cell-specific effects. Since respiratory epithelia and alveolar macrophages are fundamental members and the initiators of IAV-induced innate immune response, we aimed to characterize any distinct effects sphingolipid therapy elicits under infected and non-infected conditions. The intracellular enzymes that stringently regulate sphingolipid levels have demonstrated potential for immunotherapy during viral infection, with specific focus on the enzymes associated with sphingosine 1-phosphate metabolism. Overexpression of sphingosine 1-phosphate lyase (SPL) or treatment with a sphingosine kinase inhibitor (SKi) impairs influenza virus replication and virus-related cytopathic effect *in vitro*. Conversely, overexpression of sphingosine kinase enhanced cell susceptibility to viral infection, which was demonstrated by increased viral loads and cytopathic effect compared to WT HEK293 cells. We hypothesized that treatment with S1P and FTY720 would suppress the expression of pro-inflammatory mediators in A549 and MH-S cells following high dose influenza A challenge. Treatment with novel sphingosine kinase inhibitors SK1i, SK2i and DMS would dampen pro-inflammatory mediator expression in MH-S and A549 cells, as well as decrease viral loads in A549 and MDCK cells. We found that treating cells with S1P or FTY720 had no effect on viral loads or inflammatory gene expression. However, prophylactic and therapeutic treatment with SK inhibitors and Enigmol reduced 24h viral loads by 1-2 logs in A549 epithelial cells. These compounds also altered gene and protein expression of key influenza-induced cytokines, such as CCL2, CCL5, IL-8 and CXCL10. SK inhibitors had an overall dampening effect on these cytokines, whereas Enigmol

generally enhanced the expression of these cytokines. Our data indicate that these novel SK inhibitors and Enigmol show great potential for immunomodulatory therapy during influenza viral infection, and possibly other inflammatory diseases. The mechanisms of their activity are clearly diverse and require further investigation.

## Methods and Materials

### Preparation of sphingolipids, sphingosine analogs and sphingosine kinase inhibitors

D-erythro-sphingosine ((2S,3R,4E)-2-amino-4-octadecene-1,3-diol; Avanti Polar Lipids), D-erythro-sphingosine-1-phosphate ((2S,3R,4E)-2-amino-4-octadecene-1,3-diol-1-phosphate; Avanti Polar Lipids), FTY720·HCl (2-amino-2-[2-(4-octylphenyl)ethyl]-1,3-propanediol, hydrochloride; Cayman Chemical), proprietary SK1 and SK2 inhibitors (generously provided by W. Santos, VT Chemistry Department), N,N-dimethylsphingosine (2S-(dimethylamino)-4E-octadecene-1,3R-diol; Cayman Chemical), and Enigmol ((2S,3S,5S)-2-aminooctadecane-3,5-diol; generously provided by A.H. Merrill, Jr., Georgia Tech) were used in cell culture experiments. Sphingosine, sphingosine 1-phosphate and Enigmol were prepared in a 1:1 molar complex with fatty-acid free bovine serum albumin (FAF-BSA; Calbiochem). FTY720 and dimethylsphingosine (DMS) were prepared as 20mM stocks in DMSO. SK1i and SK2i were prepared as 1mM stocks in sterile $dH_2O$. Toxicity studies were performed in the cells lines utilized in these experiments, and a non-toxic 1μM dose was chosen for each compound.

### Cell culture and virus

Human type II alveolar epithelial cells (A549), murine alveolar macrophages (MH-S) and Madin-Darby Canine Kidney epithelial cells (MDCK) previously obtained from the American Type Culture Collection (ATCC) were grown and maintained in Dulbecco's Modified Eagle's Medium supplemented with 10% fetal bovine serum (Atlanta Biologicals) and penicillin/streptomycin (100U/100μg per ml). Sterile-filtered charcoal-stripped FBS (csFBS) at 2% or 0.1% supplementation was used during studies to remove any exogenous lipids, specifically S1P, that would interfere with signaling. Influenza A/Udorn/72 (H3N2) virus, a filamentous

laboratory-adapted human clinical isolate that had been previously prepared and titrated in MDCK cells, was used for *in vitro* experiments.

**Prophylactic treatment of A549 cells with sphingolipid compounds**

To evaluate cell-specific effect of prophylactic sphingolipid therapy in lung epithelial tissue, we utilized A549 cells as an *in vitro* model. Cells were seeded at confluency in 12-well TC plates (approx. $5x10^5$ cells/well) to mimic an intact pulmonary epithelial layer, with each treatment in triplicate. Cells were given 6-8 hours to adhere, then media was aspirated and DMEM/2% csFBS was added to each well for an overnight incubation (37˚C, 5% $CO_2$). All treatments (sphingosine, S1P, FTY720, SK1i, SK2i, DMS and Enigmol) were diluted to 1μM in DMEM/2% csFBS. The vehicle used was a 1:1000 dilution of sterile $dH_2O$ in DMEM/2% csFBS. After overnight incubation, media was aspirated and 1ml of each treatment was added to the appropriate wells, which were incubated for 24 hours before infection. Cells were removed from two extra wells and counted for the multiplicity of infection (MOI) calculation. Mock samples were incubated with 300μl $PBS^{+/+}$, while influenza-infected samples were incubated with $6x10^5$ $TCID_{50}$ (1 MOI) in 300μl $PBS^{+/+}$ per well. After a 1h adsorption period, inoculum was aspirated and cells were washed twice with PBS. Fresh media with corresponding treatments were added back to the cells. At 24hpi, supernatants were collected in microfuge tubes and RNA*later* CellProtect (Qiagen) was added to cells. Cells in the supernatants were pelleted (300xg, 5 min) and pre-cleared supernatants were divided into two new microfuge tubes: one for viral load analysis, the other for protein analysis. Cells in RNA*later* CellProtect were transferred to corresponding cell pellets. Supernatants were flash frozen in liquid nitrogen, then stored at -80˚C until use. Cells in RNA*later* were stored at 4˚C for 2 days before RNA extraction.

**Therapeutic treatment of A549 cells with SK inhibitors and Enigmol**

After finding no remarkable differences in viral loads (Fig. S4) or gene expression with sphingosine, S1P or FTY720 treatment in A549 cells (data not shown), subsequent studies focused on the impact of specific SK1 and SK2 inhibitors, DMS, a non-specific SK inhibitor, and Enigmol treatments on virus infection.

A549 cells were seeded at $8x10^4$ cells per well in 12-well TC plates (or $1x10^4$ cells per well in 48-well TC plates) and incubated until cells reached 75% confluency, which was about 24 hours (37˚C, 5% $CO_2$). Media was aspirated and DMEM/0.1% csFBS was added to all wells for an overnight incubation. The next morning, cells from two wells were counted, and a 1 MOI virus suspension was prepared in $PBS^{+/+}$ accordingly. Mock samples were incubated with 300µl $PBS^{+/+}$, while influenza-infected samples were incubated with 1 MOI IA/Udorn in 300µl $PBS^{+/+}$ per well. After a 1h adsorption period, inoculum was aspirated and cells were washed twice with PBS. The compounds used were prepared in different solvents because of varied solubility, therefore three vehicles were necessary:

| | Control for | Solvent | Dilution in DMEM/0.1% csFBS |
|---|---|---|---|
| Vehicle 1: | SK1i, SK2i | sterile $dH_2O$ | 1:1000 |
| Vehicle 2: | DMS | DMSO | 1:10,000 = 0.01% DMSO |
| Vehicle 3: | Enigmol | 1mM FAF-BSA | 1:1000 = 1uM FAF-BSA |

1ml (12-well plate) or 300µl (48-well plate) of vehicles, 1µM SK1i, 1µM SK2i, 1µM DMS or 1µM Enigmol in DMEM/0.1% csFBS was added to the appropriate wells. Cells were incubated for 5 or 24 hours. At 5hpi, cells in the 12-well plates were collected in RNA*later* CellProtect and transferred to microfuge tubes for storage at 4˚C. At 24hpi, supernatants were collected from 48-well plates. Cell debris was pelleted and pre-cleared supernatant was transferred to 2 separate

microfuge tubes- one for viral loads, the other for protein analysis. Supernatants were flash frozen in liquid nitrogen and stored at -80˚C until analysis.

Viral loads and protein levels were measured at 24hpi to ensure time for viral replication and translation of mRNA transcripts. For this, cells were seeded in separate 48-well TC plates with cell numbers and media volumes scaled down accordingly. Otherwise, experiments were identical and performed in tandem.

**Therapeutic treatment of MH-S cells with SK inhibitors and Enigmol**

This study was set up in the same manner as the previous study to evaluate therapeutic treatment in A549 cells. MH-S cells were seeded at 50% confluency in 12-well TC plates, and allowed to grow until 70% confluent. Cells were serum starved overnight (DMEM/0.1% csFBS), counted, then infected with mock ($PBS^{+/+}$) or 1 MOI IA/Udorn/72 in 300µl/well. After a 1h adsorption period, inoculum was aspirated and cells were washed twice with PBS. As in the previous study, 1ml of vehicles, 1µM SK1i, 1µM SK2i, 1µM DMS or 1µM Enigmol in DMEM/0.1% csFBS were added to the wells. Cells were incubated for 5 hours, then supernatants and cells were collected (in RNA*later* CellProtect).

**Viral load assays**

Viral loads were measured in supernatants collected from A549 and MDCK epithelial cells to determine if the compounds reduced productive virus. Titers were determined using the previously described Reed-Muench 50% tissue culture infectious dose ($TCID_{50}$) assay in a 96-well TC plate format. Briefly, serial 10-fold dilutions of pre-cleared cell supernatants were incubated with MDCK cells for 1 hour (37˚C, 5% $CO_2$) to allow for virus adsorption. Inoculum was aspirated

from cells, which were then incubated with 2ug/ml TPCK-treated trypsin in DMEM for 72 hours (37˚C, 5% $CO_2$). Cytopathic effect was recorded and used to calculate titers, expressed in $TCID_{50}$/ml.

**RNA extraction and cDNA synthesis**

Cells in RNA*later* CellProtect were pelleted and supernatant was discarded. RNA was extracted following the RNeasy Mini Kit protocol. Briefly, cells were resuspended in 500µl RLT lysis buffer and mixed thoroughly to ensure complete cell lysis. An equal volume of 70% ethanol was added to the supernatants and mixed, then transferred to a mini spin-column with collection tube to bind RNA. After DNA clean-up with RNase-free DNase I (Qiagen) and washing with RW and RPE wash buffers, RNA was eluted in 30nuclease free $dH_2O$. RNA was quantified using a NanoDrop spectrophotometer.

Complementary DNA (cDNA) was synthesized using the iScript cDNA synthesis kit from Bio-Rad. Briefly, 4ul 5x reaction mix and 1ul reverse transcriptase was added to 500ng of RNA template in 0.2ml PCR tubes. The volume was brought up to 20µl with nuclease free $dH_2O$, and samples were incubated at 42˚C in a water bath for 30 minutes. The reverse transcriptase was deactivated by incubation at 85˚C for 5 minutes in a heat block or thermocycler. Tubes were spun down to remove condensation from lid and sides, then samples were diluted 1:10 with nuclease free $dH_2O$.

**Real-time PCR analysis**

Quantitative real-time PCR was performed according to the SensiMix™ SYBR & Fluorescein kit (Bioline) instructions. All primers used (Table S1) were designed with a $T_m$ of 58-

60˚C and 80-120 bp amplicon. Each reaction consisted of 7.5ng cDNA template, 0.5uM forward primer, 0.5uM reverse primer and 1x SensiMix™ in a total volume of 15ul. Real-time PCR analysis was conducted with the Bio-Rad iQ5 Thermal Cycler with the following reaction conditions: 95˚C x 10 min for polymerase activation, then 45 cycles of denaturation (95˚C x 15s), annealing (60˚C x 15s), elongation (72˚C x 30s) and fluorescence acquisition. A melt curve analysis was performed at the end of cycle 45 to ensure product specificity. Relative quantification of transcripts were determined with the $2^{-\Delta\Delta Ct}$ method as previously described [105].

**Cytometric Bead Array (CBA) Assay**

Key chemokine protein levels were measured in lung homogenates using a Human Chemokine CBA kit (BD) as per manufacturer's protocol. This 5-plex kit quantitated levels of CCL-2, CCL-5, CXCL9, CXCL10 and IL-8. Briefly, a 50µl aliquot from previously frozen lung homogenate supernatants was incubated with 50µl capture beads and 50µl PE detection reagent for 3 hours at room temperature. Beads were pelleted (200xg for 5 min) and washed twice with the provided wash buffer prior to analysis. CBA samples were acquired with BD FACSAria Cell Sorter by Melissa Makris. Data analysis was completed using FCAP Array software.

**Statistical analysis**

Statistical analysis was conducted with Prism software (GraphPad). Difference in viral loads, gene and protein expression were analyzed with ANOVA using Tukey's or Dunnett's multiple comparisons test or Kruskal-Wallis test for non-parametric data.

## Results

### A549 alveolar epithelial cells rapidly respond to influenza with robust pro-inflammatory gene expression

A549 cells, a type II human alveolar epithelial cell line, responded rapidly to high dose (1 MOI) IA/Udorn infection with a prolific pro-inflammatory response evident at 5hpi (Fig. 4-1A). At this early time point, there was already a significant increase in the expression of all cytokines evaluated in these studies, except IL-8. CCL5, IL-6, CXCL10 and TNFα were decidedly elevated by 150- to 600-fold levels compared to mock. CCL2 and CXCL11 were also increased, but to a much lesser extent. However, it is important to note that the increases observed were magnified by the fact that these genes were very lowly expressed, essentially turned off, under steady state (control) conditions.

In a separate study, but under similar conditions, 24hpi gene expression revealed that transcript levels of these cytokines were not only maintained, but were further increased at this later time point (Fig. 4-1B). At this time, CCL5 and CXCL10 expression had reached extraordinarily high levels. IAV infection was able to induce these chemokines, which were basically non-expressed at basal state, to levels comparable with glyceraldehyde 3-phosphate dehydrogenase (GAPDH), a glycolysis-related housekeeping gene commonly used for data normalization.

### Sphingosine kinase inhibitors and Enigmol reduce viral loads in A549, but not MDCK, epithelial cells

In three separate experiments, anti-viral activity of various treatments was measured in A549 and MDCK cells. Viral loads were measured in the supernatants of A549 cells at 24hpi

(Fig. 4-2), and MDCK cells at 48 hpi (Supplemental Figure S3). Both cell lines are epithelial cells that permit influenza viral infection and multiple rounds of replication. For these events to successfully occur, cells must be adhered and arranged in a confluent monolayer. However, TPCK-treated trypsin must be supplemented after infection to cleave viral HA, a critical step for production of infectious viral progeny [118]. MDCK cells are not adversely affected, but A549 cells quickly detach from tissue-culture treated plates in the presence of trypsin. Therefore, we utilized MDCK cells to determine sphingolipid therapeutic effect during low-dose IAV infection (0.001 MOI) and subsequent rounds of replication and infection. A549 cells were used for comparison of prophylactic versus therapeutic treatment after a high-dose IAV infection (1 MOI) with subsequent viral replication and production of non-infectious virions. To activate these viral progeny, supernatants were treated with TPCK-trypsin for 30 minutes prior to viral load assay.

Prophylactic treatment of A549 cells and the low-dose MDCK studies were performed first, with all sphingolipid compounds, analogs and inhibitors at 1μM: SO, S1P, FTY720, SK1i, SK2i, DMS and Enigmol (discussed later). As shown in Supplemental Figure S3, there was no significant difference in viral loads among vehicle, SO, S1P or FTY720 treatment in either cell line. There was a significant (1-1.5 log) decrease in A549 24h viral loads with SK1i, SK2i and DMS treatment (Fig. 4-2A), but this was not found in MDCK cells at 48 hpi (Fig. S3B). There was a slight viral load reduction (< 0.5 log), but it did not meet significance. Although MDCK cells have been shown to respond to SK inhibition with D,L-*threo*-dihydrosphingosine (tDHS) [119] and DMS [120], these effects may not be the same as in human alveolar epithelia (A549). Based on these results, and the lack of substantial gene expression changes with SO, S1P or FTY720 treatment (data not shown), we decided to focus exclusively on the actions of the three sphingosine kinase inhibitors for subsequent studies.

Next, we wanted to verify if this anti-viral effect could be achieved in A549 cells with therapeutic treatment as well. Treating cells for 24 hours after viral infection also reduced viral loads comparable to prophylactic treatment (Fig. 4-2C). Despite these reductions, there was no obvious difference in CPE between treatments and vehicle in either study as CPE was minimal at 24hpi anyway. This indicates that the anti-viral action of these inhibitors is rapid, and does not necessarily require pre-treatment. To validate these measurable viral load reductions, we then evaluated IA/Udorn-specific HA gene expression with RNA isolated from these cells. Real-time PCR analysis confirmed our findings by demonstrating a significant increase in ΔCt values, which translates to decreased expression of the virus-specific gene (Fig. 4-2B,D). Reduction of gene expression suggests that the decrease in viral load results from an inhibition of virus to replicate within the cell.

**Prolonged exposure to SK inhibitors downregulates SK1 gene expression**

Having established that A549 cells respond to IAV infection with a robust pro-inflammatory response, and that inhibition of sphingosine kinases reduces viral loads and replication, we next wanted to evaluate how treatment effects expression of these influenza-induced cytokines as well as select sphingolipid-metabolizing enzymes.

Real-time PCR analysis revealed that pre-treatment with SK1i, SK2i and DMS prior to and after mock or IA/Udorn infection caused downregulation of sphingosine kinase 1 (Fig. 4-3A), but not sphingosine kinase 2 or ceramide kinase (Supplementary Table S5). This effect was more profound in mock-infected cells, which were essentially exposed to treatment for 48 hours before RNA collection. These SK inhibitors decreased SK1 expression 6- to 8-fold compared to vehicle under mock conditions, but only 3- to 4-fold under influenza-infected conditions. Influenza

infection itself caused a 2-fold increase in SK1 expression, which accounts for the 2-fold difference between downregulation during mock versus infected state.

**SK inhibitor pre-treatment downregulates gene and protein expression of select inflammatory mediators**

In general, sphingosine kinase inhibitors shared a trend of downregulating the cytokines that were induced by IAV infection (Fig 4-1). Expression of CXCL11, IL-6, TNF-α, CXCL10 and CCL2 was not altered when mock-infected, but was diminished 4- to 6-fold at 24hp IA/Udorn challenge (Fig. 4-3B and 4-4A,C). IL-8 gene expression was not altered by treatment at all, but CCL5 expression pattern was unexpected, but interesting. SK1i and SK2i treatment in mock cells increased CCL5 expression by 14-fold and 5-fold, respectively. However, because CCL5 was expressed at very low basal levels, this increase may not be as substantial. In opposition to SK1i and SK2i, DMS was actually able to downregulate gene expression, which indicates that DMS effectively shut off CCL5 gene expression. Surprisingly, pre-treatment with SK inhibitors did not alter the expression of CCL5 during an influenza infection at all. It seems that the influenza-induced CCL5 response in A549 cells was so overwhelmingly robust that the inhibitors were not able to intervene in its transcription.

Protein analysis of A549 cell supernatants gave more insight into the actual translation and secretion of these cytokine transcripts. Levels of CXCL10 and CCL5 were essentially undetected in mock cells (Fig. 4-4B), which corresponded to the high basal Ct levels obtained from real-time PCR analysis. Furthermore, CXCL10, CCL5, IL-8 and CCL2 protein concentrations in vehicle control samples were decidedly increased with IAV infection (Fig. 4-4B,D), which had also been indicated by elevated transcript levels of these cytokines (Fig. 4-1B). Prophylactic treatment with

SK1i and SK2i in A549 cells did not affect protein levels in non-infected cells, despite the increase observed in CCL5 gene expression (Fig. 4-4A). However, these treatments did significantly dampen (2-fold or greater) the levels of all 4 cytokines during influenza infection. Notably, SK1i and SK2i suppressed the expression of these proteins equally, suggesting there was no difference in the immunosuppressive abilities of these inhibitors. Like the specific SK inhibitors, DMS essentially had no effect on protein expression in a non-infected state. DMS treatment was also similar to the other inhibitors in its ability to reduce CCL5, IL-8, and CCL2 protein expression at 24hpi, but was slightly less potent, particularly with CCL5. Interestingly, DMS pre-treatment actually doubled CXCL10 protein levels during IAV infection.

**Therapeutic treatment with SK1i enhances viral-induced pro-inflammatory response**

As a compliment to the prophylactic treatment study, we evaluated therapeutic treatment with SK inhibitors in IA/Udorn-infected A549 cells. Gene expression was measured at an early time point (5 hpi), and protein expression at the later 24 hour time point. Unexpectedly, we found that 5 hour treatment with SK1i increased CXCL10 and CXCL11 gene expression in non-infected cells by 20-fold and 10-fold, respectively (Supplemental Table S6 and Fig. 4-5A). When cells had been infected with 1 MOI IA/Udorn, SK1i treatment had no effect on CXCL10 gene expression, yet further increased CXCL11 expression. In fact, 5 hour treatment increased CXCL11 gene expression 5-fold beyond that of influenza itself.

Protein analysis of 24-hour supernatants confirmed this pro-inflammatory effect, which was only evident following viral challenge. This differed from upregulated gene expression, which was prominently seen in mock cells. As before, high-dose influenza viral infection caused a dramatic increase in these extracellular cytokines. The protein levels measured in this study were

lower than those in the previous study, which may be explained by decreased cell number and the inherent variations between experiments. Though the values were lower, the trends we the same. At 24hpi, SK1i therapeutic treatment caused elevated levels of CCL5, IL-8 and CCL2 proteins. However, the increase in CXCL10 protein expression was negligible, and somewhat surprising given the marked upregulation of gene expression at 5 hours.

**SK2i and DMS therapeutic treatment has varied immunomodulatory effects on A549 inflammatory state**

Like SK1i, 5 hour treatment with SK2i or DMS led to increased CXCL10 gene expression. This increase was much less than that induce by SK1i, but still significant at 5-fold that of the vehicle control (Fig. 4-5A). Otherwise, these treatments had minimal effect on the expression of genes assessed in our panel (Supplemental Table S6). Perhaps measuring gene expression at a later time point (24 hours), would demonstrate a greater difference.

In contrast to therapeutic SK1i treatment, SK2i and DMS treatment reduced levels of cytokines elicited by IAV at 24 hpi. SK2i dampened CCL5, IL-8 and CCL2 protein concentration, whereas DMS only dampened IL-8 (Fig. 4-5B,D). These results are interesting, because they suggest SK1i actually shifts the cell to more of a pro-inflammatory state when given therapeutically, but SK2i and DMS generate anti-inflammatory conditions as seen with prophylactic treatment. This contrast illustrates just how diverse these two enzymes are, even though they perform the same biochemical reaction.

**MH-S influenza-induced early pro-inflammatory response is marginally modulated by therapeutic SK inhibitor treatment**

The resident alveolar macrophage (AM) is another key regulator of immune response following influenza A viral infection. Our previous studies demonstrated that these cells are highly susceptible to synergistic upregulation of pro-inflammatory cytokines and a likely contributor to the lethal cytokine storm associated with superinfection (Supplemental Figure S2). We found that AMs isolated from the BALF of aged mice at 21 days following mild IA/Udorn/72 infection responded to *ex vivo* secondary *Streptococcus pneumoniae* challenge with an exacerbated pro-inflammatory response. Chemokines CXCL1, CXCL2, CXCL10, CCL2 and CCL4, interleukins IL-1β and IL-6, TNFα and IFNγ were among the genes synergistically upregulated. Bio-Plex analysis of secreted proteins revealed that gene upregulation was a strong indicator of protein expression, as many were also synergistically upregulated. Due to the limited number of primary alveolar macrophages that can be isolated from the murine respiratory tract, MH-S, a transformed murine alveolar macrophage cell line, was chosen to represent this cell type *in vitro*. Although macrophages are susceptible to influenza, the virus does not typically replicate within these cells, so a 24-hour time point was not necessary. Therefore, we decided to just look at early influenza-induced gene expression in this preliminary study.

Expression of pro-inflammatory cytokines was rapidly induced by 1 MOI IA/Udorn infection. By 5hpi, IL-1β and IL-6 gene expression had increased by 100-fold or more compared to mock (Fig. 4-6B). IFNβ, CXCL1, CXCL2 and CXCL9 expression was also elevated 20- to 50-fold that of mock. Other cytokines were increased as well, but not to the extent of those mentioned above (Fig. 4-6A). Expression of IA/Udorn-specific HA was measured as an indicator for intracellular viral replication. ΔCt values were undetermined in mock cells, but very high (almost

at L19 expression levels) in infected cells (Supplemental Table S7). This verified that MH-S cells were infected and that virus was replicating within the cells.

Sphingosine kinase inhibitors had varied effects on MH-S cells after 5-hour treatment. All 3 inhibitors downregulated CXCL11 and TNFα expression about 4- and 2-fold, respectively (Fig. 4-7A). Otherwise, gene expression profiles were different. SK1i uniquely upregulated IL-12p40 6-fold; SK2i and DMS downregulated IL-1β 4-fold; and DMS distinctively downregulated IL-6 expression. When cells were challenged with high-dose influenza before treatment, the resulting gene expression profile was almost identical among the inhibitors. All treatments demonstrated a 2- to 4- fold decrease in CXCL2 and CXCL10 expression, and 3-fold increase in TGFβ expression (Fig. 4-7B).

**The novel sphingosine analog Enigmol reduces viral loads in A549**

Enigmol is a compound with therapeutic potential in cancer treatment. Although it is a potent activator of apoptosis at high concentrations [101], its immunomodulatory effects at low concentrations have not been examined. Cytotoxicity assays determined that Enigmol levels below 2uM were non-toxic to confluent A549 and MH-S cells. Therefore, we included 1μM Enigmol treatment in our *in vitro* experiments.

When Enigmol was given prophylactically (24h pre-treatment) and therapeutically with high dose IA/Udorn, viral loads at 24hpi were significantly reduced (Fig. 4-8A). Prophylactic treatment reduced viral loads by 2 logs, and therapeutic treatment by 1 log. Despite this reduction, there was no obvious difference in CPE between Enigmol and vehicle treatment as CPE was minimal at 24hpi anyway. As with the sphingosine kinase inhibitors, when MDCK cells were

treated with 1μM Enigmol during a low-dose IA/Udorn infection, viral load reduction was insignificant at < 0.5 log (Supplemental Fig. S3).

**Immunomodulatory effects of Enigmol on gene and protein expression are diverse and cell-type dependent**

Prophylactic treatment with Enigmol decreased SK1 and SK2(S) expression 3-fold in non-infected A549 cells (Fig. 4-9A). When cells were infected, Enigmol pre-treatment dampened SK1 expression even more (6-fold), which counteracted the influenza-induced increase in gene expression. The effect of Enigmol pre-treatment was overall pro-inflammatory, when cells had not been infected. CCL2, CXCL10, IL-6, IL-8 and TNFα were all elevated to some extent. Again, it should be noted that CXCL10, IL-6, and TNFα were expressed at very low basal levels, so these increases may not have been as considerable as fold values suggest. Interestingly, when cells were infected after 24h pre-treatment, Enigmol effects were immunosuppressive. Expression of CCL5, CXCL11, IL-6 and TNFα was decreased 3- to 6-fold below that of infected vehicle controls, which is fairly substantial because these cytokines were notably induced by influenza at 24hpi (Fig. 4-1B). Changes in gene expression were somewhat mirrored by protein expression in 24hpi supernatants. Not surprisingly, CXCL10 and CCL5 were not detected in Enigmol-treated mock cells, even with the 10-fold increase in CXCL10 gene expression (Fig. 4-10A). On the other hand, IL-8 and CCL2 proteins were substantially increased, which was indicated by a 7-fold and 5-fold increase in gene expression (Fig. 4-10B). With the addition of IAV infection, CCL5 and CXCL10 proteins were significantly decreased, but IL-8 and CCL2 were increased. CCL5 and CXCL10 protein levels corresponded to the downregulation in gene expression, but the considerable increase in IL-8 and CCL2 did not. The disparity between some gene expression changes being

reflected in protein levels, and others not suggests that modulation mechanisms of Enigmol are complex and varied. While some seem to be controlled at the point of transcription (CCL5 and CXCL10), others may be at the post-transcriptional or translational level (IL-8 and CCL2).

Therapeutic treatment with Enigmol revealed immunomodulatory capacity in A549 cells, but not to the extent observed with prophylactic treatment. Gene expression changes were overall insignificant, but they were measured at 5 hours following treatment. Cytokines under mock conditions and sphingolipid-metabolizing enzymes were unaffected at this early time point (Fig. 4-9B; Supplemental Table S6). Only the addition of IA/Udorn infection produced any marginal change. Again, Enigmol treatment was immunosuppressive with regards to CCL2, CCL5, CXCL10, IL-6 and IL-8 gene expression. These changes were fairly comparable to those seen with prophylactic treatment, with the exception of CXCL11. Pre-treatment significantly decreased 24h gene expression following IAV infection, but therapeutic treatment had no effect on 5h gene expression (Fig. 4-9A vs B). Although direct comparison cannot be made, this discrepancy may indicate that modulation of CXCL11 is time-dependent, which may be correlated with the late induction of gene expression by influenza viral infection. Protein quantification at 24h was a better indicator for the differences between therapeutic methods, which were noteworthy. Therapeutic Enigmol treatment of non-infected cells did induce an increase in IL-8 and CCL2 protein levels (Fig. 4-10D), but nowhere near the levels elicited by prophylactic treatment (Fig. 4-10B). When treated after infection, Enigmol had no effect on CXCL10 and CCL5 protein expression, but surprisingly decreased IL-8 and CCL2 levels. Though gene expression of IL-8 and CCL2 was downregulated at 5hpi, this was also seen with prophylactic treatment at 24hpi, yet protein levels were substantially elevated.

Finally, preliminary gene expression analysis of MH-S cells demonstrated the cell-type dependent effects of Enigmol. Fold changes in gene expression were generally minute, but there was a clear pro-inflammatory trend (Fig. 4-9C). In non-infected cells, 5 hour Enigmol treatment elicited significant upregulation of CXCL1, IL-1β, IL-6 and TNFα. Upregulation of these genes, and even others that did not meet significance, is noteworthy. With the exception of CXCL1 and IL-6, these genes are expressed at relatively high basal levels in MH-S cells. When genes are constitutively "on" at this level, even minor changes in gene regulation are considerable. This was magnified when MH-S cells were infected with IA/Udorn. As discussed earlier high-dose influenza infection elicited a rapid and robust pro-inflammatory response at 5h post-infection. IL-1β and IL-6 were the two most prominently upregulated cytokines, at 250-fold and 100-fold mock levels, respectively (Fig. 4-7). Yet, Enigmol further upregulated these genes another 2- and 3-fold. These results suggest that at low concentration, Enigmol may be a potent immunomodulator. Further evaluation is needed to determine whether these effects would be beneficial or deleterious *in vivo* for inflammatory alleviation.

## Discussion

A549 cells clearly respond to influenza A viral infection with a robust pro-inflammatory response. These findings directly correlate with the gene profile reported in live IAV-infected primary human alveolar type II cells at 4 and 24 hours post-infection [37]. They found the greatest increases in CXCL10 and CXCL11, both of which were induced 1000-fold above mock. A549 cells were alike with respect to CXCL10, but not CXCL11. This difference is not surprising, as A549 cells are adenocarcinomas, and cancer cells are known to have disparities in gene expression patterns compared to primary cells. However, the ability to induce such a strong inflammatory response with IAV infection, and the fact that A549 cells are responsive to sphingolipids [121], make this cell line a potential candidate for an *in vitro* model of sphingolipid therapy.

SK1i, SK2i, DMS and Enigmol conferred protection against influenza A viral infection in A549 cells by significantly reducing viral loads 1-2 logs versus non-treated cells. Yet, this effect was not seen in MDCK cells, though they express both sphingosine kinases and are responsive to other SK inhibitors. Both cell lines are epithelial cells, but from different tissues and animals (mouse lung versus canine kidney). SK1 and SK2 may be localized in different compartments of MDCK cells as compared to A549 cells, and therefore inhibition of these enzymes may not have the same anti-viral effect as in A549 cells.

SK1 and SK2 inhibition both resulted in a downregulation of influenza viral-induced cytokines, such as CCL2, CCL5, IL-6, IL-8, CXCL10, CXCL11 and TNFα in the lungs. This is an appealing feature in addition to the reduction of viral loads in A549 cells. Reducing expression of these major inflammatory cytokines may provide even greater protection against viral or dual infection-induced cytokine storm *in vivo*. CCL and CXCL proteins and interleukins are

chemotactic for leukocytes and lymphocytes, so their dampening would theoretically lead to a protective decrease in recruitment of these cells to the lungs during inflammation.

The ability of Enigmol to induce apoptosis may be a factor in viral load reduction. Apoptotic cells would quickly limit viral spread by eliminating host cells before viral infection or during replication after infection. However, the lack of noticeable CPE suggests that this was not a widespread effect because the monolayer was still intact at 24hpi. Therefore, there are most likely other signaling events that take place within the cell to confer this anti-viral activity.

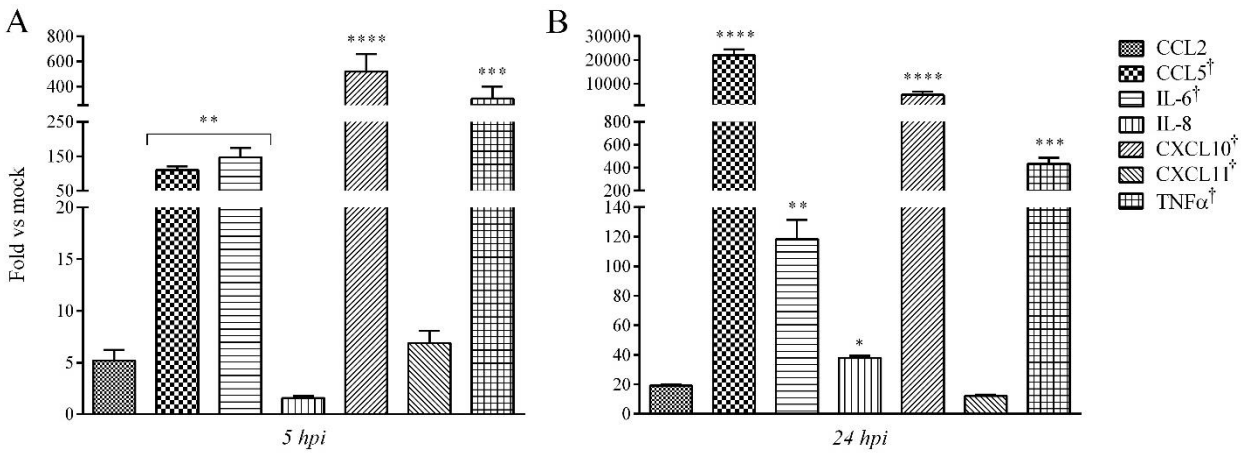


**Figure 4-1. Early and late gene expression profile of influenza-infected A549 cells.** Confluent A549 cells were infected with 1 MOI IA/Udorn/72. RNA was isolated from the cells at 5h (A) and 24h (B) post-infection. Cytokine mRNA expression levels were evaluated using real-time PCR. Values are expressed as fold change over mock (PBS) after normalization to GAPDH mRNA, a human house-keeping gene. ANOVA, Dunnett's multiple comparisons test (* $p < 0.05$, ** $p < 0.01$, *** $p < 0.005$, **** $p < 0.001$). Data represent two individual studies. †indicates gene with very low basal level expression

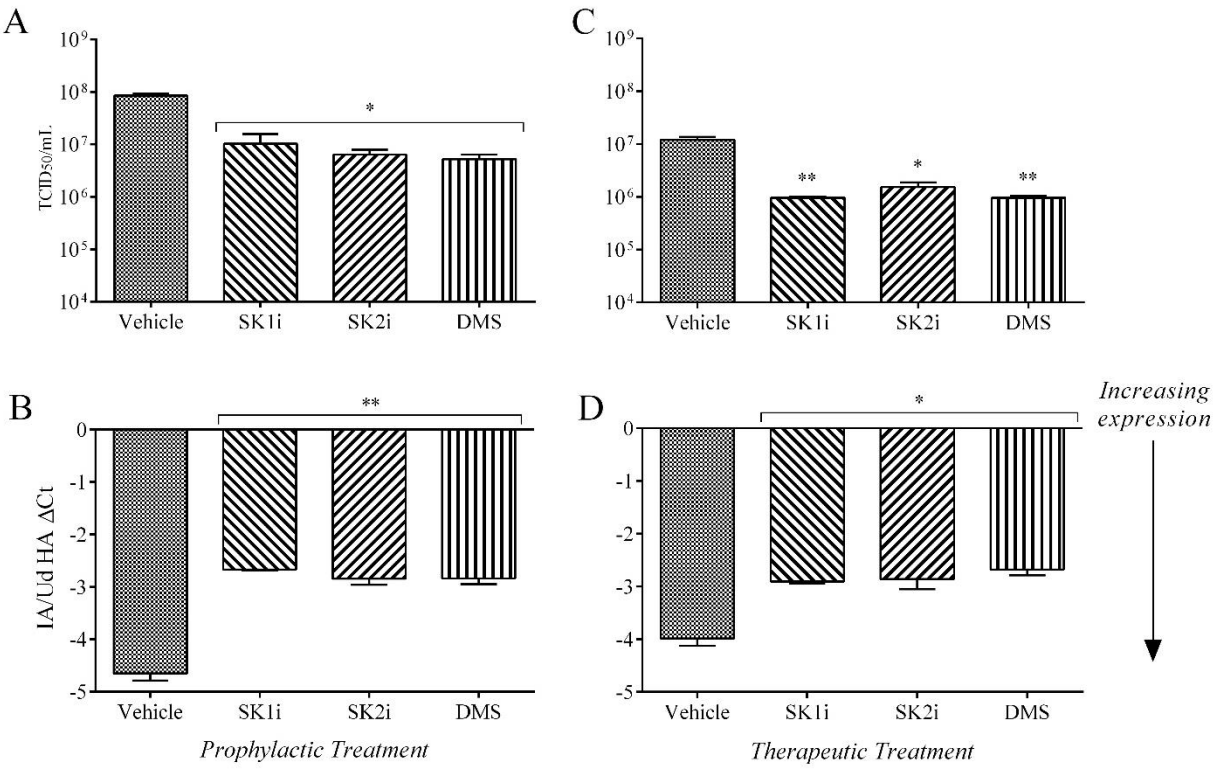


**Figure 4-2. Viral loads and IA/Udorn HA gene expression in treated A549 cells.** A549 cells were treated prophylactically with vehicle, 1uM SK1i, 1uM SK2i, or 1uM DMS for 24 hours prior to and again 24 hours following IA/Udorn infection (A,B) or therapeutically for 24 hours following infection (C,D). Cells were infected with 1 MOI IA/Udorn/72. Viral loads were measured at 24hpi (A,C). Expression of IA/Udorn HA mRNA was measured by real-time PCR and expressed as ΔCt values, which have been normalized to GAPDH (B,D). Decreasing ΔCt values indicate increasing gene expression. ANOVA, Tukey's multiple comparisons test or Kruskal-Wallis test (*$p < 0.05$, ** $p < 0.01$, *** $p < 0.005$).

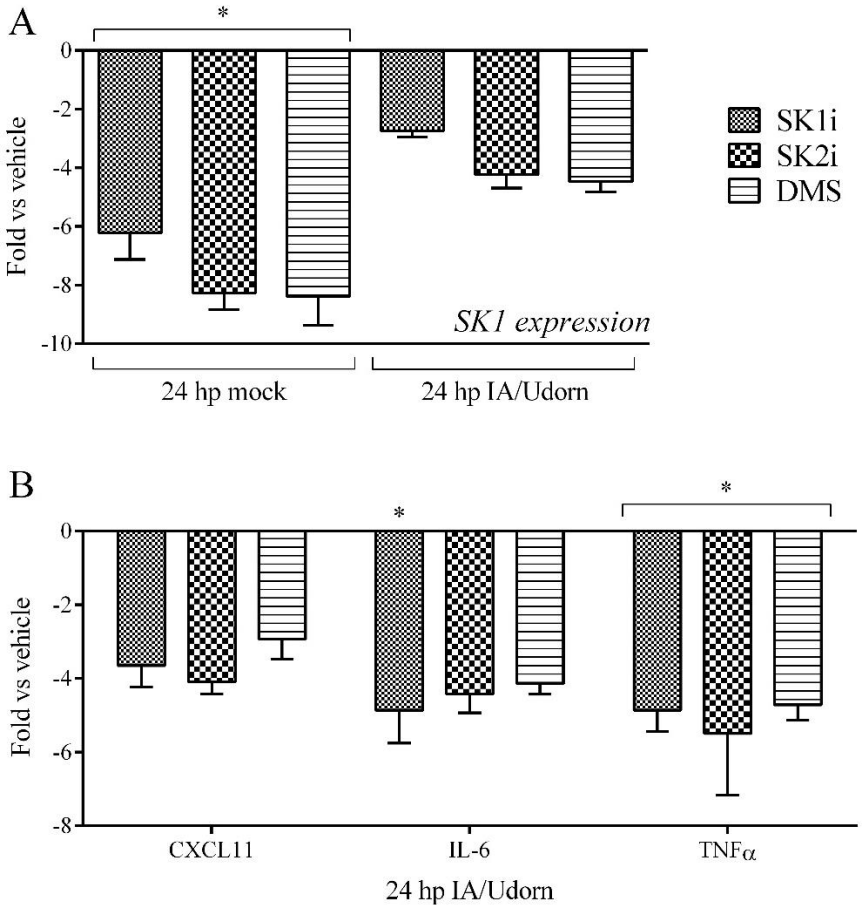


**Figure 4-3. Pre-treatment effect on gene expression in A549 cells.** A549 cells were treated with 1uM SK1i, 1uM SK2i or 1uM DMS for 24 hours prior to infection. After mock or 1 MOI IA/Udorn/72 infection, treatments were added back to cells for 24 hours. RNA was isolated from the cells at 24 hpi and mRNA transcripts were measured using real-time PCR. SK1 expression was decreased in both mock- and influenza-infected cells (A), whereas cytokine levels were only reduced during viral infection (B). Values are expressed as fold change over respective vehicle after normalization to GAPDH mRNA. ANOVA, Dunnett's multiple comparisons test (* $p < 0.05$).

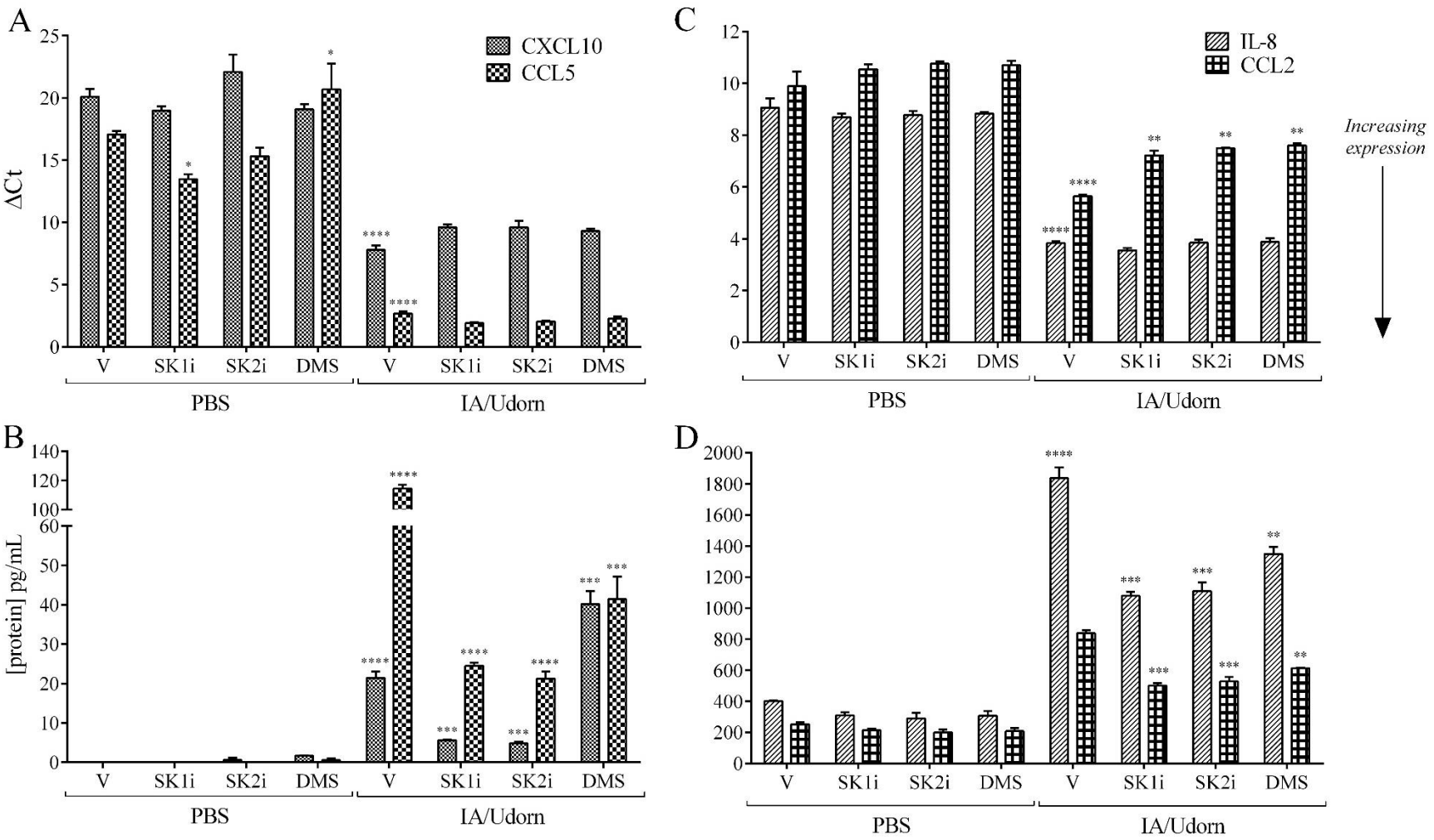


**Figure 4-4. Cytokine gene and protein expression in pre-treated A549 cells during influenza infection.** A549 cells were treated for 24 hours prior to infection. After mock or 1 MOI IA/Udorn/72 infection, treatments were added back to cells. RNA was isolated from the cells at 24hpi and cytokine mRNA expression levels were evaluated using real-time PCR (A,B). Values are expressed as ΔCt, normalized to GAPDH mRNA. Protein concentrations in 24hpi supernatants were measured by cytokine bead array (C,D). ANOVA, Tukey's multiple comparisons test (* $p < 0.05$, ** $p < 0.01$, *** $p < 0.005$). † *gene with basal Ct value < 35, which indicates gene expression is off under normal conditions.*

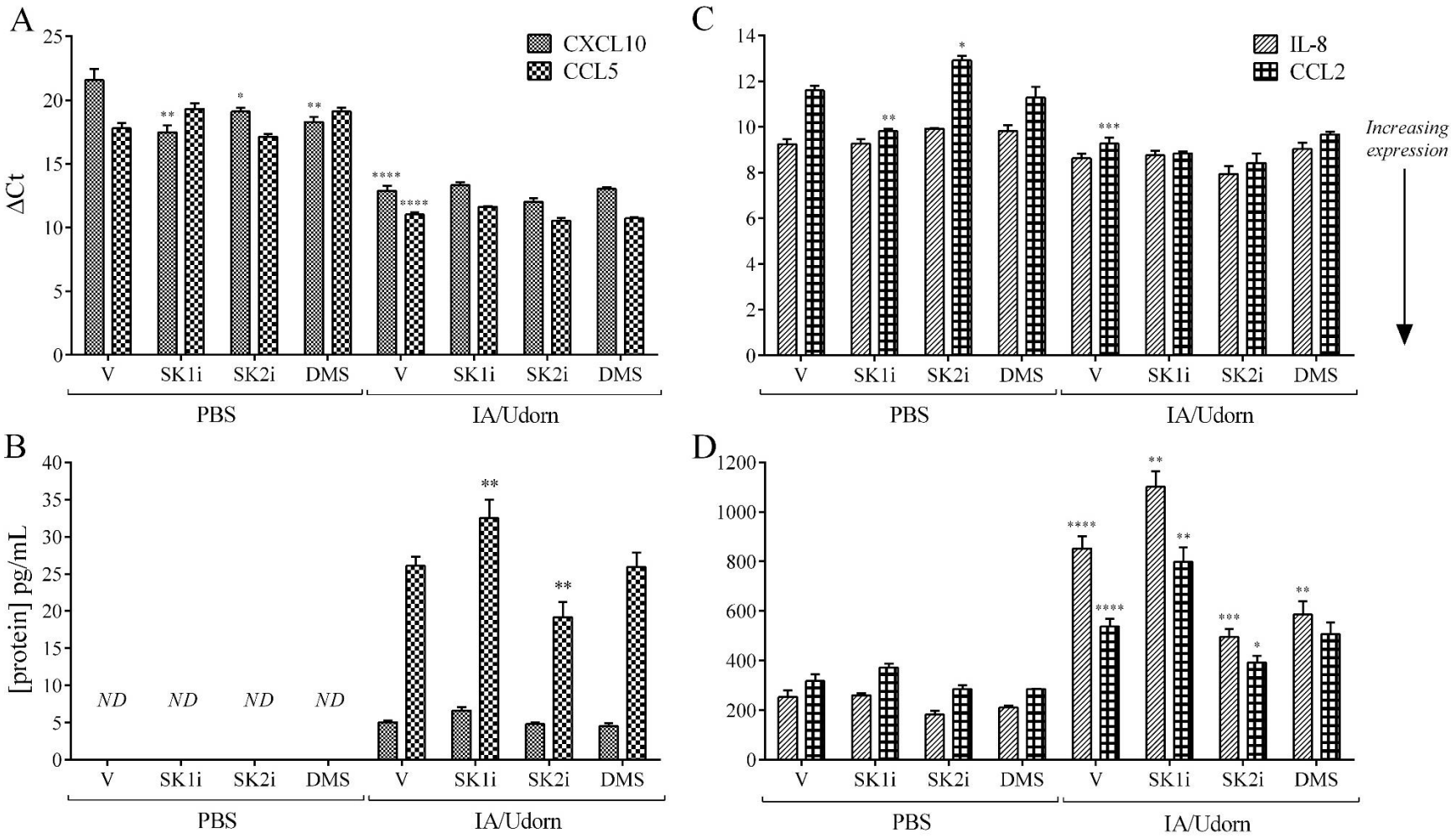


**Figure 4-5. Cytokine gene and protein expression in A549 cells treated after influenza infection.** A549 cells were treated for 5 or 24 hours after mock or 1 MOI IA/Udorn/72 infection. RNA was isolated from cells at 5hpi and cytokine expression was evaluated using real-time PCR (A,B). Values are expressed as ΔCt, normalized to GAPDH mRNA. Protein concentrations at 24hpi were measured by cytokine bead array (C,D). Mock-infected protein concentrations in panel B were below the level of detection (*ND= non-detectable*). ANOVA, Tukey's multiple comparisons test (* $p < 0.05$, ** $p < 0.01$, *** $p < 0.005$). † *gene with basal Ct value < 35, which indicates gene expression is off under normal conditions.*

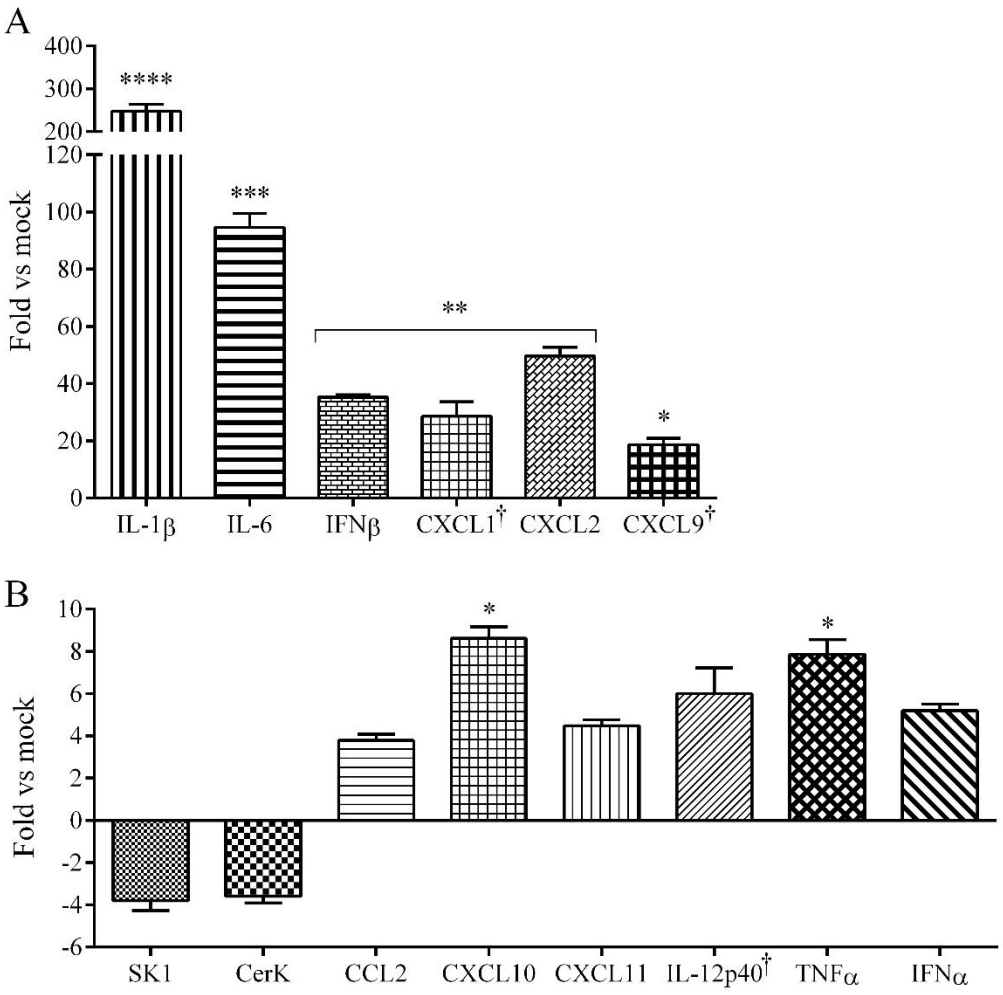


**Figure 4-6. Influenza-induced early response genes in MH-S cells.** MH-S cells were infected with mock (PBS) or 1 MOI IA/Udorn/72. RNA was isolated from the cells at 5hpi, and cytokine mRNA expression levels were evaluated using real-time PCR (A,B). Values are expressed as fold change over mock (PBS) after normalization to L19 mRNA. ANOVA, Dunnett's multiple comparisons test (* $p < 0.05$, ** $p < 0.01$, *** $p < 0.005$, **** $p < 0.001$). † *gene with basal Ct value < 35, which indicates gene expression is off under normal conditions.*

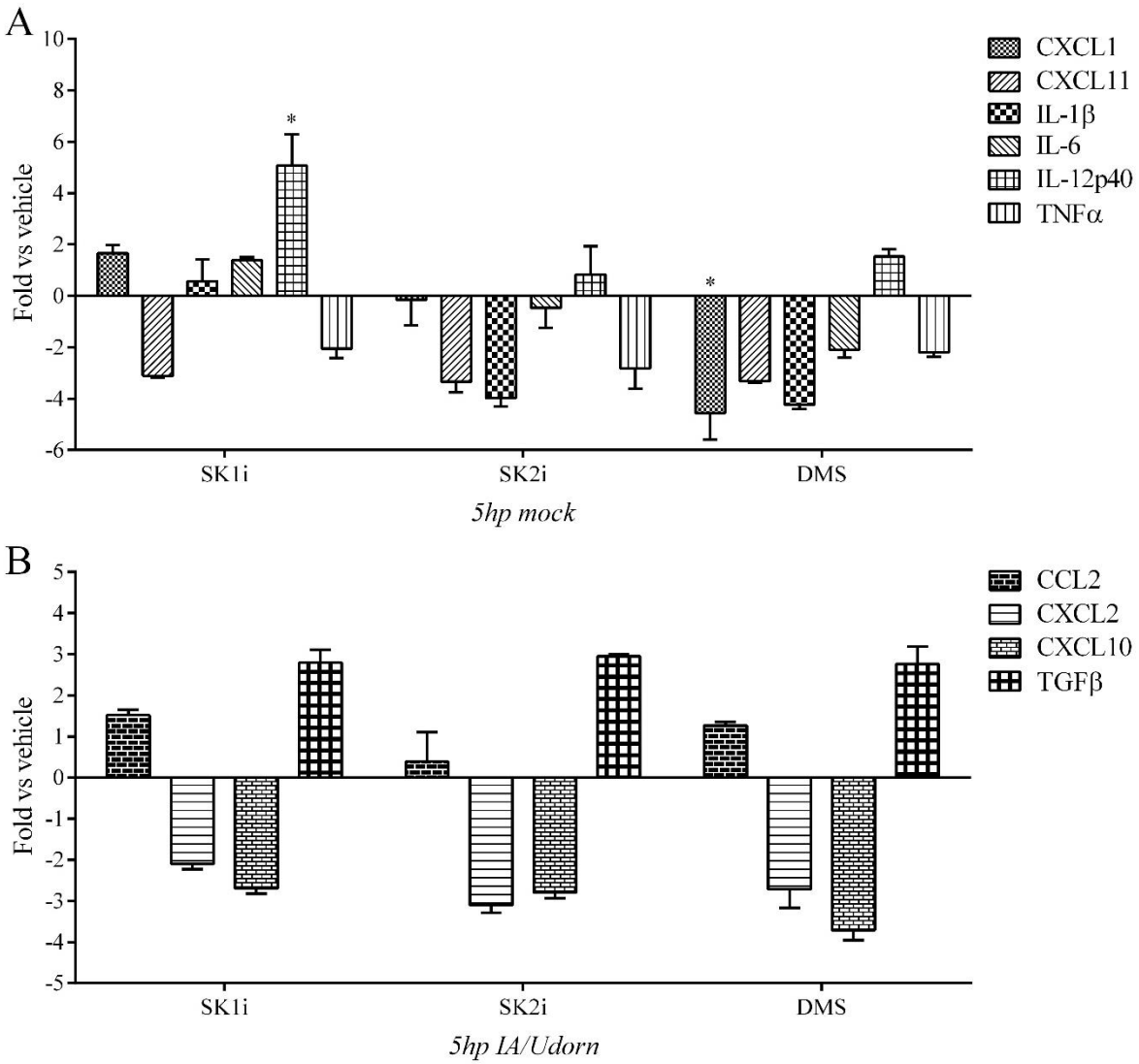


**Figure 4-7. Early cytokine response to sphingolipid treatment in MH-S cells.** MH-S cells were mock-infected (A) or infected with 1 MOI IA/Udorn/72 (B), then treated with 1uM SK1i, 1uM SK2i or 1uM DMS. RNA was isolated from the cells at 5hpi and cytokine mRNA expression levels were evaluated using real-time PCR. Values are expressed as fold change over respective vehicle after normalization to GAPDH or L19 mRNA. ANOVA, Dunnett's multiple comparisons test (* $p < 0.05$).

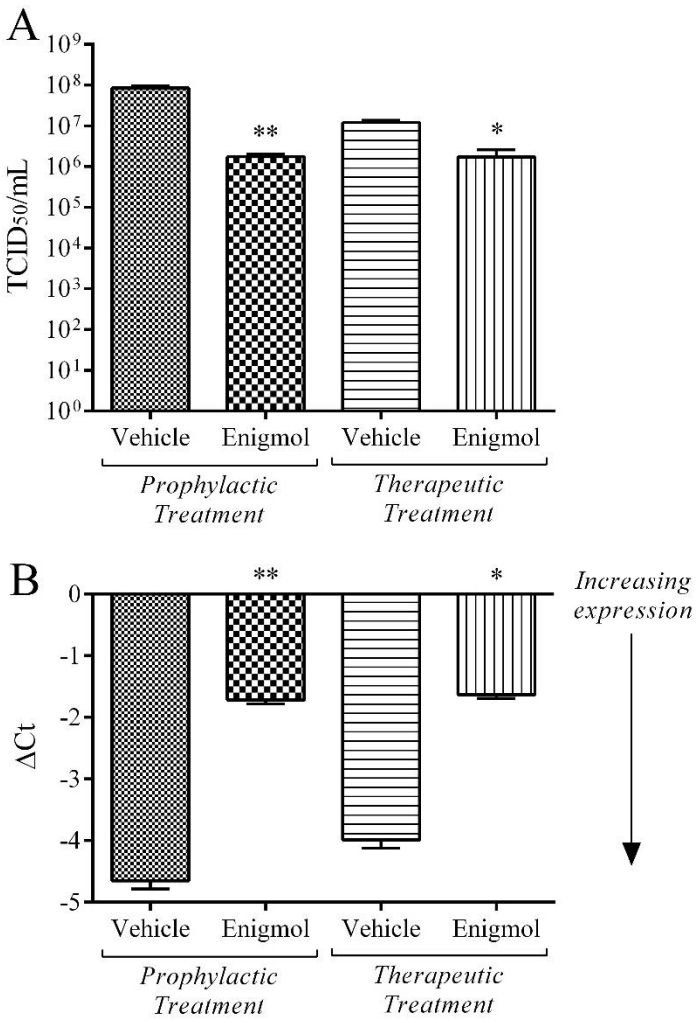


**Figure 4-8. Viral loads and IA/Udorn HA gene expression in Enigmol treated A549 cells.** A549 cells were treated prophylactically with vehicle or 1uM Enigmol for 24 hours prior to and again 24 hours following IA/Udorn infection or therapeutically for 24 hours following infection. Cells were infected with 1 MOI IA/Udorn/72. Viral loads were measured at 24hpi (A). Expression of IA/Udorn HA mRNA was measured by real-time PCR and expressed as ΔCt values, which have been normalized to GAPDH (B). Decreasing ΔCt values indicate increasing gene expression. ANOVA, Tukey's multiple comparisons test or Kruskal-Wallis test (*$p < 0.05$, ** $p < 0.01$).

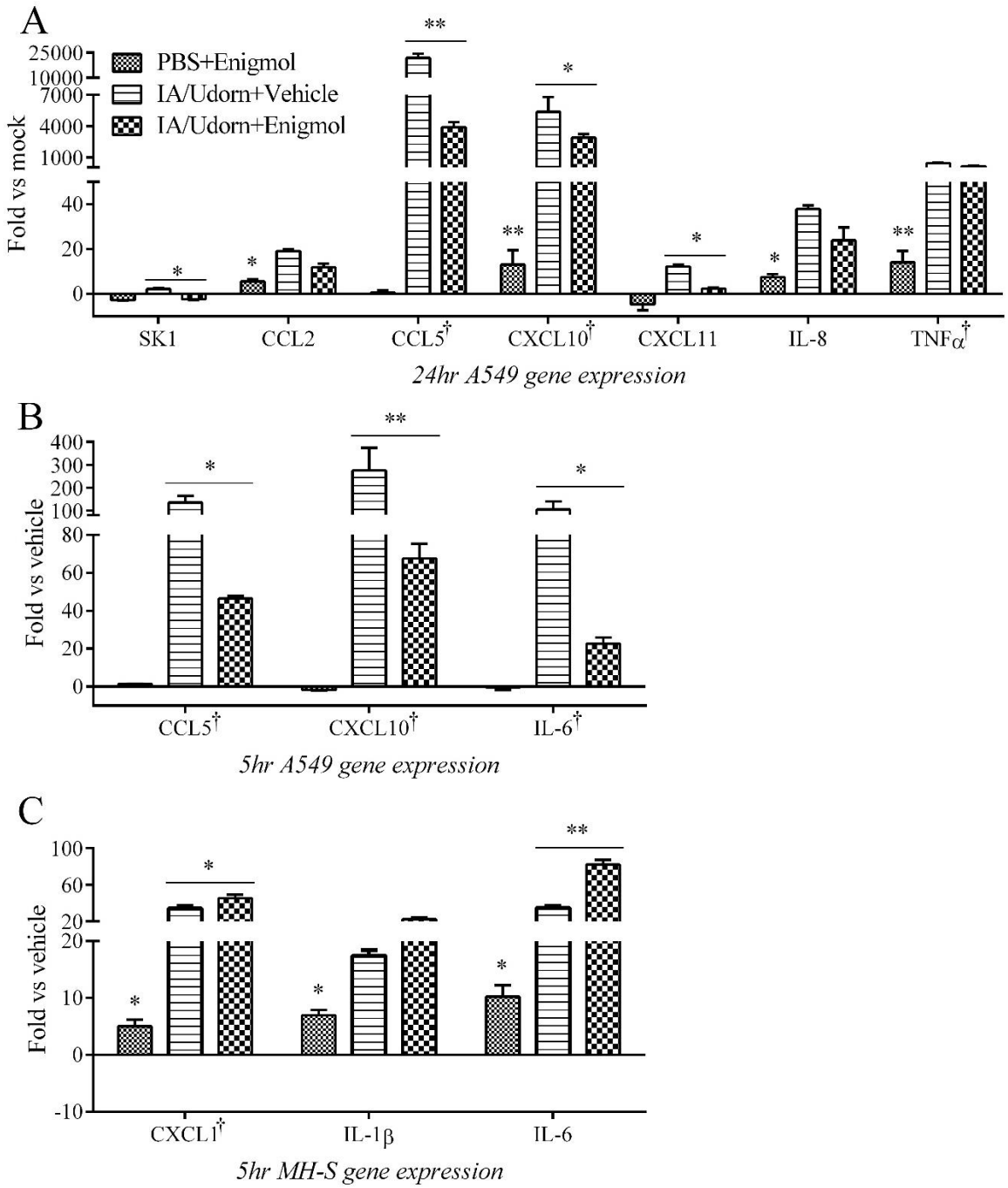


**Figure 4-9. Enigmol-induced gene expression in A549 and MH-S cells.** Cells were pretreated (A) or treated following infection (B,C) with 1μM Enigmol. A549 cells were treated with Enigmol for 24hr (A) or 5hr (B) after IA/Udorn/72 infection before RNA was harvested. MH-S cell were treated with Enigmol for 5hpi (C) before RNA collection. Cytokine mRNA expression levels were evaluated using real-time PCR. Values are expressed as fold change over respective vehicle (either mock or IA/Udorn) after normalization to L19 mRNA. ANOVA, Dunnett's multiple comparisons test (* $p < 0.05$, ** $p < 0.01$). † *indicates gene with basal Ct value < 35, which indicates gene expression is off under normal conditions.*

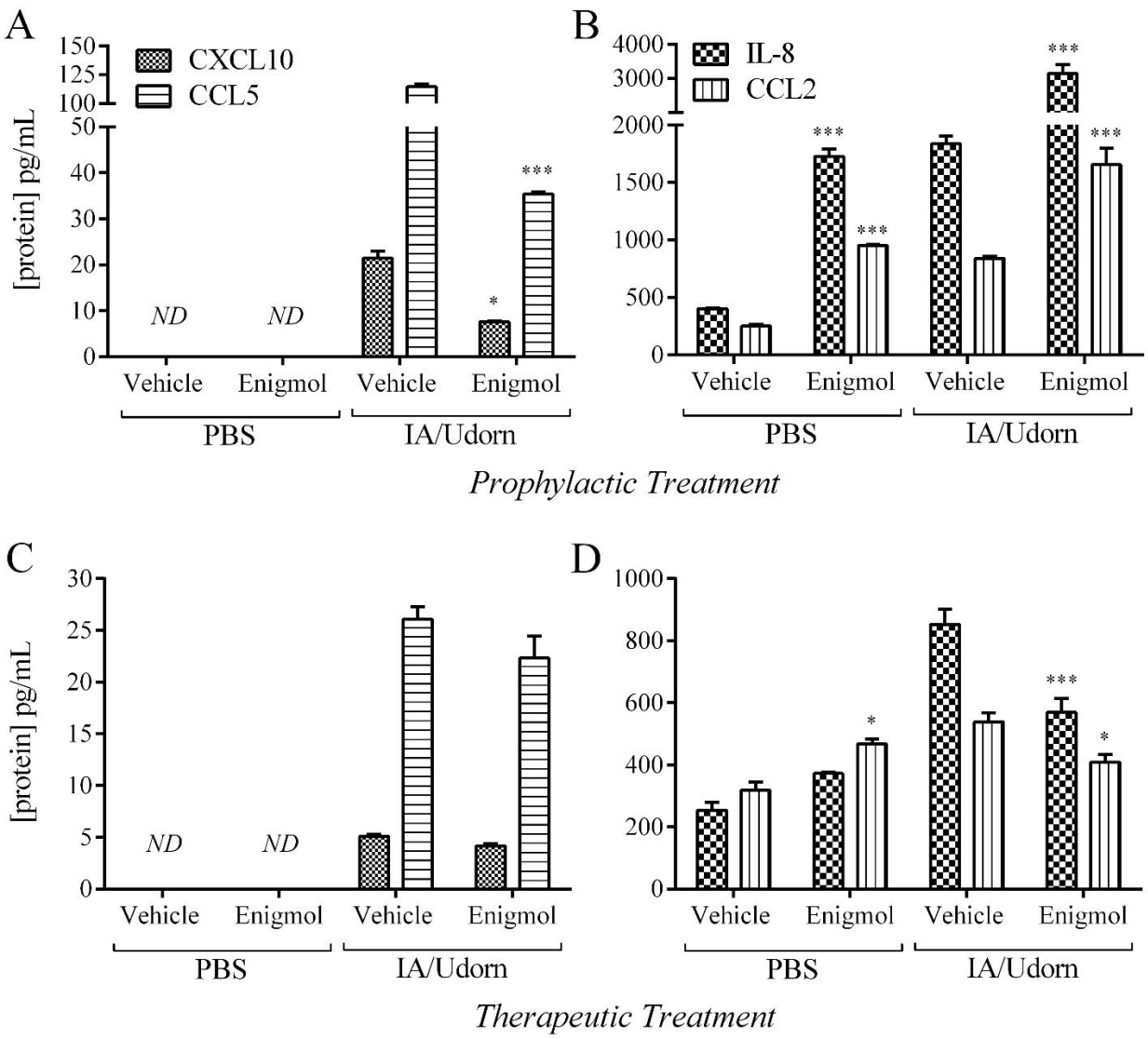


**Figure 4-10. Enigmol-induced protein expression in A549 cells.** Cells were pre-treated for 24hr with 1μM Enigmol (A,B) or not pre-treated (C,D) prior to infection with IA/Udorn/72. After viral challenge, cells were treated with Enigmol for 24hpi. Protein concentrations were measured by cytokine bead array. Mock-infected protein concentrations in panels A and C were below the level of detection (*ND= non-detectable*).. ANOVA, Dunnett's multiple comparisons test (* $p < 0.05$, ** $p < 0.01$, *** $p < 0.05$).

## **Chapter Five:** Conclusions and Future Directions

Our influenza A virus:*Streptococcus pneumoniae* dual infection study in the aged mouse model demonstrated that this population truly is at a greater risk for this devastating disease. Prolonged recovery time from even a mild seasonal IAV infection, let alone pandemic or HPAI strains, seems to contribute to the extended susceptibility to secondary bacterial pneumonia. Although we evaluated this susceptibility only up to 3 weeks after primary viral infection, it is highly likely that vulnerability to this lethal synergistic disease continues for months after viral clearance and supposed resolution of airway inflammation. One may argue that a naïve aged mouse model is flawed because humans are exposed to influenza viruses nearly every year even without vaccination, which confers at least some cross-protection. Clinical cases and statistics, however, show that this is not full-proof. A meta-analysis of 18 cohorts in the aged demographic revealed only a 27% reduction in hospitalization and 48% reduction in mortality due to influenza-associated illness [122]. Theoretically, yearly vaccination provides the greatest possible protection because of antigenic-matching and frequency of administration, yet its efficacy and potential risks for the elderly (and other groups) are still substantial limitations. Furthermore, the inadequacies of currently-approved therapeutics (NAIs and M2 channel blockers) render them completely ineffective if not administered within 48 hours of infection. This short time span is still within the incubation period of the virus, at which time the host is often asymptomatic. For these reasons, and the fact that influenza A virus is fundamentally immune to eradication, it is crucial that influenza treatment research continues to explore other avenues.

Sphingolipid modulation is one such promising avenue that is still in the nascent stages. Our findings, in addition to those of Oldstone et al. [77, 85-87] and many others, show that this

novel therapeutic target has great potential for redirecting the aberrant host response to inflammation-inducing pathogens or autoimmune disease, that may alleviate the detriment it leaves in its wake. Possibly one of the most important qualities of the therapeutics we evaluated *in vivo*, FTY720 and Enigmol, was the noted lack of adverse side effects within the non-infected mouse. In fact, we know that this property of FTY720 is extended to humans as well, since it is already an FDA-approved drug for MS treatment. Further studies are imperative to fine-tune this therapeutic, such as assessing the differences between local and systemic activity. We chose a systemic dose so as not to overwhelm the lungs with fluid, though we did test intranasal FTY720 dosing in a preliminary study. Importantly, reports with AAL-R have clearly demonstrated the necessity of local administration for its efficacy in protection against HP influenza infection [85]. Our pilot study with intranasal FTY720 administration revealed that this route induces a lymphopenic response comparable to that of systemic administration, which suggests that local treatment may be a preferable method.

Sphingosine kinase inhibitors and the sphingosine analog Enigmol offer alternative approaches to prophylaxis or therapy against influenza and similar inflammatory diseases. Their direct effect on alveolar epithelial cells to reduce viral loads is substantial in itself. The ability to limit rampant production of infectious virus could mitigate, or even prevent, the cascade of events leading to the potentially fatal dysregulated inflammatory host response, immune cell recruitment and cytokine storm. Yet, we also observed the direct modulation of the influenza-induced cytokines associated with the cytokine storm. Overall, sphingosine kinase inhibitors acted in an immunosuppressive manner by dampening, but not completely abrogating, their expression. A pro-inflammatory response is essential for combating the viral infection, so it is key that these inhibitors do not completely block the innate inflammatory response. Enigmol, on the other hand,

selectively enhanced expression of pro-inflammatory cytokine genes and proteins. Although this would seem highly unfavorable, Enigmol actually reduced viral loads in A549 cells even more than the sphingosine kinase inhibitors. This implies a different mechanism of protection than the SK inhibitors, and necessitates further exploration. As a whole, these targets bring exciting prospects for anti-influenza therapies and preventatives because they exploit the host's own naturally-occurring cellular processes. Notably, targeting the host response rather than the virus itself, In fact, the non-specific nature of these effects, as opposed to viral protein-targeting drugs, could prove invaluable to a number of other viral and inflammatory diseases. Therefore, continued research in this field to understand the exact mechanisms and implications of modulating the sphingolipid profile would vastly advance our knowledge of the nature of these metabolites and how we may employ them to combat lethal disease.

## References


1. Lamb, R., Krug, RM, *Fundamental Virology (Fourth Edition)*, ed. P.H. DM Knipe. 2001, Philadelphia: Lippincott Williams & Wilkins. 725-762.
2. Rumschlag-Booms, E., Rong, L, *Influenza A virus entry: implications in virulence and future therapeutics.* Advances in Virology, 2012. **2013**: p. 1-9.
3. Sullivan, K., AS Monto, *Population estimates of persons presenting to general practitioners with influenza-like illness, 1987-96: a study of the demography of influenza-like illness in sentinel practice networks in England and Wales, and in the Netherlands.* Epidemiology & Infection, 2000. **124**(2): p. 145-160.
4. Webster, R., Bean, WJ, Gorman, OT, Chambers, TM, Y Kawaoka, *Evolution and ecology of influenza A viruses.* Microbiological Reviews, 1992. **56**(1): p. 152-179.
5. Wille, M., Tolf, C, Avril, A, Latorre-Margalef, N, Wallerstrom, S, Olsen, B and J Waldenstrom, *Frequency and patterns of reassortment in natural influenza A virus infection in a reservoir host.* Virology, 2013. **Article in Press**: p. 1-11.
6. Tamerius, J., Nelson, MI, Zhou, SZ, Viboud, C, Miller, MA and WJ Alonso, *Global influenza seasonality: reconciling patterns across temperate and tropical regions.* Environ Health Perspect, 2011. **119**(4): p. 439-445.
7. *Influenza (seasonal) Fact sheet*. Influenza Virus. World Health Organization, April 2009.
8. *Estimating seasonal influenza-associated deaths in the United States: CDC study confirms variability of flu*. Seasonal Influenza. Centers for Disease Control and Prevention, 2011.
9. Kuiken, T., Riteau, B, Fouchier, RAM, GF Rimmelzwaan, *Pathogenesis of influenza virus infections: the good, the bad and the ugly.* Curr Opinion in Virol, 2012. **2**: p. 276-286.
10. Kreijtz, J., Fouchier, RAM, GF Rimmelzwaan, *Immune responses to influenza virus infection.* Virus Research, 2011. **162**: p. 19-30.
11. Taubenberger, J., JC Kash, *Insights on influenza pathogenesis from the grave.* Virus Research, 2011. **162**(1-2): p. 2-7.
12. Peiris, J., de Jong, MD, Y Guan, *Avian influenza virus (H5N1): a threat to human health.* Clin Microbiol Rev, 2007. **20**(2): p. 243-267.
13. Chen, W., Calvo, PA, Malide, D, Gibbs, J, Schubert, U, Bacik, I, Basta, S, O'Neill, R, Schickli, J, Palese, P, Henklein, P, Bennink, JR, JW Yewdell, *A novel influenza A virus mitochondrial protein that induces cell death.* Nat Med, 2001. **7**: p. 1306-1312.
14. Varga, Z., P Palese, *The influenza A virus protein PB1-F2.* Virulence, 2011. **2**(6): p. 542-546.
15. Julkunen, I., Sareneva, T, Pirhonen, J, Ronni, T, Melen,K, S Matikainen, *Molecular pathogenesis of influenza A virus infection and virus-induced regulation of cytokine gene expression.* Cytokine & Growth Factor Rev, 2001. **12**: p. 171-180.
16. Pinto, L., Holsinger, LJ, RA Lamb, *Influenza virus M2 protein has ion channel activity.* Cell, 1992. **69**(3): p. 517-528.
17. Salahuddin, P., AU Khan, *Structural and functional analysis of NS1 ans NS2 proteins of H1N1 subtype.* Gen Prot Bioinformatics, 2010. **8**(3): p. 190-199.
18. Matrosovich MN, M.T., Gray T, Roberts NA, Klenk HD, *Human and avian influenza viruses target different cell types in cultures of human airway epithelium.* PNAS, 2004. **101**(13): p. 4620-4624.

19. Nayak DP, H.E., Barman S, *Assembly and budding of influenza virus.* Virus Research, 2004. **106**(2): p. 147-165.
20. Hutchinson, E., von Kirchbach, JC, Gog, JR, P Digard, *Genome packaging in influenza A virus.* J of Gen Viro, 2010. **91**(313-328).
21. Hughey PG, C.R., Zebedee SL, RA Lamb, *Expression of the influenza A virus M2 protein is restricted to apical surfaces of polarized epithelial cells.* J of Virology, 1992. **66**(9): p. 5542-5552.
22. Roth MG, C.R., Giusti L, Davis AR, Nayak DP, MJ Gething, *Influenza virus hemagglutinin expression is polarized in cells infected with recombinant SV40 viruses carrying cloned hemagglutinin DNA.* Cell, 1983. **33**(2): p. 435-443.
23. Bui M, W.E., Helenius A, Whittaker GR, *Role of the influenza virus M1 protein in nuclear export of viral ribonucleoproteins.* J of Virology, 2000. **74**(4): p. 1781-1786.
24. Zhang J, P.A., Lamb RA, *Influenza virus assembly and lipid raft microdomains: a role for the cytoplasmic tails of the spike glycoproteins.* J of Virology, 2000. **74**(10): p. 4634-4644.
25. Schmitt AP, R.L., *Influenza virus assembly and budding at the viral budzone.* Adv Vir Res, 2005. **64**: p. 383-416.
26. Chen BJ, L.G., Morita E, RA Lamb, *Influenza virus hemagglutinin and neuraminidase, but not the matrix protein, are required for assembly and budding of plasmid-derived virus-like particles.* J of Virology, 2007. **81**(13): p. 7111-7123.
27. Pang, I., A Iwasaki, *Inflammasomes as mediators of immunity against influenza virus.* Trends Immunol, 2011. **32**(1): p. 34-41.
28. Diebold, S., Kaisho, T, Hemmi, H, Akira, S, C Reis e Sousa, *Innate antiviral responses by means of TLR7-mediated recognition of single-stranded RNA.* Science, 2004. **303**: p. 1529-1531.
29. Ichinohe, T., Iwasaki, A, H Hasegawa, *Innate sensors of influenza virus: clues to developing better intranasal vaccines.* Expert Rev Vaccines, 2008. **7**(9): p. 1435-1445.
30. Kato, H., S Sato, M Yoneyama, M Yamamoto, S Uematsu, K Matsui, T Tsujimura, K Takeda, T Fujita, O Takeuchi, S Akira, *Cell type-specific involvement of RIG-I in antiviral response.* Immunity, 2005. **23**: p. 19-28.
31. A Pichlmair, O.S.a.C.T., *RIG-I-mediated antiviral responses to single-stranded RNA bearing 5'-phosphates.* Science, 2006. **314**: p. 5.
32. T Ichinohe, I.P.a.A.I., *Influenza virus activates inflammasomes via its intracellular M2 ion channel.* Nat Immunol, 2010. **11**(5): p. 7.
33. Unkel, B., Hoegner, K, Clausen, BE, Lewe-Schlosser, P, Bodner, J, Gattenloehner, S, Janßen, H, Seeger, W, Lohmeyer, J, S Herold, *Alveolar epithelial cells orchestrate DC function in murine viral pneumonia.* J Clin Invest, 2012. **122**(10): p. 3652-3664.
34. Herzog, E., Brody, AR, Colby, TV, Mason, R, MC Williams, *Knowns and unknowns of the alveolus.* Proc Am Thorac Soc, 2008. **5**(778-782).
35. Yu, W., Chan, RWY, Want, J, Travanty, EA, Nicholls, JM, Peiris, JSM, Mason, RJ, MCW Chan, *Viral replication and innate host responses in primary human alveolar epithelial cells and alveolar macrophages infected with influenza H5N1 and H1N1 viruses.* J of Virology, 2011. **85**(14): p. 6844-6855.
36. Herold, S., von Wulffen, W, Steinmueller, M, Pleschka, S, Kuziel, WA, Mack, M, Srivastava, M, Seeger, W, Maus, UA, J Lohmeyer, *Alveolar epithelial cells direct*

*monocyte transepithelial migration upon influenza virus infection: impact of chemokines and adhesion molecules.* J Immunology, 2006. **177**(1817-1824).
37. Wang, J., Nikrad, MP, Phang, T, Gao, B, Alford, T, Ito, Y, Edeen, K, Travanty, EA, Kosmider, B, Hartshorn, K, RJ Mason, *Innate immune response to influenza A virus in differentiated human alveolar type II cells.* Am J Respir Cell Mol Biol, 2011. **45**: p. 582-591.
38. Hussell, T., J Goulding, *Structured regulation of inflammation during respiratory viral infection.* Lancet Infect Dis, 2010. **10**(5): p. 360-366.
39. Tumpey, T., Garcia-Sastre, A, Taubenberger, JK, Palese, P, Swayne, DE, Pantin-Jackwood, MJ, Katz, JM, CF Basler, *Pathogenicity of influenza viruses with genes from the 1918 pandemic virus: functional roles of alveolar macrophages and neutrophils in limiting virus replication and mortality in mice.* J of Virology, 2005. **79**(23): p. 14933-14944.
40. Wang, J., Nikrad, MP, Travanty, EA, Zhou, B, Phang, T, Gao, B, Alford, T, Ito, Y, Nahreini, P, Hartshorn, K, Wentworth, D, Dinarello, CA, RJ Mason, *Innate immune response of human alveolar macrophages during influenza A infection.* PLoS ONE, 2011. **7**(3): p. 1-12.
41. Rubins, J., *Alveolar macrophages: wielding the double-edged sword of inflammation.* Amer J of Resp and Critical Care Med, 2003. **167**: p. 2.
42. Haslett, C., *Granulocyte apoptosis and its role in the resolution and control of lung inflammation.* Am J Respir Crit Care Med, 1999. **160**(5-11).
43. Rathinasamy, A., Czeloth, N, Pabst, O, Forster, R, G Bernhardt, *The origin and maturity of dendritic cells determine the pattern of sphingosine 1-phosphate receptors expressed and required for efficient migration.* J Immunology, 2010. **185**: p. 4072-4081.
44. Cook, D., K Bottomly, *Innate immune control of pulmonary dendritic cell trafficking.* Proc Am Thorac Soc, 2007. **4**: p. 234-239.
45. GeurtsvanKessel, C., Willart, MAM, vanRijt, LS, Muskens, F, Kool, M, Baas, C, Thielemans, K, Bennett, C, Clausen, BE, Hoogsteden, HC, Osterhaus, ADME, Rimmelzwaan, GF, BN Lambrecht, *Clearance of influenza virus from the lung depends on migratory langerin+CD11b- but no plasmacytoid dendritic cells.* J Exp Med, 2008. **205**(7): p. 1621-1634.
46. Albert, M., Sauter, B, Bhardwaj, N, *Dendritic cells acquire antigen from apoptotic cells and induce class I-restricted CTLs.* Nature, 1998. **392**: p. 86-89.
47. Diebold, S., Montoya, M, Unger, H, Alexopoulou, I, RP Haswell, *Viral infection switches non-plasmacytoid dendritic cells into high interferon producers* Nature, 2003. **424**: p. 324-328.
48. Tisoncik, J., Korth, MJ, Simmons, CP, Farrar, J, Martin, TR, MG Katze, *Into the eye of the cytokine storm.* Microbiol and Molec Biol Reviews, 2012. **76**(1): p. 16-32.
49. Groom, J., AD Luster, *CXCR3 ligands: redundant, collaborative and antagonistic functions.* Immunol and Cell Biology, 2011. **89**: p. 207-215.
50. D Kobasa, S.J., K Shinya, JC Kash, J Copps, H Ebihara, Y Hatta, JH Kim, P Halfmann, M Hatta, F Feldmann, JB Alimonti, L Fernando, Y Li, MG Katze, H Feldmann and Y Kawaoka, *Aberrant innate immune response in lethal infection of macaques with the 1918 influenza virus.* Nature, 2007. **445**: p. 5.
51. VT Peltola, K.M.a.J.M., *Influenza virus neuraminidase contributes to secondary bacterial pneumonia.* J Infect Dis, 2005. **192**: p. 9.

52. Rehg, J.M.a.J., *Lethal synergism between influenza virus and Streptococcus pneumoniae: characterization of a mouse model and the role of platelet-activating factor receptor.* J Infect Dis, 2002. **186**: p. 10.
53. JO Hendley, M.S., PM Steward and JM Gwaltney Jr, *Spread of Streptococcus pneumoniae in families. I. Carriage rates and distribution types.* J Infect Dis, 1975. **132**(1): p. 7.
54. McCullers, J., *Insights into the interaction between influenza virus and pneumococcus.* Clin Microbiol Rev, 2006. **19**(3): p. 10.
55. JL Speshock, N.D.-R., R Rabah, MN Neely, PC Roberts, *Filamentous influenza A virus infection predisposes mice to fatal septicemia following superinfection with Streptococcus pneumoniae serotype 3.* Infection and Immunity, 2007. **75**(6): p. 10.
56. AM Smith, F.A., RM Ribeiro, RN Gutenkunst, JL McAuley, JA McCullers and AS Perelson., *Kinetics of coinfection with influenza A virus and Streptococcus pneumoniae.* PLoS ONE, 2013. **9**(13): p. 12.
57. Price, J., Jarrell, JA, Furman, D, Kattah, NH, Newell, E, Dekker, CL, Davis, MM, PJ Utz, *Characterization of influenza vaccine immunogenicity using influenza antigen microarrays.* PLoS ONE, 2013. **8**(5): p. 1-13.
58. Samson, M., Pixxorno, A, Abed, Y, G Boivin, *Influenza virus resistance to neuraminidase inhibitors.* Antiviral Res, 2013. **98**(2): p. 174-185.
59. CDC, *High levels of adamantane resistance among influenza A (H3N2) viruses and interim guidelines for use of antiviral agents.* MMWR Morb Mortal Wkly Rep, 2006. **55**(2): p. 44-46.
60. A Adan-Gokbulut, M.K.-Y., G Iskender and Y Baran, *Novel agents targeting bioactive sphingolipids for the treatment of cancer.* Curr Medicinal Chem, 2013. **20**: p. 15.
61. Pruett, S., Bushnev, A, AH Merrill, *Biodiversity of sphingoid bases and related amino alcohols.* J Lipid Research, 2008. **49**(8): p. 1621-1639.
62. Spiegel, C.C.a.S., *Sphingosine 1-phosphate and ceramide 1-phosphate: expanding roles in cell signaling.* J Cell Sci, 2005. **118**: p. 8.
63. Okada, T., Ding, G, Sonoda, H, Kajimoto, T, Haga, Y, Khosrowbeygi, A, Gao, S, Miwa, N, Jahangeer, S, S-i Nakamura, *Involvement of N-terminal-extended form of sphingosine kinase 2 in serum-dependent regulation of cell proliferation and apoptosis.* J Biol Chem, 2005. **280**(43): p. 36318-36325.
64. Neubauer, H., SM Pitson, *Roles, regulation and inhibitors of sphingosine kinase 2.* FEBS Journal, 2013: p. 1-20.
65. Wang, Z., Min, X, Xiao, S-H, Johnstone, S, Romanow, W, Meininger, D, Xu, H, Liu, J, Dai, J, An, S, Thibault, S, N Walker, *Molecular basis of sphingosine kinase 1 substrate recognition and catalysis.* Structure, 2013. **21**: p. 798-809.
66. Lima, S., S Spiegel, *Sphingosine kinase: a closer look at last.* Structure, 2013. **21**(690-692).
67. Wattenberg, B., Pitson, SM, DM Raben, *The sphingosine and diacylglycerol kinase superfamily of signaling kinases: localization as a key to signaling function.* J of Lipid Res, 2006. **47**: p. 1128-1139.
68. Xia, P., J. R. Gamble, K. A. Rye, L. Wang, C. S. Hii, P. Cockerill, Y. Khew-Goodall, A. G. Bert, P. J. Barter, and M. A. Vadas, *Tumor necrosis factor-alpha induces adhesion molecule expression through the sphingosine kinase pathway.* Proc Natl Acad Sci, 1998. **95**: p. 14196-14201.

69. Mastrandrea, L.D., S. M. Sessanna, and S. G. Laychock, *Sphingosine kinase activity and sphingosine-1 phosphate production in rat pancreatic islets and INS-1 cells: response to cytokines.* Diabetes, 2005. **54**(1429-1436).
70. Olivera, A., S Spiegel, *Sphingosine-1-phosphate as second messenger in cell proliferation induced by PDGF and FCS mitogens.* Nature, 1993. **365**: p. 557-560.
71. Meyer zu Heringdorf, D., H. Lass, I. Kuchar, M. Lipinski, R. Alemany, U. Rumenapp, and K. H. Jakobs, *Stimulation of intracellular sphingosine-1-phosphate production by G-protein coupled sphingosine-1-phosphate receptors.* Eur. J Pharmacol, 2001. **414**: p. 145-154.
72. Siow, D., Anderson, CD, Berdyshev, EV, Skobeleva, A, Pitson, SM, BW Wattenberg, *Intracellular localization of sphingosine kinase 1 alters access to substrate pools but does not affect the degradative fate of sphingosine-1-phosphate.* J Lipid Research, 2010. **51**: p. 2546-2559.
73. Obeid, Y.H.a.L., *Principles of bioactive lipid signaling: lessons from sphingolipids.* Nat Rev Mol Cell Biol, 2008. **9**(2): p. 10.
74. Spiegel, S., S Milstien, *The outs and the ins of sphingosine-1-phosphate in immunity.* Nature Reviews, 2011. **11**: p. 403-415.
75. Cyster, S.S.a.J., *Finding a way out: lymphocyte egress from lymphoid organs.* Nature Immunol, 2007. **8**: p. 7.
76. CN Jenne, A.e., R Rivera, SR Watson, AJ Bankovich, JP Pereira, Y Xu, CM Roots, JN Beilke, A Banerjee, SL Reiner, SA Miller, AS Weinmann, CC Goodnow, LL Lanier, JG Cyster and J Chun, *T-bet-dependent S1P5 expression in NK cells promotes egress from lymph nodes and bone marrow*. J Exp Med, 2009. **206**(11): p. 3.
77. MBA Oldstone, J.T., KB Walsh and H Rosen, *Dissecting influenza virus pathogenesis uncovers a novel chemical approach to combat the infection.* Virology, 2013. **435**: p. 10.
78. Konig, K., et al., *Four-and-a-half LIM domain protein 2 is a novel regulator of sphingosine 1-phosphate receptor 1 in CCL19-induced dendritic cell migration.* J Immunology, 2010. **185**: p. 1466-1475.
79. Walzer, T.e.a., *Natural killer cell trafficking in vivo requires a dedicated sphingosine 1-phosphate receptor.* Nature Immunol., 2007. **8**: p. 1337-1344.
80. Takabe, K., Paugh, SW, Milstien, S, S Spiegel, *"Inside-out" signaling of sphingosine-1-phosphate: therapeutic targets.* Pharmacol Rev, 2008. **60**(2): p. 181-195.
81. Pitson, S., et al, *Activation of sphingosine kinase 1 by ERK1/2-mediated phosphorylation.* EMBO J, 2003. **22**: p. 5491-5500.
82. Siehler, S., Wang, Y, Fan, X, Windh, RT, DR Manning, *Sphingosine 1-phosphate activates nuclear factor-κB through Edg receptors. Activation through Edg-3 and Edg-5, but not Edg-1, in human embryonic kidney 293 cells.* J Biol Chem, 2001. **276**: p. 48733-48739.
83. Jary, E., Bee, T, Walker, SR, Chung, S-K, Seo, K-C, Morris, JC, AS Don, *Elimination of a hydroxyl group in FTY720 dramatically improves the phosphorylation rate.* Molec Pharm, 2010. **78**(4): p. 685-692.
84. Don, A., Martinez-Lamenca, C, Webb, WR, Proia, RL, Roberts, E, H Rosen, *Essential requirement for sphingosine kinase 2 in a sphingolipid apoptosis pathway activated by FTY720 analogues.* J Biol Chem, 2007. **282**(21): p. 15833-15842.
85. Marsolais, D., Hahm, B, Edelmann, KH, Walsh, KB, Guerrero, M, Hatta, Y, Kawaoka, Y, Roberts, E, Oldstone, MBA H Rosen, *Local not systemic modulation of dendritic cell*

*S1P receptors in lung blunts virus-specific immune response to influenza.* Mol Pharmacol, 2008. **74**(3): p. 896-903.
86. D Marsolais, B.H., KB Walsh, KH Edelmann, D McGavern, Y Hatta, Y Kawaoka, H Rosen and MBA Oldstone, *A critical role for the sphingosine analog AAL-R in dampening the cytokine response during influenza virus infection.* PNAS, 2008. **106**(5): p. 6.
87. KB Walsh, J.T., PR Wilker, A Jatzek, DM Fremgen, SC Das, T Watanabe, M Hatta, K Shinya, M Suresh, Y Kawaoka, H Rosen and MBA Oldstone, *Suppression of cytokine storm with a sphingosine analog provides protection against pathogenic influenza virus.* PNAS, 2011. **108**(29): p. 6.
88. J Chun, H.-P.H., *Mechanism of action of oral fingolimod (FTY720) in multiple sclerosis.* Clin Neuropharmacol, 2010. **33**(2): p. 11.
89. Kihara, A., Y Igarashi, *Production and release of sphingosine 1-phosphate and the phosphorylated form of the immunomodulator FTY720.* Biochemica et Biophysica Acta, 2008. **1781**: p. 496-502.
90. Brinkmann, V., Cyster, JG, T Hla, *FTY720: sphingosine 1phosphate receptor-1 in control of lymphocyte egress and endothelial barrier function.* Amer J of Transplantation, 2004. **4**: p. 1019-1025.
91. Mullershausen, F., Zecri, F, Cetin, C, Billich, A, Guerini, D, K Seuwen, *Persistent signaling induced by FTY720-P is medated by internalized S1P1 receptors.* Nature Chem Biol, 2009. **5**(6): p. 428-434.
92. Gasperini, C., Ruggieri, S, Mancinelli, CR, C Pozilli, *Advances in the treatment of relapsing-remitting multiple sclerosis- critical appraisal of fingolimod.* Ther Clin Risk Manag, 2013. **9**: p. 73-85.
93. Foster, C., Howard, LM, Schweitzer, A, Persohn, Hiestand, PC, Balatoni, B et al., *Brain penetration of the oral immunomodulatory drug FTY720 and its phosphorylation in the central nervous system during experimental autoimmune encephalomyelitis: consequences for mode of action in multiple sclerosis.* J Pharmacol Exp Ther, 2007. **323**(2): p. 469-475.
94. Brinkmann, V., *Review FTY720 in multiple sclerosis: therapeutic effects in the immune and the central nervous system.* Br J Pharmacol, 2009. **158**(5): p. 1173-1182.
95. MR Pitman, J.W., AF Lopez, SM Pitson, *Molecular Targets of FTY720 (Fingolimod)*, in *Curr Molec Medicine*2012. p. 1207-1219.
96. Nagahara, Y., Ikekita, M, T Shinomiya, *T cell selective apoptosis by a novel immunosuppressant, FTY720, is closely related with Bcl-2.* Br J Pharmacol, 2002. **137**: p. 953-962.
97. Matsuoka, Y., Nagahara, Y, Ikekita, M, T Shinomiya, *A novel immunosuppressive agent FTY720 induced Akt dephosphorylation in leukema cells.* Br J Pharmacol, 2003. **138**: p. 1303-1312.
98. Lahiri, S., Park, H, Laviad, EL, et al., *Ceramide synthesis is modulated by the sphingosine analog FTY720 via a mixture of uncompetitive and noncomptetitive inhibition in an acyl-CoA chain length-dependent manner.* J Biol Chem, 2009. **284**: p. 16090-8.
99. Lim, K., Tonelli, F, Li, Z, et al, *FTY720 analogues as SK1 inhibitors: enzyme inhibition kinetics, allosterism, proteasomal degradation, and actin rearrangement in MCF-7 breast cancer cells.* J Biol Chem, 2011. **286**: p. 18633-40.

100. Bandhuvula P, T.Y., Oskouian B, JD Saba JD, *The immune modulator FTY720 inhibits sphingosine-1-phosphate lyase activity.* J Biol Chem, 2005. **280**: p. 33697-700.
101. Symolon, H., Bushnev, A, Peng, Q, Ramaraju, H, Mays, SG, Allegood, JC, Pruett, ST, Sullards, MC, Dillehay, DL, Liotta, DC, AH Merrill Jr, *Enigmol: a novel sphingolipid analogue with anticancer activity against cancer cell lines and in vivo models for intestinal and prostate cancer.* Mol Cancer Therapy, 2011. **10**(10): p. 648-658.
102. Saddoughi, S., Song, P, Ogretmen, B, *Roles of bioactive sphingolipids in cancer biology and therapeutics.* Subcell Biochem, 2008. **49**: p. 413-440.
103. KS Kang, N.L., MS Shin, SD Kim, Y Yu, S Mohanty, RB Belshe, RR Montgomery, AC Shaw and I Kang, *An altered relationship of influenza vaccine-specific IgG responses with T cell immunity occurs with aging in humans.* Clin Immunology, 2013. **147**(2): p. 10.
104. Reed, L.J.a.H.M., *A simple method of estimating fifty percent end points.* Amer J Hyg, 1938. **27**(493-497).
105. Livak, K., TD Schmittgen, *Analysis of relative gene expression data using real-time quantitative PCR and the 2(-Delta Delta C(T)) method.* Methods, 2001. **25**(4): p. 402-408.
106. Ramos, C., Canetti, C, Souto JT, Silva, JS, Hogaboam, CM, Ferreira, SH, FQ Cunha, *MIP-1alpha acting on the CCR1 receptor mediates neutrophil migration in immune inflammation via sequential release of TNF-alpha and LTB4.* J Leukoc Biol, 2005. **78**(1): p. 167-177.
107. Dorrington, M., DME Bowdish, *Immunosenescence and novel vaccination strategies for the elderly.* Front Immunol, 2013. **4**(171): p. 1-10.
108. Lelic, A., Verschoor, CP, Ventresca, M, Parsons, R, Evelegh, C, D Bowdish, *The polyfunctionality of human memory CD8+ T cells elicited by acute and chronic infections is not influenced by age.* PLoS Path, 2012. **8**.
109. Olivieri, F., Rippo, MR, Prattichizzo, F, Babini, L, Graciotti, L, Recchioni, R, AD Procopio, *Toll like receptor signaling in "inflammaging": microRNA as new players.* Immun Ageing, 2013. **10**(11): p. 1-10.
110. Legge, K., TJ Braciale, *Respiratory dendritic cells: maturation and migration following pulmonary influenza virus infection.* International Congress Series, 2004. **1263**: p. 149-152.
111. McGill, J., Rooijen, NV, KL Legge, *Protective influenza-specific CD8 T cell responses require interactions with dendritic cells in the lungs.* J Exp Med, 2008. **205**(7): p. 1635-1646.
112. Legge, K., TJ Braciale, *Accelerated migration of respiratory dendritic cells to the regional lymph nodes is limited to the early phase of pulmonary infection.* Immunity, 2003. **18**: p. 265-277.
113. Matheu, M., Teijaro, JR, Walsh, KB, Greenberg, ML, Marsolais, D, Parker, I, Rosen, H, Oldstone, MBA, Cahalan, MD., *Three phases of CD8 T cell response in the lung following H1N1 influenza infection and sphingosine 1-phosphate agonist therapy.* PLoS ONE, 2013. **8**(3).
114. K Chiba, Y.Y., Y Masubuchi, H Kataoka, T Kawaguchi, M Ohtsuki and Y Hoshino, *FTY720, a novel immunosuppressant, induces sequestration of circulating mature lymphocytes by acceleration of lymphocyte homing in rats. I. FTY720 selectively*

*decreases the number of circulating mature lymphocytes by acceleration of lymphocyte homing.* J Immunology, 1998. **160**(10): p. 8.
115. Lan, Y., De Creus, A, Colvin, BL, Abe, M, Brinkmann, V, Coates, PTH, AW Thomson, *The sphingosine-1-phosphate receptor agonist FTY720 modulates dendritic cell trafficking in vivo.* Amer J of Transplantation, 2005. **5**: p. 2649-2659.
116. Reichel, C., Rehber, M, Lerchenberger, M, Berberich, N, Bihari, P, Khandoga, AG, Zahler, S, F Krombach, *CCL2 and CCL3 mediated neutrophil recruitment via induction of protein synthesis and generation of lipid mediators.* Arterioscler Thromb Vasc Biol, 2009. **29**(11): p. 1787-1793.
117. Yamada, M., Gomez, JC, Chugh, PE, Lowell, CA, Dinauer, MC, Dittmer, DB, CM Doerschuk, *Interferon-γ production by neutrophils during bacterial pneumonia in mice.* Am J Respir Crit Care Med, 2011. **183**(10): p. 1391-1401.
118. Su B, W.S., Rameix-Welti M-A, Dwyer D, van der Werf S, et al, *Enhancement of the influenza A HA-mediated cell-cell fusion and virus entry by the viral NA.* PLoS ONE, 2009. **4**(12).
119. Nieto, F., Pescio, LG, Favale, NO, Adamo, AM, NB Sterin-Speziale, *Sphingolipid metabolism is a crucial determinant of cellular fate in nonstimulated proliferating MDCK cells.* J Biol Chem, 2008. **283**: p. 25682-25691.
120. Lee WK, T.B., Kohistani N, Thévenod F, *ABCB1 protects kidney proximal tubule cells against cadmium-induced apoptosis: roles of cadmium and ceramide transport.* Toxicol Sci, 2011. **121**(2): p. 343-356.
121. J Milara, M.M., MD Mauricio, E Donet, EJ Morcillo and J Cortijo, *Sphingosine-1-phosphate increases human alveolar epithelial IL-8 secretion, proliferation and neutrophil chemotaxis.* Eur J of Pharm, 2009. **609**: p. 8.
122. Vu, T., Farish, S, Jenkins, M, H Kelly, *A meta-analysis of effectiveness of influenza vaccine in persons aged 65 years and over living in the community.* Vaccine, 2002. **20**(13): p. 1831-1836.

# Appendix. Supplemental Figures and Tables

**Mouse Primer Sets**

| Gene ID | Alt. Names | Forward (5' - 3') | Reverse (5' - 3') |
|---|---|---|---|
| L19 (housekeeping) | | CAAGAAGGAAGAGATCATCAAGAC | GTACAGACACGAGGGAAGC |
| CCL2 | MCP-1 | CTTCTGGGCCTGCTGTTCA | CCAGCCTACTCATTGGGATCA |
| CCL3 | MIP-1α | CTCTGTCACCTGCTCAAC | AATAGTCAACGATGAATTGG |
| CCL4 | MIP-1β | GTTCTCAGCACCAATGGG | GGTCAGGAATACCACAGC |
| CCL5 | RANTES | CGAAGGAACCGCCAAGTG | AGGACTAGAGCAAGCAATGAC |
| CCL8 | MCP-2 | TACGAGAGAATCAACAATATCC | CTACACAGAGAGACATACCC |
| CCL9 | MIP-1γ | ATGTTGGGTGTTATGTAGTC | AGTTGTAAGAATGAGGAAGG |
| CCL17 | TARC | TAAGACCTCAGTGGAGTGTTC | AAATGCCTCAGCGGGAAG |
| CXCL1 | KC, GRO1 | CTAAAAGGTGTCCCCAAGTAAC | ATTGTATAGTGTTGTCAGAAGCC |
| CXCL2 | MIP-2α, GRO2 | ACCTATTTATTCATTAGTTTCTGG | ACTCTCCTCGGTGCTTAC |
| CXCL3 | MIP-2β, GRO3 | GTTAGGGAGTTATATTGCTATTTC | ATGTGACACCGTAAGACC |
| CXCL9 | MIG | TCCTCTTGGGCATCATCTTC | TCTCCGTTCTTCAGTGTAGC |
| CXCL10 | IP-10 | ATCCCGAGCCAACCTTCC | CCCACTCAGACCCAGCAG |
| CXCL11 | I-TAC | GTTGAAGTGATTGTTACTATGAAG | TGGCACAGAGTTCTTATTGG |
| CXCL13 | BLC | GTTGAACTCCACCTCCAG | AATCACTCCAGAACACCTAC |
| IL-1b | | CAACCAACAAGTGATATTCTCCATG | GATCCACACTCTCCAGCTGCA |
| IL-6 | | TCCATCCAGTTGCCTTCTTG | GGTCTGTTGGGAGTGGTATC |
| IL-10 | | TGATGGGAGGGGTTCTTC | GTTTCTTCACAACTCTCTTAGG |
| IL-12p35 | | GTCTTAGCCAGTCCCGAAAC | GGTCCCGTGTGATGTCTTC |
| IL-12p40 | | CCAGGCACATCAGACCAG | GCAGGGAGTTAGCGACAG |
| IL-23p19 | | TGGCTGTGCCTAGGAGTAGCA | TTCATCCCTCTTCTTCTCTTAGTGATTCATA |
| iNOS | | AGTGGTGTTCTTTGCTTC | GCTTGCCTTATACTGGTC |
| TNFα | | CCAGGAGGGAGAACAGAAAC | CCAGTGAGTGAAAGGGACAG |
| TGFβ | | GACTCCTGCTGCTTTCTCC | CTCGGCAAAGGTGGGATG |
| IFNα | | GGATTCCCGCAGGAGAAG | GAATGAGTCTAGGAGGGTTG |
| IFNβ | | AGGAAAAGCAAGAGGAAAGATTG | ACCACCATCCAGGCGTAG |
| IFNγ | | GCGTCATTGAATCACACCTG | GACCTCAAACTTGGCAATACTC |

**Mouse Primer Sets**

| Gene ID | Alt. Names | Forward (5' - 3') | Reverse (5' - 3') |
|---|---|---|---|
| G-CSF | | TTCCTCCTGCCTCCTCTG | AACGAAGTCCCTAAAGAAACAG |
| GM-CSF | | GTGGTCTACAGCCTCTCAG | GACGACTTCTACCTCTTCATTC |
| SK1 | SO kinase 1 | GAAACCCCTGTGTAGCCTCC | CCTGCTCGTACCCAGCATAG |
| SK2 | SO kinase 2 | TTGGAACCTTCTGACGAGCC | GACCAGCCTCTGGGTGTCT |
| Sgpp | S1P phosphatase | CTGTCATCAAGCTGGAGGTCTTC | GCCCGTAGATAAGAGGATACTGC |
| Sgpl | S1P lyase | TCCACAGCCTGAGGAGAC | GCTTGAGGAGGTCCGTC |
| Smpd2 | Sphingomyelin- | CCACCGAAGGACCTAAGAATC | GCGACTCCTGCGTTACTG |
| Smpd3 | phosphodiesterase | CATACCCACCACCTATGAGAAGC | ACCAGAAGATGAACCCGAGAAAG |
| CerK | Ceramide kinase | GCCAGAGCGACAGACTAG | AGGATGAGGAGCAGAAAAGG |

**Human Primer Sets**

| Gene ID | | Forward (5' - 3') | Reverse (5' - 3') |
|---|---|---|---|
| GAPDH (housekeeping) | | GCCATCAATGACCCCTTCATT | TCTCGCTCCTGGAAGATGG |
| SK1 | SO kinase 1 | GGGCTTCATTGCTGATGTGGAC | TGCCTGCCATTACAACTGTCC |
| SK2(S) | SO kinase 2 (short | CTGTCTGCTCCGAGGACTGC | CAAAGGGATTGACCAATAGAAGC |
| SK2(L) | SO kinase 2 (long) | ATGATGGACACCTTGAAGCAG | CATGGCCTTAGCCCTGACCAG |
| CerK | Ceramide kinase | TGGTTGGGTCTTGCCAGATAC | ACTTCCCACAGACGACTTGC |
| CCL2 | MCP-1 | GCTCATAGCAGCCACCTTCA | ACAATGGTCTTGAAGATCACAGC |
| CCL5 | RANTES | CCCAGCAGTCGTCTTTGTCA | TGATGTACTCCCGAACCCATTTT |
| CXCL10 | IP-10 | CTGCTTTGGGGTTTATCAGA | CCACTGAAAGAATTTGGGC |
| CXCL11 | I-TAC | CAAGACCAAACTGGCCAAGG | GAATCCTGCACCCACTTCTTCT |
| IL-6 | | GTACATCCTCGACGGCACCTC | GGCAAGTCTCCTCATTGAATC |
| IL-8 | | ATTAGCCACCATCTTACCTCACAG | GTGCTTCCACATGTCCTCACA |
| TNFα | | CGAGTGACAAGCCTGTAGC | GGTGTGGGTGAGGAGCACAT |

**Influenza A Primer Set**

| Gene ID | | Forward (5' - 3') | Reverse (5' - 3') |
|---|---|---|---|
| IA/Udorn HA | Hemagglutinin | TGCACCTATTGGCACCTGCATTTC | CCTGTTGCCAACTTCAGGGTGTTT |

**Supplemental Table S1. SYBR green real-time PCR primer sequences.**

| Treatment | CXCL1 | CXCL2 | CXCL3 | CXCL9 | CXCL10 | CXCL11 |
|---|---|---|---|---|---|---|
| 21d PBS + 2d PBS | 6.33 (0.97) | 8.60 (0.94) | 17.70 (0.25) | 12.05 (2.12) | 6.72 (1.15) | 13.87 (1.64) |
| 21d IA/Ud + 2d PBS | 7.37 (0.33) | 9.29 (0.57) | 17.12 (0.47) | 13.10 (1.93) | 6.68 (0.10) | 12.89 (0.80) |
| 21d PBS + 2d *S.pn* | 3.84 (0.46) | 5.08 (0.12) | 11.46 (0.33) | 6.76 (0.93) | 1.47 (1.09) | 7.42 (0.37) |
| 21d IA/Ud + 2d *S.pn* | 2.09 (0.66) | 2.22 (0.76) | 12.22 (0.31) | 7.58 (1.33) | 0.06 (0.65) | 4.60 (1.66) |
| | CXCL13 | CCL2 | CCL3 | CCL4 | CCL8 | CCL9 |
| 21d PBS + 2d PBS | 6.90 (1.63) | 7.55 (0.95) | 17.70 (0.25) | 6.39 (1.00) | 5.06 (2.12) | 16.05 (0.67) |
| 21d IA/Ud + 2d PBS | 6.48 (0.72) | 8.12 (0.24) | 18.47 (0.20) | 7.20 (0.19) | 5.06 (0.37) | 16.69 (0.82) |
| 21d PBS + 2d *S.pn* | 2.54 (0.18) | 2.85 (0.98) | 14.42 (2.26) | 3.81 (0.53) | 2.79 (0.33) | 14.32 (0.59) |
| 21d IA/Ud + 2d *S.pn* | 2.16 (0.44) | 2.06 (1.04) | 16.26 (0.45) | 2.26 (1.02) | 2.88 (0.27) | 14.66 (0.66) |
| | CCL17 | IL-1b | IL-6 | IL-10 | IL-12p35 | TNFa |
| 21d PBS + 2d PBS | 6.29 ( 0.93) | 5.46 (0.97) | 8.20 (0.19) | 17.70 (0.25) | 10.79 (1.48) | 6.85 (0.93) |
| 21d IA/Ud + 2d PBS | 6.44 (0.26) | 5.66 (0.20) | 9.68 (0.17) | 18.47 (0.20) | 9.44 (0.37) | 6.98 (0.36) |
| 21d PBS + 2d *S.pn* | 5.70 (0.15) | 3.62 (0.46) | 5.71 (0.45) | 18.57 (0.18) | 9.11 (0.76) | 4.57 (0.48) |
| 21d IA/Ud + 2d *S.pn* | 4.67 (0.32) | 2.70 (0.33) | 3.24 (0.76) | 17.49 (0.38) | 8.24 (0.28) | 3.49 (0.73) |
| | G-CSF | GM-CSF | IFNa | IFNb | IFNg | |
| 21d PBS + 2d PBS | 13.28 (0.25) | 7.41 (0.94) | 11.81 (2.35) | 12.85 (2.18) | 8.57 (0.53) | |
| 21d IA/Ud + 2d PBS | 13.19 (0.48) | 6.70 (0.21) | 15.46 (0.35) | 15.12 (0.93) | 8.74 (0.07) | |
| 21d PBS + 2d *S.pn* | 6.77 (0.19) | 6.53 (0.25) | 12.55 (0.76) | 10.56 (1.13) | 7.44 (0.50) | |
| 21d IA/Ud + 2d *S.pn* | 5.09 (0.70) | 5.79 (0.32) | 12.91 (1.28) | 9.76 (0.22) | 6.17 (0.36) | |

**Supplemental Table S2. Gene expression in the lungs of aged mice after viral:bacterial infection.** Cytokine mRNA expression levels in 18 month old female Balb/c mice superinfected at day 21 post-virus infection. RNA was isolated from the lung tissue of animals two days after secondary infection, and mRNA levels were measured using real-time PCR. All Ct values were normalized to L19, a murine house-keeping gene, to obtain a ΔCt value. Values are reported as ΔCt (±SEM).

| | CCL2 | | CCL3 | | CCL4 | |
|---|---|---|---|---|---|---|
| Treatment | Mock | IA/Udorn | Mock | IA/Udorn | Mock | IA/Udorn |
| 2d Vehicle | 7.98 (0.31) | 3.31 (0.30) | 8.55 (0.63) | 7.05 (0.69) | 9.11 (0.22) | 5.10 (0.64) |
| 2d FTY720 | 7.73 (0.65) | 3.06 (0.71) | 10.44 (0.14) | 7.71 (0.49) | 9.96 (0.13) | 5.41 (1.25) |
| 7d Vehicle | 9.36 (0.25) | 7.66 (0.27) | 10.89 (0.21) | 8.55 (0.45) | 9.62 (0.29) | 6.47 (0.52) |
| 7d FTY720 | 8.28 (0.22) | 5.87 (0.19) | 11.19 (0.12) | 8.46 (0.49) | 10.25 (0.11) | 6.98 (0.96) |

| | CCL5 | | CXCL1 | | CXCL2 | |
|---|---|---|---|---|---|---|
| | Mock | IA/Udorn | Mock | IA/Udorn | Mock | IA/Udorn |
| 2d Vehicle | 4.00 (0.12) | 2.76 (0.22) | 7.87 (0.26) | 5.92 (0.52) | 9.01 (0.41) | 7.32 (0.82) |
| 2d FTY720 | 4.40 (0.07) | 3.15 (0.76) | 7.88 (0.47) | 5.02 (0.48) | 9.24 (0.63) | 6.65 (0.49) |
| 7d Vehicle | 3.31 (0.24) | 2.48 (0.09) | 8.13 (0.27) | 6.01 (0.49) | 11.89 (0.39) | 9.78 (0.34) |
| 7d FTY720 | 4.05 (0.39) | 2.66 (0.45) | 8.87 (0.35) | 6.05 (0.61) | 11.96 (0.10) | 9.62 (0.39) |

| | CXCL10 | | CXCL11 | | IL-1β | |
|---|---|---|---|---|---|---|
| | Mock | IA/Udorn | Mock | IA/Udorn | Mock | IA/Udorn |
| 2d Vehicle | 9.28 (0.10) | 1.58 (0.27) | 14.06 (0.35) | 4.66 (0.30) | 6.34 (0.38) | 4.66 (0.50) |
| 2d FTY720 | 8.09 (0.85) | 1.88 (0.45) | 14.41 (0.28) | 5.02 (1.25) | 6.84 (0.07) | 5.19 (0.56) |
| 7d Vehicle | 9.51 (0.25) | 2.14 (0.41) | 14.36 (0.46) | 5.92 (0.60) | 7.35 (0.08) | 5.17 (0.43) |
| 7d FTY720 | 8.32 (0.67) | 2.42 (0.59) | 15.11 (0.58) | 5.52 (0.75) | 6.30 (0.13) | 5.78 (0.61) |

| | IL-6 | | IL-10 | | IL-12p40 | |
|---|---|---|---|---|---|---|
| | Mock | IA/Udorn | Mock | IA/Udorn | Mock | IA/Udorn |
| 2d Vehicle | 11.23 (0.34) | 6.91 (0.31) | 13.70 (0.75) | 10.25 (0.33) | 11.45 (0.92) | 12.06 (0.11) |
| 2d FTY720 | 8.79 (1.36) | 5.77 (0.15) | 13.99 (0.10) | 10.64 (0.08) | 11.31 (1.84) | 11.71 (2.37) |
| 7d Vehicle | 11.88 (0.93) | 8.46 (0.48) | 15.02 (0.09) | 10.23 (0.31) | 12.00 (1.52) | 12.65 (0.42) |
| 7d FTY720 | 11.85 (0.20) | 7.92 (0.64) | 15.95 (0.68) | 10.58 (0.95) | 12.85 (0.79) | 11.93 (1.20) |

| | IL-23p19 | | TNFα | | TGFβ | |
|---|---|---|---|---|---|---|
| | Mock | IA/Udorn | Mock | IA/Udorn | Mock | IA/Udorn |
| 2d Vehicle | 15.76 (0.30) | 16.53 (0.35) | 8.56 (0.46) | 7.07 (0.54) | 9.78 (0.25) | 9.78 (0.34) |
| 2d FTY720 | 17.54 (0.83) | 15.96 (0.72) | 7.87 (1.05) | 6.56 (0.75) | 10.56 (0.26) | 9.93 (0.24) |
| 7d Vehicle | 15.68 (0.23) | 17.44 (0.74) | 9.99 (0.43) | 8.75 (0.27) | 11.38 (1.31) | 10.46 (0.71) |
| 7d FTY720 | 17.48 (0.38) | 16.85 (0.38) | 10.48 (0.09) | 8.46 (0.56) | 10.69 (0.59) | 9.49 (0.38) |

| | IFNα | | IFNβ | | IFNγ | |
|---|---|---|---|---|---|---|
| | Mock | IA/Udorn | Mock | IA/Udorn | Mock | IA/Udorn |
| 2d Vehicle | 12.71 (0.89) | 9.57 (0.35) | 14.97 (1.29) | 6.86 (0.37) | 10.60 (0.44) | 8.74 (0.35) |
| 2d FTY720 | 8.00 (1.80) | 7.92 (1.83) | 10.31 (1.86) | 6.27 (0.53) | 8.04 (1.56) | 7.02 (1.11) |
| 7d Vehicle | 10.66 (1.18) | 13.78 (1.41) | 11.73 (0.91) | 10.48 (0.58) | 10.87 (0.67) | 7.97 (0.55) |
| 7d FTY720 | 13.63 (1.46) | 14.54 (2.24) | 15.74 (2.67) | 9.22 (0.74) | 11.92 (0.12) | 8.11 (0.74) |

| | iNOS | | IA/Udorn HA | |
|---|---|---|---|---|
| | Mock | IA/Udorn | Mock | IA/Udorn |
| 2d Vehicle | 8.03 (0.06) | 8.13 (0.10) | *ND* | 2.28 (0.42) |
| 2d FTY720 | 8.08 (0.09) | 7.94 (0.52) | *ND* | 1.49 (0.67) |
| 7d Vehicle | 9.90 (0.46) | 8.68 (0.13) | *ND* | 4.69 (0.82) |
| 7d FTY720 | 9.79 (0.51) | 8.68 (0.21) | *ND* | 4.58 (0.54) |

**Supplemental Table S3. Gene expression in the lungs of mice after influenza infection and treatment with FTY720.** Balb/c mice were intranasally infected with $1x10^4$ $TCID_{50}$ IA/Udorn/72 or PBS, then given vehicle or FTY720 by i.p. injection 4 hours later. Mice were sacrificed at day 2 and 7 following infection. RNA was isolated from lungs, and mRNA levels were measured using real-time PCR. All Ct values were normalized to L19 mRNA to obtain a ΔCt value. Values are reported as ΔCt (±SEM). Undetermined (*ND*) values are those that failed to reach threshold by 45 cycles (i.e. Ct > 45), indicating the gene was not expressed.

| Treatment | SK1 | SK2 | Sgpp | Sgpl | SMPD1 | SMPD3 |
|---|---|---|---|---|---|---|
| Vehicle | 6.25 (0.08) | 10.12 (0.15) | 5.28 (0.13) | 5.02 (0.19) | 7.10 (0.13) | 8.75 (0.13) |
| Sphingosine | 6.22 (0.17) | 10.44 (0.32) | 5.20 (0.11) | 5.09 (0.14) | 7.08 (0.10) | 9.03 (0.08) |
| Enigmol | 6.03 (0.13) | 9.96 (0.28) | 5.09 (0.09) | 6.58 (0.16) | 6.94 (0.17) | 9.49 (0.21) |
| | CerK | CCL2 | CCL3 | CCL4 | CCL5 | CXCL1 |
| Vehicle | 10.26 (0.14) | 8.09 (0.24) | 10.71 (0.37) | 8.69 (0.11) | 4.13 (0.15) | 10.78 (0.62) |
| Sphingosine | 10.42 (0.23) | 7.71 (0.15) | 10.95 (0.19) | 9.00 (0.11) | 4.51 (0.14) | 11.22 (0.76) |
| Enigmol | 10.29 (0.31) | 8.05 (0.20) | 11.07 (0.46) | 8.83 (0.20) | 5.11 (0.14) | 11.70 (0.34) |
| | CXCL2 | CXCL10 | CXCL11 | IL-1β | IL-6 | IL-10 |
| Vehicle | 10.71 (0.65) | 7.29 (0.14) | 15.98 (0.53) | 5.29 (0.32) | 10.83 (0.32) | 16.78 (0.42) |
| Sphingosine | 11.12 (0.54) | 7.06 (0.17) | 16.10 (0.39) | 5.68 (0.20) | 10.87 (0.13) | 15.98 (0.35) |
| Enigmol | 11.54 (0.47) | 7.04 (0.28) | 15.92 (0.36) | 5.88 (0.29) | 11.27 (0.21) | 15.63 (0.47) |
| | IL-12p40 | TNFa | TGFβ | IFNα | IFNβ | iNOS |
| Vehicle | 13.13 (0.10) | 7.68 (0.30) | 8.89 (0.27 | 18.15 (0.62) | 17.69 (0.64) | 7.09 (0.25) |
| Sphingosine | 12.01 (0.21) | 7.46 (0.30) | 8.60 (0.18) | 16.53 (0.78) | 19.01 (0.50) | 7.35 (0.15) |
| Enigmol | 12.32 (0.21) | 7.68 (0.28) | 8.61 (0.15) | 16.31 (0.55) | 19.07 (0.53) | 7.50 (0.39) |

**Supplemental Table S4. Gene expression in the lungs following 4 days of systemic sphingosine or Enigmol treatment.** Balb/c mice were treated each day for 4 days with intraperitoneal injections of vehicle, 0.5mg/kg sphingosine or 0.5 mg/kg Enigmol. After 4 days of consecutive treatment, mice were sacrificed and lungs were collected. RNA was isolated from lungs, and mRNA levels were measured using real-time PCR. All Ct values were normalized to L19 mRNA to obtain a ΔCt value. Values are reported as ΔCt (±SEM).

| | SK1 | | SK2(S) | | SK2(L) | |
|---|---|---|---|---|---|---|
| Treatment | PBS | 24h Flu | PBS | 24h Flu | PBS | 24h Flu |
| Vehicle | 9.39 (0.50) | 8.28 (0.24) | 8.14 (0.41) | 9.37 (0.23) | 10.78 (0.48) | 11.30 (0.19) |
| SK1i | 11.99 (0.23) | 9.72 (0.11) | 8.89 (0.18) | 9.69 (0.01) | 11.67 (0.13) | 11.38 (0.09) |
| SK2i | 12.43 (0.10) | 10.34 (0.16) | 9.06 (0.10) | 9.79 (0.01) | 11.78 (0.03) | 11.60 (0.04) |
| DMS | 12.44 (0.16) | 10.43 (0.11) | 9.04 (0.19) | 9.74 (0.05) | 11.92 (0.20) | 11.66 (0.03) |
| Enigmol | 10.82 (0.20) | 10.63 (0.20) | 9.62 (0.34) | 10.25 (0.06) | 10.47 (0.34) | 11.12 (0.14) |

| | CerK | | CCL2 | | CCL5 | |
|---|---|---|---|---|---|---|
| | PBS | 24h Flu | PBS | 24h Flu | PBS | 24h Flu |
| Vehicle | 9.35 (0.45) | 10.33 (0.42) | 9.89 (0.18) | 5.64 (0.16) | 17.08 (0.28) | 2.68 (0.16) |
| SK1i | 9.22 (0.17) | 10.94 (0.15) | 10.55 (0.04) | 7.23 (0.04) | 13.47 (0.41) | 1.91 (0.08) |
| SK2i | 9.59 (0.10) | 11.46 (0.15) | 10.76 (0.03) | 7.50 (0.07) | 15.32 (0.67) | 2.02 (0.09) |
| DMS | 9.41 (0.19) | 11.10 (0.16) | 10.70 (0.03) | 7.60 (0.06) | 18.70 (2.08) | 2.28 (0.16) |
| Enigmol | 9.90 (0.38) | 11.78 (0.08) | 8.12 (0.05) | 6.34 (0.16) | 16.80 (0.38) | 5.18 (0.19) |

| | CXCL10 | | CXCL11 | | IL-6 | |
|---|---|---|---|---|---|---|
| | PBS | 24h Flu | PBS | 24h Flu | PBS | 24h Flu |
| Vehicle | 20.02 (0.61) | 7.79 (0.36) | 16.47 (0.16) | 12.86 (0.09) | 19.46 (1.63) | 11.05 (0.16) |
| SK1i | 18.99 (0.35) | 9.62 (0.23) | 17.23 (0.63) | 14.70 (0.22) | 22.50 (0.23) | 13.28 (0.27) |
| SK2i | 22.10 (1.39) | 9.60 (0.52) | 17.18 (0.31) | 14.89 (0.11) | 18.50 (0.30) | 13.18 (0.17) |
| DMS | 19.08 (0.43) | 9.31 (0.20) | 17.49 (0.05) | 14.35 (0.30) | 22.69 (0.16) | 13.09 (0.10) |
| Enigmol | 16.72 (0.69) | 8.61 (0.17) | 18.17 (0.85) | 15.36 (0.32) | 17.81 (0.42) | 12.97 (0.30) |

| | IL-8 | | TNFα | | A/Udorn HA | |
|---|---|---|---|---|---|---|
| | PBS | 24h Flu | PBS | 24h Flu | PBS | 24h Flu |
| Vehicle | 9.07 (0.35) | 3.83 (0.06) | 22.33 (0.14) | 13.60 (0.20) | *ND* | -4.65 (0.13) |
| SK1i | 8.69 (0.15) | 3.55 (0.09) | 21.91 (0.50) | 15.86 (0.16) | *ND* | -2.67 (0.01) |
| SK2i | 8.77 (0.16) | 3.84 (0.13) | 22.23 (0.40) | 15.93 (0.41) | *ND* | -2.84 (0.12) |
| DMS | 8.83 (0.06) | 3.88 (0.15) | 21.69 (0.19) | 15.83 (0.12) | *ND* | -2.84 (0.12) |
| Enigmol | 6.21 (0.26) | 4.59 (0.37) | 18.70 (0.52) | 14.94 (0.14) | *ND* | -1.72 (0.06) |

**Supplemental Table S5. Gene expression in pre-treated A549 cells.** Cytokine mRNA expression levels were evaluated in A549 cells pre-treated for 24 hours, sham or IA/Udorn-challenged and then treated for another 24 hours following infection. RNA was isolated from cells at 24hpi, and mRNA levels were measured using real-time PCR. All Ct values were normalized to GAPDH, a human house-keeping gene, to obtain a ΔCt value. Values are reported as ΔCt (±SEM). Undetermined (*ND*) values are those that failed to reach threshold by 45 cycles (i.e. Ct > 45), indicating the gene was not expressed.

| | SK1 | | SK2(S) | | SK2(L) | |
|---|---|---|---|---|---|---|
| Treatment | PBS | 5h Flu | PBS | 5h Flu | PBS | 5h Flu |
| Vehicle 1 | 12.87 (0.32) | 12.67 (0.16) | 10.70 (0.11) | 11.29 (0.31) | 12.62 (0.16) | 13.51 (0.19) |
| Vehicle 2 | 12.43 (0.47) | 12.75 (0.11) | 10.68 (0.06) | 11.15 (0.11) | 12.43 (0.16) | 13.04 (0.20) |
| Vehicle 3 | 12.58 (0.33) | 11.72 (0.30) | 10.61 (0.31) | 10.60 (0.38) | 12.69 (0.30) | 12.46 (0.53) |
| SK1i | 11.34 (0.19) | 12.96 (0.18) | 10.70 (0.14) | 10.94 (0.01) | 12.71 (0.11) | 13.09 (0.15) |
| SK2i | 12.58 (0.13) | 11.64 (0.34) | 9.54 (0.32) | 10.66 (0.44) | 12.60 (0.40) | 12.58 (0.44) |
| DMS | 12.41 (0.15) | 12.68 (0.14) | 9.62 (0.44) | 11.81 (0.17) | 12.25 (0.17) | 13.42 (0.10) |
| Enigmol | 12.18 (0.13) | 12.49 (0.04) | 10.30 (0.35) | 11.51 (0.06) | 12.16 (0.43) | 13.12 (0.07) |

| | CerK | | CCL2 | | CCL5 | |
|---|---|---|---|---|---|---|
| | PBS | 5h Flu | PBS | 5h Flu | PBS | 5h Flu |
| Vehicle 1 | 10.03 (0.11) | 10.13 (0.19) | 11.59 (0.21) | 9.27 (0.27) | 17.78 (0.43) | 11.02 (0.16) |
| Vehicle 2 | 10.03 (0.08) | 10.04 (0.12) | 10.16 (0.07) | 8.90 (0.10) | 17.46 (0.47) | 11.65 (0.14) |
| Vehicle 3 | 10.10 (0.30) | 9.83 (0.34) | 8.78 (0.03) | 8.17 (0.41) | 17.28 (0.21) | 10.22 (0.19) |
| SK1i | 10.03 (0.05) | 9.96 (0.03) | 9.81 (0.10) | 8.84 (0.09) | 19.30 (0.43) | 11.63 (0.04) |
| SK2i | 10.40 (0.34) | 9.42 (0.37) | 12.91 (0.21) | 8.43 (0.41) | 17.13 (0.22) | 10.55 (0.22) |
| DMS | 10.24 (0.38) | 10.56 (0.04) | 11.28 (0.47) | 9.67 (0.12) | 19.12 (0.30) | 10.73 (0.10) |
| Enigmol | 10.42 (0.13) | 10.86 (0.07) | 9.97 (0.37) | 9.65 (0.11) | 16.82 (0.09) | 11.74 (0.04) |

| | CXCL10 | | CXCL11 | | IL-6 | |
|---|---|---|---|---|---|---|
| | PBS | 5h Flu | PBS | 5h Flu | PBS | 5h Flu |
| Vehicle 1 | 21.57 (0.87) | 12.88 (0.39) | 18.52 (0.35) | 15.79 (0.88) | 22.72 (0.26) | 15.56 (0.28) |
| Vehicle 2 | 20.72 (0.61) | 14.14 (0.39) | 18.42 (0.26) | 17.19 (1.11) | 21.65 (0.60) | 16.47 (0.16) |
| Vehicle 3 | 20.24 (0.12) | 12.20 (0.30) | 17.33 (0.17) | 15.58 (0.67) | 20.54 (0.19) | 13.91 (0.33) |
| SK1i | 17.48 (0.53) | 13.33 (0.22) | 15.65 (0.48) | 14.05 (0.51) | 21.77 (0.40) | 16.90 (0.46) |
| SK2i | 19.10 (0.28) | 12.03 (0.29) | 17.33 (0.28) | 14.66 (0.34) | 21.65 (0.20) | 15.07 (0.48) |
| DMS | 18.30 (0.40) | 13.05 (0.10) | 19.15 (0.39) | 16.26 (0.34) | 22.68 (0.18) | 16.01 (0.17) |
| Enigmol | 20.92 (0.27) | 14.18 (0.18) | 19.86 (0.48) | 15.12 (0.78) | 20.83 (0.59) | 16.08 (0.23) |

| | IL-8 | | TNFα | | A/Udorn HA | |
|---|---|---|---|---|---|---|
| | PBS | 5h Flu | PBS | 5h Flu | PBS | 5h Flu |
| Vehicle 1 | 9.24 (0.21) | 8.62 (0.20) | 21.59 (0.64) | 13.47 (0.42) | *ND* | -4.22 (0.19) |
| Vehicle 2 | 9.64 (0.09) | 8.54 (0.10) | 21.84 (1.24) | 14.33 (0.34) | *ND* | -3.98 (0.29) |
| Vehicle 3 | 8.82 (0.37) | 7.58 (0.36) | 20.73 (0.28) | 15.37 (0.49) | *ND* | -3.77 (0.23) |
| SK1i | 9.26 (0.20) | 8.76 (0.20) | 22.41 (0.26) | 14.71 (0.11) | *ND* | -2.91 (0.03) |
| SK2i | 9.92 (0.03) | 7.94 (0.34) | 22.85 (0.29) | 14.55 (0.24) | *ND* | -2.86 (0.19) |
| DMS | 9.83 (0.24) | 9.04 (0.26) | 22.91 (0.65) | 12.75 (0.58) | *ND* | -2.68 (0.10) |
| Enigmol | 8.23 (0.30) | 8.82 (0.06) | 21.06 (0.78) | 15.24 (0.30) | *ND* | -1.63 (0.06) |

**Supplemental Table S6. Gene expression in A549 cells treated after influenza infection.** Cytokine mRNA expression levels were evaluated in A549 cells treated for 5 hours following sham or IA/Udorn viral challenge. RNA was isolated from cells at 5hpi, and mRNA levels were measured using real-time PCR. All Ct values were normalized to GAPDH, a human house-keeping gene, to obtain a ΔCt value. Values are reported as ΔCt (±SEM). Undetermined (*ND*) values are those that failed to reach threshold by 45 cycles (i.e. Ct > 45), indicating the gene was not expressed.

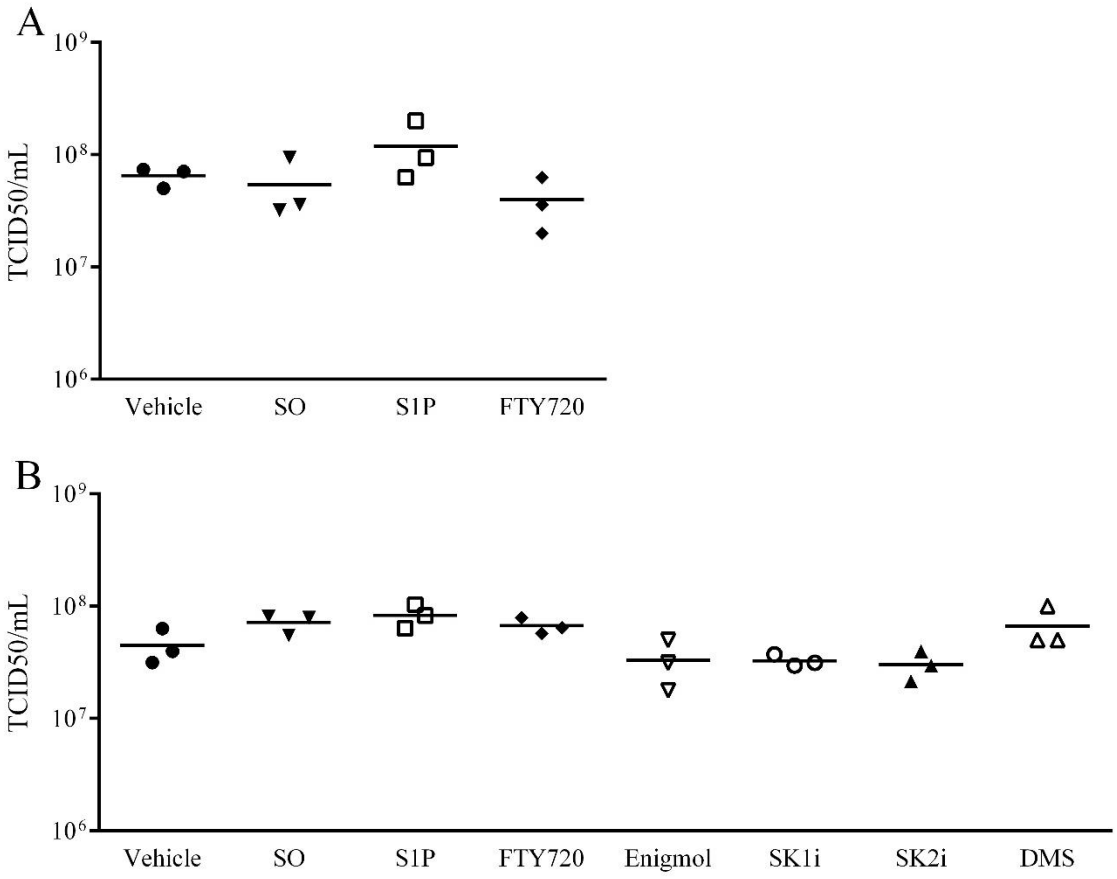


**Supplemental Figure S1. Viral loads in treated A549 or MDCK cells post-influenza challenge.** A549 cells were pre-treated with vehicle, 1uM SO, 1uM S1P or 1uM FTY720 for 24 hours, then infected with 1 MOI IA/Udorn. Treatments were added back to cells and supernatants were collected and titrated at 24hpi (A). MDCK cells were seeded at confluency in a 96-well tissue culture plate. They were pre-treated for 24 hours with vehicle, 1uM SO, 1uM S1P, 1uM FTY720, 1uM SK1i, 1uM SK2i, 1uM DMS or 1uM Enigmol in DMEM/2% charcoal-stripped FBS, then challenged with a low dose of IA/Udorn in 50ul $PBS^{+/+}$ (100 $TCID_{50}$/well). After a 1-hour adsorption period, inoculum was aspirated, cells were washed and treatments were added back to cells in the presence of 2ug/ml TPCK-treated trypsin. At 48hpi, supernatants were collected, serially diluted and titrated on MDCK cells. Cytopathic effect was observed over a 72-hour period. Viral loads are reported as 50% tissue culture infectious dose units ($TCID_{50}$/ml) as determined by the Reed-Muench method. ANOVA, Kruskal-Wallis test.

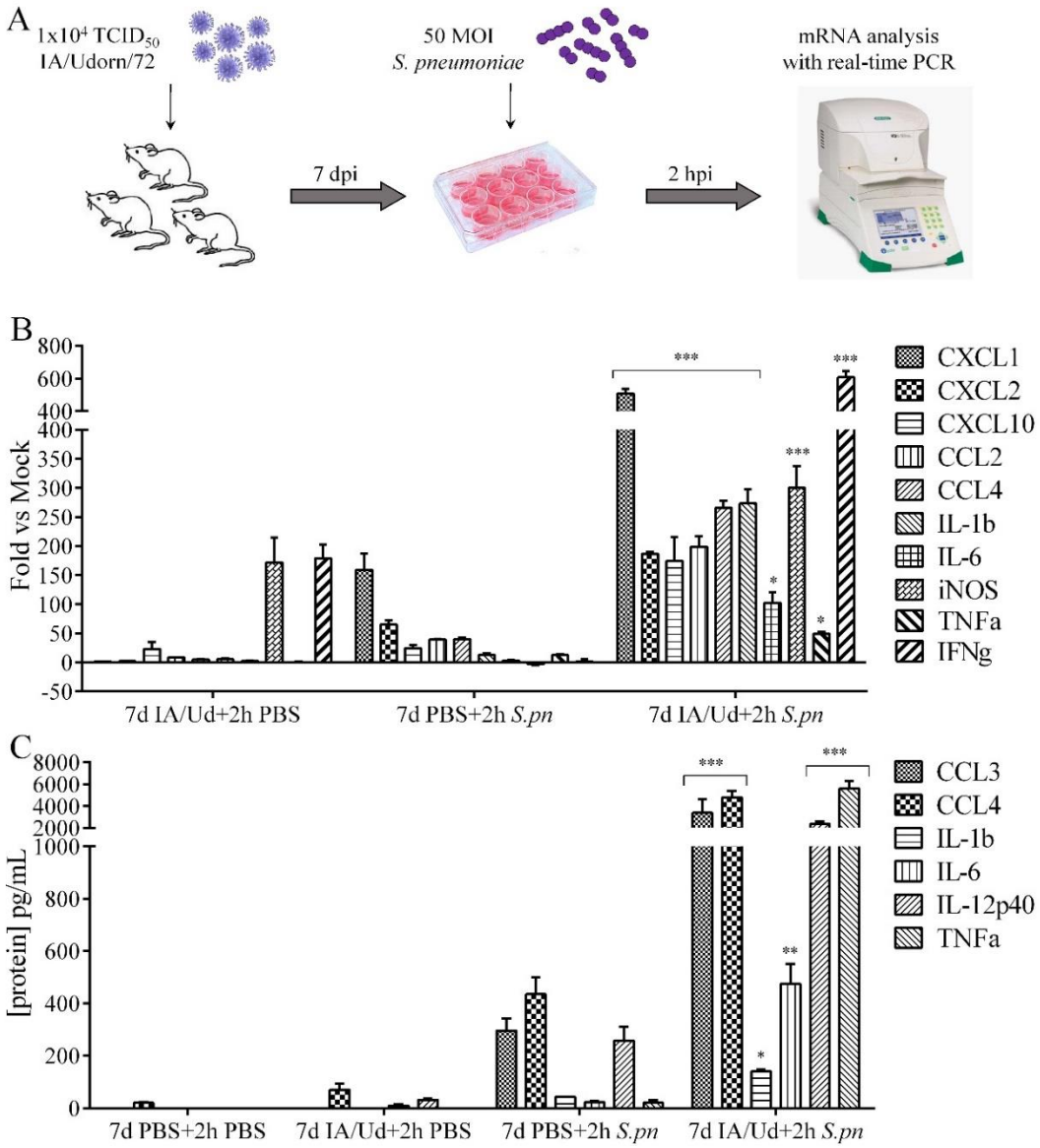


**Supplemental Figure S2. Viral:bacterial synergistic exacerbation in primary murine alveolar macrophages.** To obtain primary alveolar macrophages (AMs), young adult (3m) female Balb/c mice were intranasally infected with 1x10$^4$ TCID$_{50}$ IA/Udorn/72 or PBS. Seven days later, mice were euthanized and AMs were isolated by plating cells harvested from bronchoalveolar lavage. Adherent cells, 95% alveolar macrophages (confirmed by FACS), were washed 6 hours after plating then challenged with 50 MOI *S.pneumoniae* for 2 hours. RNA was extracted from cells after infection and cytokine analysis was performed by real-time PCR (A). Expression values are shown as fold change over mock infection (7 PBS+2h PBS) after normalization to L19 mRNA (B). Cell supernatants were also collected at 2 hours after *ex vivo* challenge for protein analysis (C). ANOVA, Dunnett's multiple comparisons test (* $p < 0.05$, ** $p < 0.01$, *** $p < 0.005$).

| | SK1 | | SK2 | | Sgpl | |
|---|---|---|---|---|---|---|
| Treatment | PBS | 5h Flu | PBS | 5h Flu | PBS | 5h Flu |
| Vehicle 1 | 12.17 (0.04) | 14.08 (0.17) | 6.44 (0.17) | 6.75 (0.16) | 7.63 (0.14) | 8.48 (0.13) |
| Vehicle 2 | 12.59 (0.14) | 13.71 (0.08) | 6.33 (0.07) | 6.62 (0.08) | 7.49 (0.1) | 8.31 (0.06) |
| Vehicle 3 | 12.25 (0.16) | 13.59 (0.11) | 6.91 (0.01) | 6.52 (0.14) | 7.64 (0.06) | 8.22 (0.01) |
| SK1i | 12.41 (0.18) | 13.67 (0.06) | 7.29 (0.24) | 7.13 (0.13) | 7.94 (0.3) | 8.75 (0.12) |
| SK2i | 12.26 (0.09) | 14.01 (0.06) | 7.12 (0.12) | 6.98 (0.13) | 7.73 (0.07) | 8.72 (0.11) |
| DMS | 11.73 (0.06) | 13.68 (0.06) | 7.34 (0.18) | 6.93 (0.23) | 7.61 (0.07) | 8.41 (0.17) |
| Enigmol | 13.15 (0.07) | 13.65 (0.11) | 6.64 (0.22) | 6.92 (0.11) | 8.15 (0.11) | 8.52 (0.11) |

| | Sgpp | | CerK | | CCL2 | |
|---|---|---|---|---|---|---|
| | PBS | 5h Flu | PBS | 5h Flu | PBS | 5h Flu |
| Vehicle 1 | 6.86 (0.06) | 7.76 (0.09) | 9.1 (0.19) | 11.12 (0.16) | 3.77 (0.15) | 2.11 (0.08) |
| Vehicle 2 | 6.78 (0.08) | 7.53 (0.08) | 9.21 (0.14) | 10.82 (0.12) | 4.03 (0.21) | 1.91 (0.07) |
| Vehicle 3 | 6.86 (0.02) | 7.38 (0.12) | 9.22 (0.13) | 11.06 (0.24) | 2.41 (0.03) | 2.03 (0.06) |
| SK1i | 7.16 (0.17) | 8.21 (0.11) | 9.43 (0.22) | 11.68 (0.16) | 3.42 (0.22) | 1.52 (0.13) |
| SK2i | 6.94 (0.08) | 8.19 (0.05) | 8.96 (0.16) | 11.54 (0.21) | 4.35 (0.06) | 2.03 (0.07) |
| DMS | 6.89 (0.11) | 8.09 (0.17) | 9.12 (0.12) | 11.12 (0.11) | 3.64 (0.04) | 1.57 (0.11) |
| Enigmol | 7.72 (0.08) | 7.92 (0.03) | 10.55 (0.14) | 11.76 (0.08) | 1.34 (0.04) | 0.53 (0.06) |

| | CCL4 | | CCL5 | | CXCL1 | |
|---|---|---|---|---|---|---|
| | PBS | 5h Flu | PBS | 5h Flu | PBS | 5h Flu |
| Vehicle 1 | 3.67 (0.09) | 2.64 (0.07) | 3.75 (0.13) | 2.61 (0.12) | 16.68 (0.33) | 11.37 (0.06) |
| Vehicle 2 | 3.67 (0.04) | 2.5 (0.07) | 4.02 (0.03) | 2.54 (0.16) | 15.29 (0.18) | 11.18 (0.04) |
| Vehicle 3 | 3.49 (0.11) | 2.29 (0.02) | 3.08 (0.14) | 2.29 (0.11) | 15.85 (0.19) | 10.76 (0.11) |
| SK1i | 4.15 (0.16) | 2.7 (0.01) | 3.41 (0.02) | 2.14 (0.08) | 16.01 (0.31) | 11.43 (0.22) |
| SK2i | 4.72 (0.03) | 3.11 (0.02) | 3.47 (0.07) | 2.19 (0.13) | 16.51 (0.37) | 12.42 (0.07) |
| DMS | 4.2 (0.05) | 3.15 (0.06) | 3.81 (0.03) | 2.32 (0.11) | 17.41 (0.31) | 12.02 (0.04) |
| Enigmol | 2.28 (0.2) | 2.22 (0.06) | 1.88 (0.11) | 0.83 (0.03) | 13.59 (0.32) | 10.35 (0.11) |

| | CXCL2 | | CXCL9 | | CXCL10 | |
|---|---|---|---|---|---|---|
| | PBS | 5h Flu | PBS | 5h Flu | PBS | 5h Flu |
| Vehicle 1 | 8.57 (0.06) | 2.95 (0.22) | 19.46 (0.58) | 15.68 (0.18) | 5.37 (0.16) | 2.31 (0.21) |
| Vehicle 2 | 8.29 (0.22) | 2.68 (0.04) | 20.19 (0.25) | 15.55 (0.11) | 5.45 (0.09) | 2.31 (0.05) |
| Vehicle 3 | 5.29 (0.33) | 2.37 (0.11) | 18.51 (0.41) | 15.33 (0.44) | 4.51 (0.03) | 1.78 (0.09) |
| SK1i | 8.14 (0.21) | 4.01 (0.09) | 20.84 (0.58) | 15.89 (0.21) | 6.49 (0.15) | 3.75 (0.07) |
| SK2i | 9.61 (0.09) | 4.58 (0.09) | 20.35 (0.45) | 15.88 (0.11) | 6.72 (0.09) | 3.81 (0.07) |
| DMS | 9.45 (0.15) | 4.09 (0.23) | 21.87 (0.09) | 16.63 (0.33) | 6.98 (0.03) | 4.22 (0.09) |
| Enigmol | 4.02 (0.13) | 2.65 (0.09) | 17.22 (0.33) | 15.37 (0.15) | 3.57 (0.17) | 2.51 (0.13) |

| | CXCL11 | | IL-1β | | IL-6 | |
|---|---|---|---|---|---|---|
| Treatment | PBS | 5h Flu | PBS | 5h Flu | PBS | 5h Flu |
| Vehicle 1 | 9.48 (0.13) | 7.63 (0.17) | 10.02 (0.32) | 1.94 (0.13) | 13.54 (0.27) | 6.91 (0.11) |
| Vehicle 2 | 9.72 (0.07) | 7.41 (0.09) | 9.68 (0.32) | 1.88 (0.08) | 13.32 (0.28) | 6.85 (0.09) |
| Vehicle 3 | 9.41 (0.06) | 6.86 (0.08) | 5.73 (0.69) | 1.61 (0.08) | 11.59 (0.53) | 6.48 (0.08) |
| SK1i | 11.12 (0.03) | 8.37 (0.11) | 9.77 (0.27) | 2.15 (0.03) | 13.07 (0.13) | 6.97 (0.13) |
| SK2i | 11.22 (0.18) | 8.74 (0.08) | 12.01 (0.11) | 2.89 (0.06) | 13.72 (0.15) | 7.47 (0.09) |
| DMS | 11.45 (0.03) | 9.07 (0.14) | 11.76 (0.05) | 2.99 (0.15) | 14.36 (0.23) | 7.74 (0.09) |
| Enigmol | 7.63 (0.31) | 6.91 (0.09) | 2.95 (0.19) | 1.26 (0.11) | 8.29 (0.26) | 5.25 (0.09) |

| | IL-10 | | IL-12p40 | | TNFα | |
|---|---|---|---|---|---|---|
| | PBS | 5h Flu | PBS | 5h Flu | PBS | 5h Flu |
| Vehicle 1 | 10.37 (0.16) | 10.58 (0.14) | 18.08 (0.29) | 16.11 (0.29) | 6.91 (0.13) | 4.18 (0.17) |
| Vehicle 2 | 10.42 (0.13) | 10.21 (0.05) | 18.09 (0.43) | 15.31 (0.47) | 6.98 (0.09) | 3.82 (0.11) |
| Vehicle 3 | 10.74 (0.21) | 10.55 (0.11) | 16.84 (0.39) | 15.28 (0.41) | 5.71 (0.09) | 3.49 (0.12) |
| SK1i | 10.93 (0.02) | 10.41 (0.11) | 15.84 (0.37) | 15.54 (0.19) | 7.91 (0.25) | 5.12 (0.15) |
| SK2i | 11.26 (0.21) | 10.56 (0.09) | 17.68 (0.52) | 15.89 (0.25) | 8.31 (0.37) | 5.47 (0.11) |
| DMS | 11.88 (0.19) | 10.94 (0.07) | 17.53 (0.29) | 15.45 (0.34) | 8.11 (0.11) | 5.03 (0.21) |
| Enigmol | 10.47 (0.17) | 10.62 (0.01) | 15.93 (0.71) | 14.91 (0.14) | 4.62 (0.13) | 4.13 (0.07) |

| | TGFβ | | IFNα | | IFNβ | |
|---|---|---|---|---|---|---|
| | PBS | 5h Flu | PBS | 5h Flu | PBS | 5h Flu |
| Vehicle 1 | 12.46 (0.22) | 12.97 (0.12) | 14.32 (0.32) | 12.05 (0.09) | 11.99 (0.08) | 6.88 (0.06) |
| Vehicle 2 | 12.27 (0.15) | 12.81 (0.18) | 13.92 (0.35) | 11.46 (0.14) | 11.96 (0.14) | 6.81 (0.04) |
| Vehicle 3 | 11.67 (0.17) | 12.84 (0.12) | 13.57 (0.14) | 11.42 (0.18) | 10.74 (0.03) | 7.03 (0.05) |
| SK1i | 12.69 (0.53) | 11.51 (0.16) | 13.87 (0.14) | 11.88 (0.22) | 12.22 (0.31) | 6.74 (0.11) |
| SK2i | 12.55 (0.17) | 11.41 (0.03) | 13.78 (0.31) | 11.74 (0.26) | 12.04 (0.13) | 7.05 (0.09) |
| DMS | 12.84 (0.15) | 11.38 (0.23) | 14.34 (0.11) | 12.01 (0.19) | 12.84 (0.17) | 7.22 (0.12) |
| Enigmol | 10.76 (0.11) | 11.19 (0.19) | 14.20 (0.13) | 11.42 (0.16) | 10.24 (0.16) | 7.04 (0.17) |

| | IFNγ | | IA/Udorn HA | |
|---|---|---|---|---|
| | PBS | 5h Flu | PBS | 5h Flu |
| Vehicle 1 | 18.48 (0.35) | 18.93 (0.94) | *ND* | 2.29 (0.10) |
| Vehicle 2 | 17.43 (0.45) | 18.21 (1.94) | *ND* | 2.44 (0.04) |
| Vehicle 3 | 17.68 (0.42) | 19.92 (1.29) | *ND* | 2.50 (0.09) |
| SK1i | 16.98 (0.52) | 19.12 (1.55) | *ND* | 2.04 (0.05) |
| SK2i | 19.13 (1.41) | 18.21 (1.13) | *ND* | 2.01 (0.09) |
| DMS | 18.63 (1.85) | 16.47 (0.23) | *ND* | 3.84 (0.13) |
| Enigmol | 18.83 (1.33) | 19.41 (1.25) | *ND* | 2.09 (0.06) |

**Supplemental Table S7. Gene expression in MH-S cells treated after influenza infection.** Cytokine mRNA expression levels were evaluated in A549 cells treated for 5 hours following sham or IA/Udorn viral challenge. . RNA was isolated from cells at 5hpi, and mRNA levels were measured using real-time PCR. All Ct values were normalized to L19 to obtain a ΔCt value. Values are reported as ΔCt (±SEM). Undetermined (*ND*) values are those that failed to reach threshold by 45 cycles (i.e. Ct > 45), indicating the gene was not expressed.